UNIVERSITÀ DEGLI STUDI DI MILANO

GRADUATE SCHOOL IN PHARMACOLOGICAL SCIENCES

DEPARTMENT OF PHARMACOLOGICAL AND BIOMOLECULAR SCIENCES

PhD COURSE IN PHARMACOTOXICOLOGICAL, PHARMACOGNOSTIC SCIENCES AND PHARMACOLOGICAL BIOTECHNOLOGY
XXVI CICLO

PhD THESIS

THE ROLE OF VALVE INTERSTITIAL CELLS IN THE PATHOGENESIS OF CALCIFIC AORTIC VALVE DISEASE

BIO/14

Paolo Poggio
Matricola R 09310

TUTOR: Chiar.ma Prof.ssa Elena TREMOLI
CORRELATORE: Chiar.mo Prof. Giovanni FERRARI
COORDINATORE: Chiar.mo Prof. Alberto PANERAI

ANNO ACCADEMICO 2012-2013

ABSTRACT

Calcific aortic valve disease (CAVD) is the most common etiology of acquired aortic valve disease. The early stage is characterized by thickening of the leaflets and none or marginal effect on the mechanical properties of the valve, while the end stage disease is associated with impaired leaflet motion and resistances to blood flow. These conditions are known as aortic valve sclerosis (AVSc) and calcific aortic valve stenosis (AVS), respectively. AVSc is present in 25–30% of patients over 65 years of age and in up to 40% of those over 75 years of age. Moreover, since AVSc hemodynamics are comparable to healthy controls, the presentation of the disease is largely asymptomatic and almost 10% of these patients will progress to AVS within 10 years from the diagnosis. Patients with severe AVS have a life expectancy of less than 10 years if untreated. Currently the main indication for AVS is aortic valve replacement (AVR).

Over the last decade several clinical trials have been performed to halt the progression of CAVD with contradictory results. The early enthusiastic findings documenting a reduction in the progression of CAVD have been questioned by later randomized studies, which show substantial equivalence between treatments and placebo. It has been proposed that CAVD therapy may have been initiated too late in the course of the disease to have the desired effect. In conclusion, there is currently no definitive therapy supported by prospective and randomized studies to halt or delay the progression of CAVD, leaving AVR the treatment of choice. Therefore, the identification of high-risk patients at early stages of degeneration will open new perspectives for the appropriate timing of therapeutic intervention on future clinical trials.

We implemented *in vitro* and *ex vivo* experiments to better characterize the early asymptomatic stage of CAVD and to evaluate osteopontin (OPN) as a potential biomarker in the progression of this degenerative disease. Moreover, we focused on OPN role in valve endothelial cells (VEC) migration, as well as valve interstitial cells (VIC) osteoblastic-like activation and biomineralization. Our results supported the

correlation between CAVD progression and increased OPN levels in aortic valve tissue and blood. Interestingly, in advance stages of calcification, we demonstrated that the overexpressed OPN had different post-translational modification compared to healthy controls. Moreover, we analyzed bone morphogenetic protein 4 (BMP4) pathway and mechanical tensile stretch as cause of VIC osteogenic-like transdifferentiation and calcium accumulation.

Table of Contents

Chapter 1

Introduction

1.1 The Heart

The heart is shaped roughly like a cone and consists of four muscular chambers (two atria and two ventricles), where the right and the left ventricles are the main pumping chambers (Figure 1.1). Starting with the right atrium, the systemic deoxygenated blood arrives from the superior and inferior vena cava and it is directed to the right ventricle. This ventricle is triangular in shape and its superior aspect forms a cone-shaped outflow tract, which leads the blood flow to the pulmonary artery towards the lungs. The oxygenated blood return to the hart in the left atrium from the four pulmonary veins and it is directed to the left ventricle. This last chamber is approximately cone shaped, longer then the right ventricle and pumps the oxygenated blood into the systemic circulation towards the aorta.

Four major valves direct the blood flow in one direction only, from the atria to the respective ventricles. The atrioventricular valves (tricuspid and mitral) separate the atria and ventricles, whereas the semilunar valves (pulmonic and aortic) separate the ventricles from the great arteries (Figure 1.1).

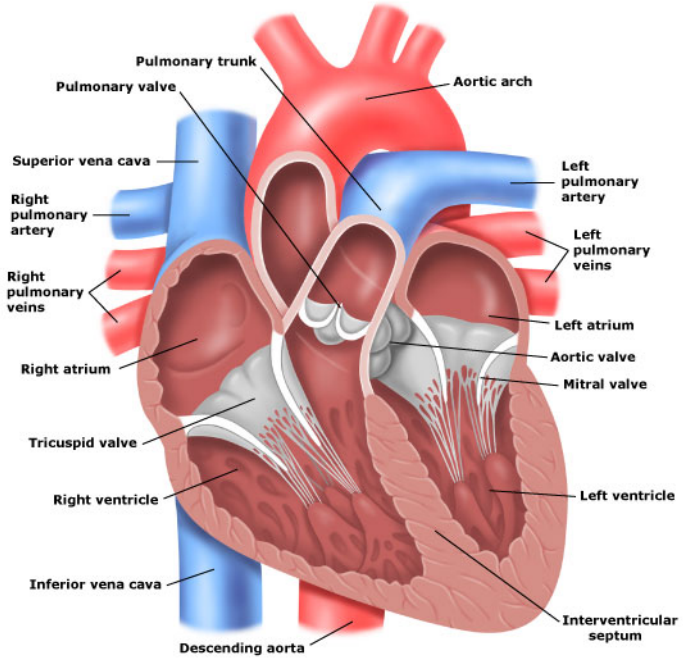

Figure 1.1. Illustration of the anatomy of the human heart.

Adapted from http://nursingmedic.blogspot.com/2010/11/anatomy-of-heart.html

1.1.1 The Cardiac Cycle

The cardiac cycle consist in the sequence of mechanical and electrical events that are responsible for the rhythmic atrial and ventricular contractions, and they occur on the right side of the heart as on the left side. The cardiac cycle can be divided in in four phases based on ventricles and valves positions: *inflow phase*, the inlet valve is open and the outlet valve is closed; *isovolumetric contraction*, both valves are open with no blood flow; *outflow phas*e, the outlet valve is open and the inlet valve is closed; *isovolumetric relaxation*, both valves are closed, with no blood flow. It is common to divides these four phases in two parts, the systole refers to ventricular contraction and the diastole refers to ventricular relaxation. Throughout the cardiac cycle the atria accept blood returning to the heart and during the diastole the blood passes from the atrium to the ventricles through the tricuspid and mitral valves. When the systole occurs the atrioventricular valves close and the semilunar valves open allowing the blood to proceed from the right and left ventricles to the pulmonary and aorta arteries, respectively.

The cardiac cycle has an average time of 800 ms and the cardiac valves open and close approximately 40 million times a year, and more than 3 billion times during the average human lifetime[1]. A common point of failure in the system is the aortic valve, since this valve regulates the highest-pressure chamber within the heart[2].

1.2 Aortic Valve

The aortic valve is located in the outflow tract of left ventricle (LV) and maintains unidirectional blood flow throughout the cardiac cycle. It provides an open tract during systolic period and a close tract during diastole preventing blood regurgitation from systemic circulation (Figure 1.2), in healthy patients blood flows through the aortic valve accelerating to a peak value of 1.35 ± 0.4m/s (Otto, 2001). The aortic vavle should functionally be considered part of the entire left ventricular outflow track and be viewed in conjunction with the aortic root[3].

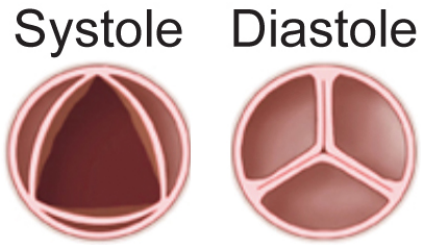

Figure 1.2. Aortic valve representation.

Adapted from: http://www.webmd.com/heart-disease/heart-failure/aortic-valve-with-stenosis

The aortic root is a cylinder and extends from the basal attachments of the leaflets within the left ventricle to the sinutubular junction. The discrete anatomic ventriculo-aortic junction is a circular locus within this root, formed where the supporting ventricular structures give way to the fibro-elastic walls of the aortic valvar sinuses[4] (Figure 1.3). In functional terms, all three sinuses of the root, and their contained leaflets, are identical. Anatomically, however, two of the valvar sinuses give rise to the coronary arteries and these can be nominated as the right, left and non coronary aortic sinuses[4]. The root provides the supporting structures for the leaflets of the aortic valve and forms the bridge between the left ventricle and the ascending aorta.

The aortic valve is normally composed of three leaflets, which attach to the aortic root in a semilunar fashion, ascending to the commissures (where the adjacent leaflets come together) ad descending to the basal attachment of each leaflet to the aortic wall (Figure 1.3).

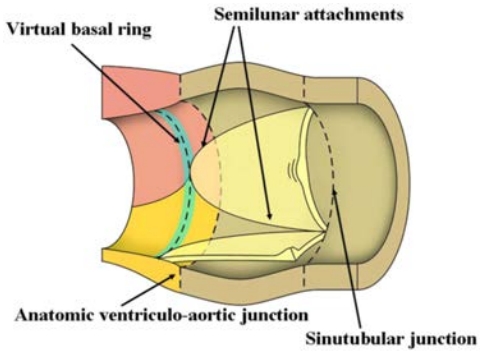

Figure 1.3. Aortic root representation.

Adapted from[4]: Anderson, R. H. The surgical anatomy of the aortic root. *Multimedia Manual of Cardio-Thoracic Surgery* **2007,** (2007).

The aortic leaflets are flexible structures that come together to seal the valve orifice during diastole. Vascularization of the valve is not necessary because the leaflets are thin enough for the diffusion of oxygen, nutrients, and waste between the tissue and the surrounding blood[5]. The leaflets are a highly specialized structure divided into three functionally specific layers: the *fibrosa* layer, facing the aorta, rich in densely packed collagen in circumferential directions, which provides the strength and stiffness of the leaflets and it is responsible for absorbing the diastolic and systolic stresses; the *ventricularis* layer, closest to the left ventricle, composed largely of elastin fibers align radially, which can extend in diastole and recoil in systole to minimize the leaflet area; and the *spongiosa* layer, located between the previous two, mainly constitute by glycosaminoglycans, which accommodate shear forces of the leaflet during the cardiac cycle and allow the outer layers to slide easily over one another during leaflet motion[3,5,6] (Figure 1.4). The collagen-rich fibrosa, the elastin-rich ventricularis, and the glycosaminoglycan-rich spongiosa made up 41%, 29%, and 30% of the whole aortic valve tissue, respectively[7].

Figure 1.4. Aortic valve structure.

F = Fibrosa layer; S = Spongiosa layer; V = Ventricularis layer. The fibrosa layer face the aorta while the ventricularis layer face the left ventricle. Scale bar is 200 μm. Adapted from[8]: Chen, J.-H. & Simmons, C. A. Cell-matrix interactions in the pathobiology of calcific aortic valve disease: critical roles for matricellular, matricrine, and matrix mechanics cues. *Circ. Res.* **108,** 1510–1524 (2011).

The *ventricularis* layer is exposed to rapid, pulsatile, unidirectional shear stress (Figure 1.5 left panel), while the *fibrosa* layer experiences an oscillatory stress[9] (Figure 1.5 right panel). This oscillatory stress has been linked to increase in the expression of inflammatory receptors and bone morphogenic proteins (BMPs)[10]; it also decreases the expression of inhibitors of fibrosis and calcification[11].

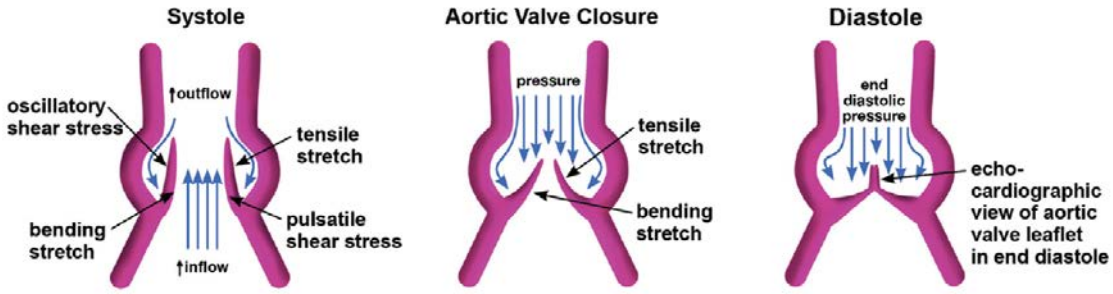

Figure 1.5. Hemodynamic flow across the aortic valve.

Schematic representation of diastole and systole hemodynamics in the aortic root affecting aortic valve leaflet. Adapted from[12]: Rajamannan, N. M. *et al.* Calcific Aortic Valve Disease: Not Simply a Degenerative Process: A Review and Agenda for Research From the National Heart and Lung and Blood Institute Aortic Stenosis Working Group * Executive Summary: Calcific Aortic Valve Disease - 2011 Update. *Circulation* **124,** 1783–1791 (2011).

1.2.1 Aortic Valve Cell Populations

The native aortic valve consists of two types of cells: valve endothelial cells (VECs) that cover the surface with a single monolayer, and a heterogeneous population called valve interstitial cells (VICs) that reside in the bulk tissue matrix.

The VECs (Figure 1.6), much like the endothelial cells covering the vasculature, serve as a protective lining for the underlying tissue by regulating permeability, mediating inflammation, and preventing thrombosis[13]. Transcriptional profiling of vascular versus valve endothelial cells demonstrated significant differences between the two cell types *in vivo*[14]. VECs are oriented circumferentially across the leaflets and perpendicular to the direction of the blood flow, in contrast to vascular endothelium, which aligns parallel to the blood flow[3,15]. In addition, the hemodynamic forces exerted on the two sides of the leaflets are different. It has been hypothesized that the differences in opposite side endothelium may play a critical role in the typical predominant localization of pathologic aortic valve calcification near the outflow surface (*fibrosa* layer)[16].

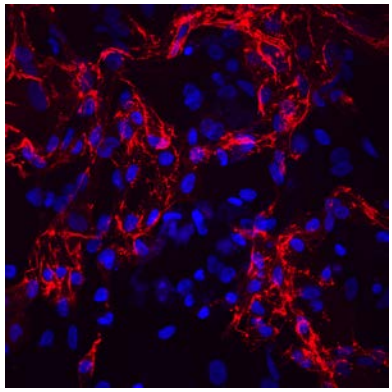

Figure 1.6. Valve endothelial cells.

Immunofluorescence image showing isolated human valve endothelial cells (VEC) at 40x magnification. Red signal represent platelet endothelial adhesion molecule (PCAM1) also known as cluster of differentiation 31 (CD31).

The VICs (Figure 1.7) reside within the aortic valve leaflets, where they synthesize and maintain the extracellular matrix that forms the tissue architecture[6]. In healthy adult valve, the 95% of VICs have a fibroblast-like phenotype and the rest 5% is divided in myofribroblasts-like and smooth muscle cells (SMC)[17-21]. Studies of the interstitial cell population have revealed that there is no particular localization within the layers of the leaflet and the VICs are present throughout the tissue[20,22,23]. VIC phenotype is believed to be plastic and reversible, with fibroblasts in healthy valves representing the majority of the cells. Fibroblast are a quiescent population (qVIC) that, in response to injury or disease, acquire a secretory myofribloblast-like phenotype (aVIC)[18,24,25], where the principal indicator for aVICs is α-smooth muscle actin (SMA)[26,27]. This process allows the secretion and turn over of extracellular matrix (ECM) proteins, which repair the tissue micro-damage and enable the long-term durability of the leaflets structure[3,17]. The local environment (paracrine endothelium-derived signals)[28], the inflammatory cytokines (TGF-β1 and BMPs)[29], the biochemical and biomechanical properties of the ECM[11,30-36], and mechanical stimuli induced by hemodynamic forces (normal or pathological stretching of the valve tissue) regulate the VIC phenotype and function[1,37-40].

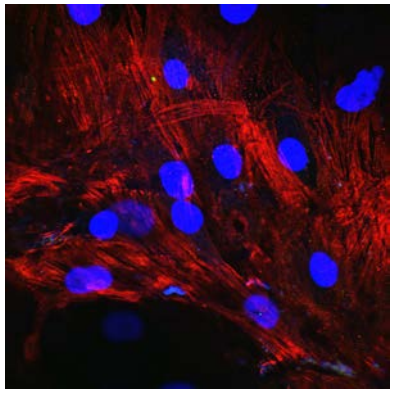

Figure 1.7. Valve interstitial cells.

Immunofluorescence image showing isolated human valve interstitial cells (VIC) at 60x magnification. Red signal represent alpha smooth muscle actin (SMA).

1.3 Calcific Aortic Valve Diseases

CAVD is a progressive disease that eventually leads to calcification of the aortic valve, which causes left ventricular outflow react obstruction. Our understanding of the pathophysiology has evolved in the past decades. Previously, valve calcification was seen as an inevitable consequence of ageing that only has clinical significance once symptoms due to valve obstruction occur[41]. Today, CAVD is view as the result of an active, multi-factorial potentially modifiable pathological process[41].

CAVD is the most common heart valve disease with a prevalence of ≈ 30% in adults over 65 years in the sub-clinical asymptomatic form, called aortic valve sclerosis (AVSc)[42]. Importantly, between 16% - 33% of patients with AVSc will progress to aortic valve stenosis (AVS)[43,44], the most common cause of sudden death among valve heart diseases[45]. Moreover, the incidence of CAVD continues to rise due to the aging population[46], as such, calcific aortic valve disease has a serious impact on general health.

AVSc in characterized by focal sub-endothelial plaque-like lesions on the aortic side of the leaflet that extend to the adjacent fibrosa layer[6]. Moreover, it has been reported a prominent accumulation of low-density lipoprotein (LDL), LDL oxidation

and microscopic calcification[47-51], resulting in macroscopic, progressive valve thickening[6]. Advance stages of CAVD (AVS) are associated with impaired leaflet motion and resistance to blood flow due to the calcium deposition and matrix degradation[6]. Once aortic sclerosis is detectable, the risk of cardiovascular events is increased by 50%[52]. At the onset of mild symptoms, survival deviates considerably from the even-free curve, with a dramatic decline in survival with severe symptomatic aortic stenosis (Figure 1.8).

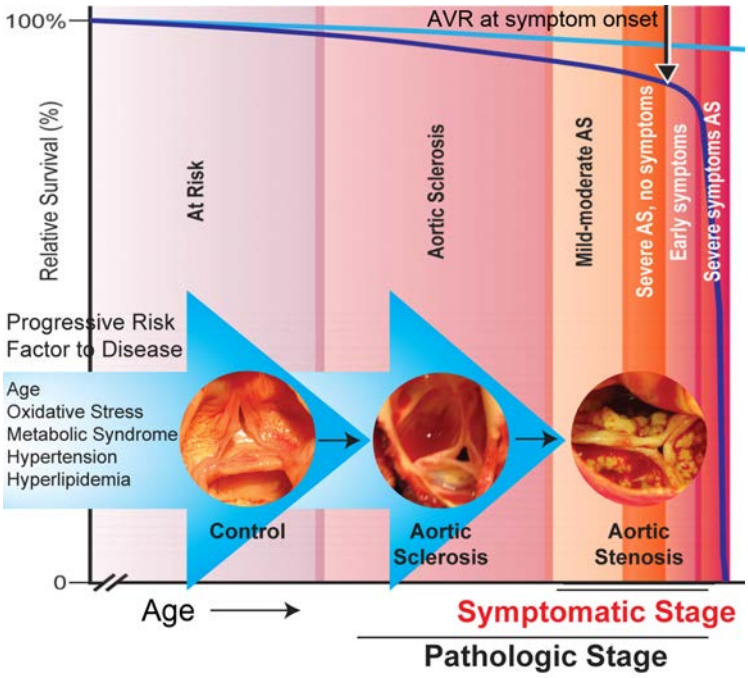

Figure 1.8. Aortic valve degeneration: conceptual framework.

Adapted from[12,41]: Otto, C. M. Calcific aortic valve disease: outflow obstruction is the end stage of a systemic disease process. *European Heart Journal* **30,** 1940–1942 (2009).

Rajamannan, N. M. *et al.* Calcific Aortic Valve Disease: Not Simply a Degenerative Process: A Review and Agenda for Research From the National Heart and Lung and Blood Institute Aortic Stenosis Working Group * Executive Summary: Calcific Aortic Valve Disease - 2011 Update. *Circulation* **124,** 1783–1791 (2011).

Several evidence suggest that CAVD, due to the pathophysiological similarities to atherosclerosis, share many risk factors, such as male gender, age, tobacco use, diabetes mellitus, hypercholesterolemia, hypertension, hyperparathyroidism, renal disease, decreased bone density, and metabolic syndrome. This overlapping of risk

factors has led to the hypothesis that calcific aortic valve disease and atherosclerosis have similar etiologies, but there are epidemiological discrepancies. In atherosclerosis, the main cell population is represented by SMC, while in the aortic valve the key players are the VICs (fibroblasts and myofibroblasts)[6]. Moreover, calcification occurs earlier and in more substantial amount in AVS versus atherosclerotic plaques[6]. Furthermore, only 50% of patients with severe AVS have significant coronary artery disease (CAD), and the majority of patients with CAD have no sign of CAVD[53].

An additional major risk factor for CAVD is the presence of a bicuspid aortic valve (BAV). BAV disease is one of the most frequent observed congenital heart abnormalities affecting 0.5-1.4% of the general population and has a 3:1 male predominance[54-57]. Patients with BAV develop aortic valve calcification at an earlier age compared with degenerative tricuspid aortic valve[51,58,59] and up to 50% of the adults who present with AVS show evidence of BAV disease[60]. A fairly high incidence of familial clustering exists, which suggests autosomal-dominant inheritance with reduce penetrance[61]. The anatomic features of BAV are characterized by smooth cusps margins and the fusion of two cusps of unequal size (Figure 1.9). The largest cusp often contains a raphe instead of a commissure. The most commonly seen variant of BAV is characterized by one raphe between the left and right coronary cusps (L-R BAV), which is seen in 70-86% of the BAV cases, whereas the fusion of the right and non-coronary cusps (R-N BAV) are observed in 12-28% and the left and non-coronary cusps (L-N BAV) in 0.5-3% of the cases[62-64]. BAV with two aortic sinuses and no raphe is uncommon and is called type 0[61].

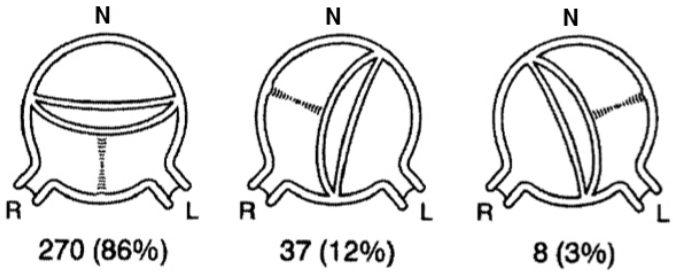

Figure 1.9. Schematic representation of bicuspid aortic valve classification.

Adapted from[63]: Sievers, H.-H. & Schmidtke, C. A classification system for the bicuspid aortic valve from 304 surgical specimens. *The Journal of Thoracic and Cardiovascular Surgery* **133,** 1226–1233 (2007).

1.3.1 Pathophysiology of Calcific Aortic Valve Disease

Early aortic lesions seem to be initiated by increased mechanical or decreased shear stress, in combination with endothelial dysfunction, followed by lipids deposition. Researchers as shown that endothelium subjected to abnormal blood flow seems more susceptible to inflammatory cytokines[65,66], and more important, high stretch loading induces upregulation of pro-inflammatory cytokines expression on the fibrosa layer of the aortic valve[67]. Consequently, monocytes infiltrate the endothelial layer via adhesion molecules and differentiate into macrophages. Activated T lymphocytes further increase cytokines release, which activate quiescent VICs into myofibroblasts and furthermore in osteoblast-like cells, eventually causing calcium deposition[42,68,69].

Srivatsa[70], Mohler[71] and Rajamannan[72] have described a molecular and cellular heterogeneity of the biomineralization process. Osteoblastic-like cells can derive from circulating myeloid calcifying cell, circulation osteogenic precursor, endothelial progenitor cells, valve endothelial cells, valve interstitial cells, and valve annulus chondrocytes (Figure 1.10)[73].

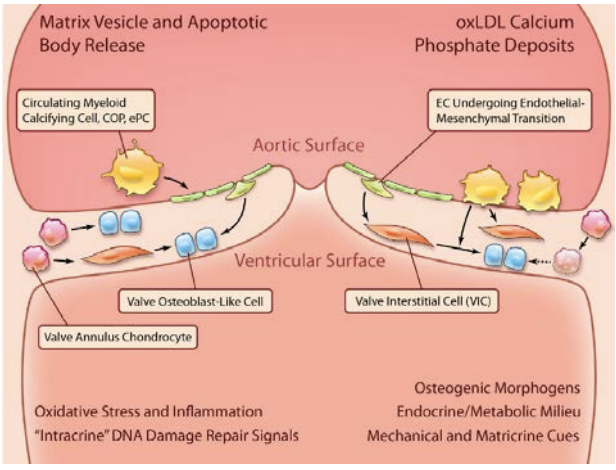

Figure 1.10. Possible sources of osteogenic-like cell.

Adapted from[73]: Towler, D. A. Molecular and cellular aspects of calcific aortic valve disease. *Circ. Res.* **113,** 198–208 (2013).

Cytokines involved in the pro-osteogenic signaling cascade that induce osteogenic-like transdifferentiation are part of the Wnt, and Notch signaling family as well as of the transforming growth factor (TGF)-β superfamily, including the bone morphogenetic proteins (BMPs)[73,74], which has been investigated further in the result section of this dissertation.

BMPs are secreted polypeptides, a subgroup of the transforming growth factor (TGF)-b superfamily. BMPs elicit their effects through activation of receptor complexes composed of type I and type II Ser/Thr kinase receptors[75,76]. When the ligand binds, the type II receptors phosphorylate and activate the type I receptors, which propagate the signaling by phosphorylating transcription factors (Smads) (Figure 1.8). The BMP type I receptors activate the receptor-activated Smads, which assemble into complexes together with the common mediator Smad4 and translocate to the nucleus. Smads can modulate gene expression runt-related transcription factor 2 (Runx2), alkaline phosphatase (ALP), osteopontin (OPN), and other molecules involved in VIC activation, osteoblastic-like transdifferentiation and calcium deposition. This process is also regulated by the inhibitory I-Smads, Smad6, and Smad7[77] (Figure 1.11). BMPs can activate non-Smad signaling pathways as well. One of these non-Smad signals is the paracrine Wnt/b-catenin relay that promotes ALP expression and matrix biomineralization[78,79]. Moreover, Narisawa[80] and Harmey[81] have demonstrated that ALP is able to induce a robust tissue mineralization by neutralizing natural calcification inhibitors, such as inorganic phosphate (Pi) and osteopontin (OPN).

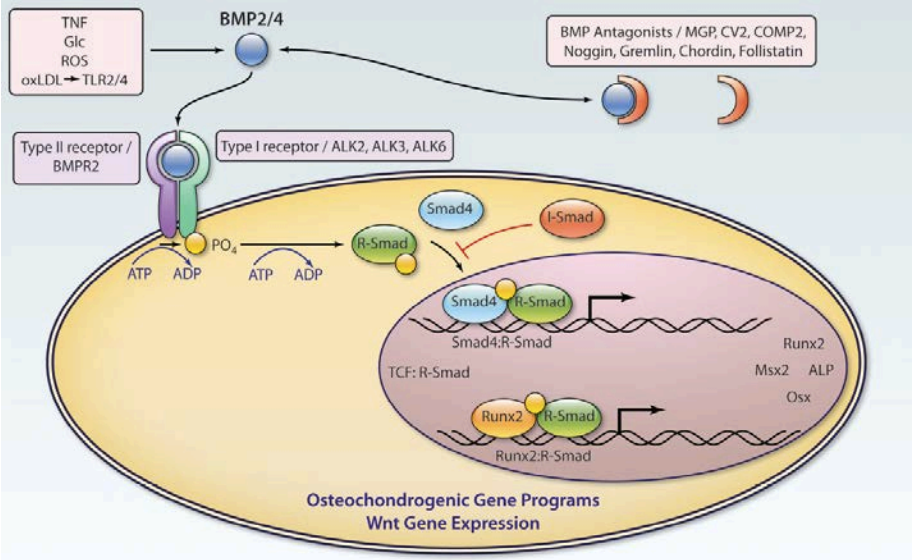

Figure 1.11. Schematic representation of BMP4 pathway.

Adapted from[82]: Boström, K. I., Rajamannan, N. M. & Towler, D. A. The regulation of valvular and vascular sclerosis by osteogenic morphogens. *Circ. Res.* **109,** 564–577 (2011).

1.3.2 Diagnosis

The initial diagnosis of aortic valve stenosis typically is based on detection of a systolic murmur followed by echocardiography confirmation. Echocardiography provides detailed, non-invasive information about the anatomy and etiology of valve disease, and the severity of valve stenosis. The first step in evaluation is the assessment of valve anatomy by two-dimensional (2D) imaging. Transthoracic imaging provides diagnostic images in the vast majority of patients with valve heart disease and is the standard approach both for the initial evaluation and for follow-up studies. Transesophageal imaging is reserved for patients for whom transthoracic images are non-diagnostic or when higher resolution images are needed for clinical decision-making. Three-dimensional (3D) echocardiographic (3DE) imaging represents a major innovation in cardiovascular ultrasound. Advancements in computer and transducer technologies permit real-time 3DE acquisition and presentation of cardiac structures from any spatial point of view[83]. Standard measures of aortic stenosis severity are the maximum velocity (V_{max}) across the stenotic valve, the mean transaortic pressure

gradient (ΔP_{mean}) calculated with the Bernoulli equation, and the functional aortic valve area (AVA) calculated with the continuity equation (Table 1.1) [84,85].

AVSc is related to thickening of the aortic cusps without obstruction to blood flow (Figure 1.12). The sclerotic lesions of the aortic valve have both similarities and differences when compared with the atherosclerotic process. Similarities include inflammatory cell infiltrates, oxidized low-density lipoprotein, and calcification, while differences between the 2 processes involve a larger calcium load and the absence of smooth muscle cell infiltration in aortic valve sclerosis as compared with coronary vessels[47,72,86-89]. The progressive degeneration of the aortic valve leads to the obstruction of the left ventricular outflow tract due to impaired leaflet motion and resistance to the blood flow, which causes several physiological changes and the symptoms of aortic valve stenosis arise.

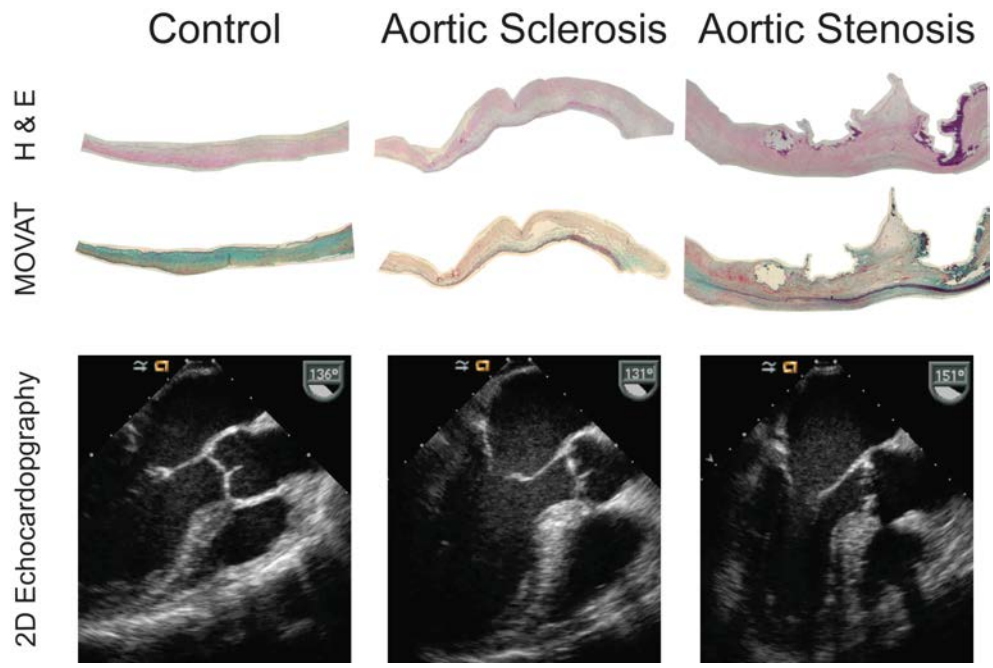

Figure 1.12. Calcific aortic valve degeneration phases.

Histological staining showing cell content and structure architectire (H&E and MOVAT) in different stage of CAVD. Lower panels show representative images of 2D echocardiography in controls, aortic valve sclerosis and stenosis patients.

Adapted from[90]: Grau, J. B. *et al.* Analysis of osteopontin levels for the identification of asymptomatic patients with calcific aortic valve disease. *Ann. Thorac. Surg.* **93,** 79–86 (2012).

Table 1.1 Classification of Calcific Aortic Valve Disease

	Valve Anatomy	Aortic Velocity (m/s)	Mean Gradient (mmHg)	Aortic Valve Area (cm^2)
Normal Aortic Valve	Transparent leaflets with normal motion	< 2.5	< 10	> 2.5
Aortic Sclerosis	Focal leaflet thickening with normal motion	< 2.5	< 10	> 2.5
Mild Aortic Stenosis	Mild leaflet thickening with mildly reduced motion	2.5 – 3	10 – 20	1.5 – 2.5
Moderate Aortic Stenosis	Mild to moderate calcium presence with moderately reduced leaflet motion	3 – 4	20 – 40	1.0 – 1.5
Severe Aortic Stenosis	Moderate to severe calcium presence with little leaflet motion	4 – 5	40 – 60	0.6 – 1.0
Critical Aortic Stenosis	Severe calcium presence with immobile leaflets	> 5	> 60	< 0.6

Adapted from[84]: Lindman, B. R., Bonow, R. O. & Otto, C. M. Current management of calcific aortic stenosis. *Circ. Res.* **113,** 223–237 (2013).

1.4 Surgical Treatments of Aortic Valve Stenosis

1.4.1 Aortic Valve Replacement

Currently in developed countries, the main indication for aortic valve stenosis due to CAVD is aortic valve replacement (AVR)[91]. Patients with severe AVS have a life expectancy of less than 10 years if untreated and if there is concomitant heart failure, 50% will die within a year[92,93]. Surgical AVR is the only effective treatment for severe AVS and has transformed the outlook of patients presenting this disease[84]. The timing of intervention is critical and is determined through specific guidelines (Figure 1.13).

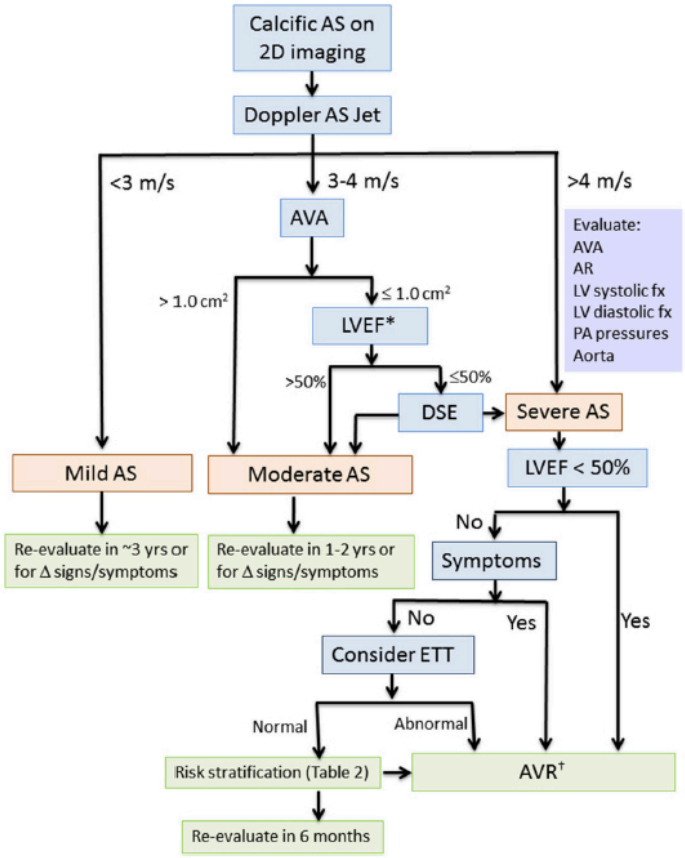

Figure 1.13. Approach to the diagnosis of calcific aortic valve disease.

Adapted from[84]: Lindman, B. R., Bonow, R. O. & Otto, C. M. Current management of calcific aortic stenosis. *Circ. Res.* **113,** 223–237 (2013).

Today, isolated AVR can be accomplished with a mini-sternotomy; although a full sternotomy is often performed if extensive concomitant coronary artery bypass grafting (CABG) is required[84]. The operative mortality associated with AVR is dependent on both patient risk factors and the skill and experience of the surgical team. Comorbidities associated with higher 30-day mortality include age, left ventricle dysfunction, concomitant coronary artery disease (CAD), previous CABG, renal insufficiency, and chronic pulmonary disease[84]. The mortality associated with AVR has decreased dramatically during the past 2 decades and 30-day mortality is currently under 3% for isolated AVR and under 4.5% for combined AVR/CABG[94,95].

In elderly and high-risk individual, the risk of death undergoing surgical aortic valve replacement is too high, for this reason transcatheter aortic valve implantation

(TAVI) has become an exciting treatment option[96,97]. In a very high-risk population, TAVI resulted in 30.7% in mortality at 1 year and in 43.3% mortality at 2 years, where standard surgical therapy had a 50.7% and 68.0% mortality at 1 and 2 years, respectively[98].

1.4.2 Prosthetic Aortic Valves

Various alternatives are available for aortic valve replacement, and matching patients to the most-appropriate type of valve is not always straightforward. Matching the right valve for the right patient is a difficult but essential process to optimize the outcome for patients undergoing AVR[99]. The most important factors that should be considered in the first place are the patient's age, life expectancy, preference, indication/contraindication for warfarin therapy, and comorbidities (Figure 1.14)[99].

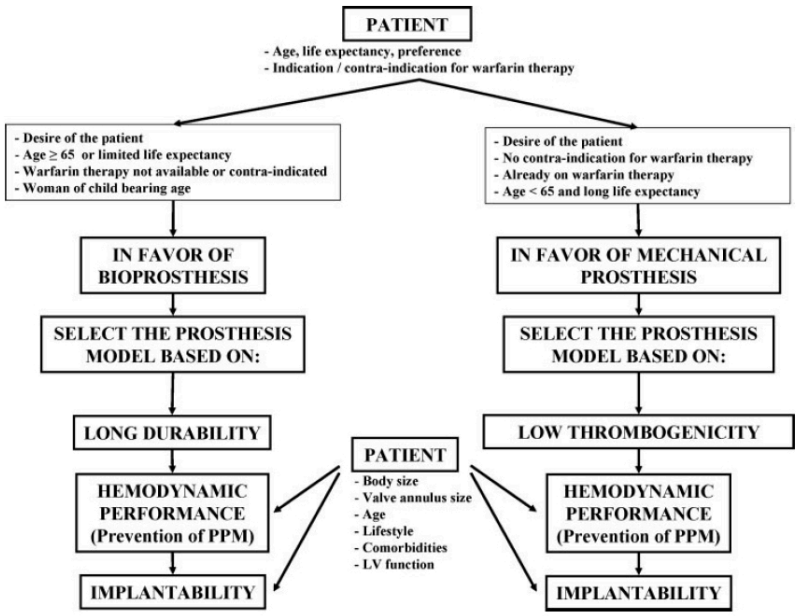

Figure 1.14. Flowchart for optimal prosthesis selection.

Adapted from[99]: Pibarot, P. & Dumesnil, J. G. Prosthetic Heart Valves: Selection of the Optimal Prosthesis and Long-Term Management. *Circulation* **119,** 1034–1048 (2009).

Commercially, there are two types of aortic valve prosthesis: mechanical and bioprosthetic (Figure 1.15). The mechanical valves currently in use are of a bileaflet design, these valves are durable but require lifelong anticoagulation with warfarin. Bioprosthetic valves do not require oral anticoagulation, but with limited durability, 10 to 15 year is the average lifespan[100]. Bioprosthetic heart valves are made with glutaraldehyde-fixed porcine aortic valves, or constructed with glutaraldehyde-fixed bovine pericardium and most of the times mounted on stent[100]. Other types of bioprosthetic valves are pulmonary autograft and aortic valve homograft. The former, also known as Ross procedure[101], is used in young patients, particularly women in childbearing years, might not wish to take oral anticoagulation therapy[100]. The latter is less in use because the realization that a homograft aortic valve has limited durability, is technically difficult to implant, is expensive to procure and cryopreserve, and might not be superior to other bioprosthetic valves[102-106].

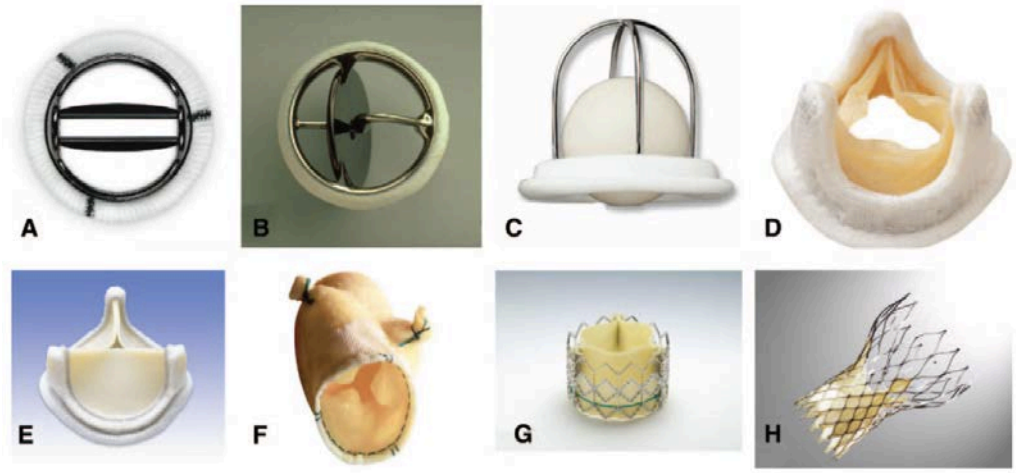

Figure 1.15. Types of prosthetic valves.

(A) Bileaflet mechanical valve (St Jude); (B) monoleaflet mechanical valve (Medtronic Hall); (C) caged ball valve (Starr-Edwards); (D) stented porcine bioprosthesis (Medtronic Mosaic); (E) stented pericardial bioprosthesis (Carpentier-Edwards Magna); (F) stentless porcine bioprosthesis (Medtronic Freestyle); (G) percutaneous bioprosthesis expanded over a balloon (Edwards Sapien); (H) self-expandable percutaneous bioprosthesis (CoreValve).

Adapted from: Pibarot, P. & Dumesnil, J. G. Prosthetic Heart Valves: Selection of the Optimal Prosthesis and Long-Term Management. *Circulation* **119,** 1034–1048 (2009).

Mechanical prostheses have an excellent durability, and structural valve degeneration (SVD) is extremely rare with contemporary valves, although the rate of SVD in bioprosthetic valves increases over time, particularly after the initial 7 to 8 years after implantation[99]. Bioprosthetic SVD is strongly influenced by the age of the patient at the time of implantation and the rate of failure is less than 10% at 10 years in elderly patients (more than 70 years of age), but is between 20% and 30% in patients older than 40 years[107,108].

It is important to note that, despite surgical treatments, the underlying mechanism of the valve degeneration is left untreated, and calcification reoccurs even in bioprosthetic valves. The pathogenesis of structural degeneration can occur due to several processes. The degenerative process of bioprosthetic valves could occur because of the tissue fixation with glutaraldehyde, this induces a calcium influx as a result of membrane damage, which provides, along with the residual phospholipids of the membranes, an environment prone to calcium crystal nucleation[108]. The immune process could occur because bioprosthetic valves are not in fact completely "immunologically inert"[109] and residual animal antigens could elicit humoral and cellular immune responses, leading to tissue mineralization and/or disruption. The only available treatment for SVD is reoperation with surgical AVR or TAVI (valve-in-valve implantation).

1.5 Pharmacological Treatments of Aortic Valve Stenosis

Therapeutic strategies able to reduce or halt the progression of CAVD are needed to delay and possibly avoid surgical valve replacement. Furthermore, The need for alternatives to surgery is emphasized by the increasing age of the general population and the rising prevalence of CAVD. Since CAVD and atherosclerosis have similar disease progression and risk factors, pharmacological treatment of patients with CAVD has been focused on 3-hydroxy-3-methylglutaryl-coenzyme A (HMG-CoA) reductase inhibitors (statins) and angiotensin-converting enzyme inhibitors (ACEi) [110,111]. Statins are used to inhibit the cholesterol synthesis in the liver and lowering plasma cholesterol levels, while ACEi interfere with the renin-angiotensin system blocking the conversion

of angiotensin I to angiotensin II causing dilation of blood vessels with consequent decrease in blood pressure and improved endothelial function[112].

Several studies have been investigating statin treatment on the progression of CAVD. The early enthusiastic findings of observational studies (retrospective and non-randomized) documenting a reduction in the progression of the disorder have been seriously questioned by later, randomized studies, which showed substantial equivalence between statin and placebo-treated patients (Table 1.2)[113]. In conclusion, there is currently no definitive therapy supported by prospective and randomized studies to halt or delay the progression of CAVD.

Table 1.2 Published nonrandomized and randomized statin trials

Study (y)	Follow Up	Grade, AS at baseline	Pro statins
Non Randomized			
Aronow (2001)	2.75 y	Mild	Yes ($p < 0.01$)
Navaro (2001)	1.75 y	Mild to moderate	Yes ($p < 0.03$)
Bellamy (2002)	3.7 y	Mild to moderate	Yes ($p < 0.04$)
Shavelle (2002)	2.5 y	N.A.	Yes ($p < 0.006$)
Rosenhek (2004)	2.0 y	Mild to severe	Yes ($p < 0.0001$)
RAAVE (2007	1.4 y	Moderate to severe	Yes ($p < 0.007$)
Randomized			
SALTIRE (2005)	2.08 y	Mild to severe	No
SEAS (2008)	4.35 y	Mild to moderate	No
ASTRONOMER (2010)	3.5 y	Mild to moderate	No

Adapted from[114,115]: Hermans, H. *et al.* Statins for calcific aortic valve stenosis: into oblivion after SALTIRE and SEAS? An extensive review from bench to bedside. *Curr Probl Cardiol* **35,** 284–306 (2010).

Chan, K. L. *et al.* Effect of Lipid lowering with rosuvastatin on progression of aortic stenosis: results of the aortic stenosis progression observation: measuring effects of rosuvastatin (ASTRONOMER) trial. *Circulation* **121,** 306–314 (2010).

The questions that were raised after the results of the randomized statin trials where related to the target choose and the timing of intervention. A recent study has been published on the genetic associations with valve calcification and aortic stenosis[116]. In this study Thanassoulis et al.[116] found a strong correlation between one single-nucleotide polymorphism (SNP) in the lipoprotein(a) (LPA) locus and the presence of aortic valve calcification, answering the question regarding the use of the statins in CAVD patients. The reason of the statin therapy failure could be due to the patient population selected for the randomized trials. The patients did have not dyslipidemia as facilitating factor for the progression of the disease, so the effect would only depend on the pleiotropic effects of statins. Moreover, only patients with at least moderate stenosis where included, as such the hemodynamic changes and inflammation could be self-perpetuating and overcome the beneficial effect of the statins[114].

The efficacy of statin therapy should be tested in earlier stages of the disease when the aortic valve functions are still in the normal range and the valve degeneration is still at the initial stage. The same problems have been notice with ACEi treatment to preventing the progression of CAVD[117]. Although these data are discouraging, there are already few studies that demonstrate the potential of statin and ACEi treatments in slowing the progression of CAVD at the sclerotic stage[118-120].

1.6 References

1. Sacks, M. S., David Merryman, W. & Schmidt, D. E. On the biomechanics of heart valve function. *J Biomech* **42,** 1804–1824 (2009).

2. LEVIN, A. R. *et al.* Intracardiac pressure-flow dynamics in isolated ventricular septal defects. *Circulation* **35,** 430–441 (1967).

3. Schoen, F. J. Evolving concepts of cardiac valve dynamics: the continuum of development, functional structure, pathobiology, and tissue engineering. *Circulation* **118,** 1864–1880 (2008).

4. Anderson, R. H. The surgical anatomy of the aortic root. *Multimedia Manual of Cardio-Thoracic Surgery* **2007,** (2007).

5. Schoen, F. J. & Levy, R. J. Tissue heart valves: current challenges and future research perspectives. *Journal of biomedical materials research* **47,** 439–465 (1999).

6. Freeman, R. V. & Otto, C. M. Spectrum of calcific aortic valve disease: pathogenesis, disease progression, and treatment strategies. *Circulation* **111,** 3316–3326 (2005).

7. Stella, J. A. & Sacks, M. S. On the biaxial mechanical properties of the layers of the aortic valve leaflet. *J Biomech Eng* **129,** 757–766 (2007).

8. Chen, J.-H. & Simmons, C. A. Cell-matrix interactions in the pathobiology of calcific aortic valve disease: critical roles for matricellular, matricrine, and matrix mechanics cues. *Circ. Res.* **108,** 1510–1524 (2011).

9. Kilner, P. J. *et al.* Asymmetric redirection of flow through the heart. *Nature* **404,** 759–761 (2000).

10. Sucosky, P., Balachandran, K., Elhammali, A., Jo, H. & Yoganathan, A. P. Altered shear stress stimulates upregulation of endothelial VCAM-1 and ICAM-1 in a BMP-4- and TGF-beta1-dependent pathway. *Arterioscler.*

Thromb. Vasc. Biol. **29,** 254–260 (2009).

11. Yip, C. Y. Y., Chen, J.-H., Zhao, R. & Simmons, C. A. Calcification by valve interstitial cells is regulated by the stiffness of the extracellular matrix. *Arteriosclerosis, Thrombosis, and Vascular Biology* **29,** 936–942 (2009).

12. Rajamannan, N. M. *et al.* Calcific Aortic Valve Disease: Not Simply a Degenerative Process: A Review and Agenda for Research From the National Heart and Lung and Blood Institute Aortic Stenosis Working Group * Executive Summary: Calcific Aortic Valve Disease - 2011 Update. *Circulation* **124,** 1783–1791 (2011).

13. Butcher, J. T. & Nerem, R. M. Valvular endothelial cells and the mechanoregulation of valvular pathology. *Philos. Trans. R. Soc. Lond., B, Biol. Sci.* **362,** 1445–1457 (2007).

14. Farivar, R. S. *et al.* Transcriptional profiling and growth kinetics of endothelium reveals differences between cells derived from porcine aorta versus aortic valve. *Eur J Cardiothorac Surg* **24,** 527–534 (2003).

15. Deck, J. D. Endothelial cell orientation on aortic valve leaflets. *Cardiovascular Research* **20,** 760–767 (1986).

16. Simmons, C. A., Grant, G. R., Manduchi, E. & Davies, P. F. Spatial heterogeneity of endothelial phenotypes correlates with side-specific vulnerability to calcification in normal porcine aortic valves. *Circ. Res.* **96,** 792–799 (2005).

17. Rabkin, E. *et al.* Activated interstitial myofibroblasts express catabolic enzymes and mediate matrix remodeling in myxomatous heart valves. *Circulation* **104,** 2525–2532 (2001).

18. Rabkin-Aikawa, E., Farber, M., Aikawa, M. & Schoen, F. J. Dynamic and reversible changes of interstitial cell phenotype during remodeling of cardiac valves. *J. Heart Valve Dis.* **13,** 841–847 (2004).

19. Taylor, P. M., Allen, S. P. & Yacoub, M. H. Phenotypic and functional characterization of interstitial cells from human heart valves, pericardium and skin. *J. Heart Valve Dis.* **9,** 150–158 (2000).

20. Bairati, A. & DeBiasi, S. Presence of a smooth muscle system in aortic valve leaflets. *Anat Embryol* **161,** 329–340 (1981).

21. Cimini, M., Rogers, K. A. & Boughner, D. R. Smoothelin-positive cells in human and porcine semilunar valves. *Histochem. Cell Biol.* **120,** 307–317 (2003).

22. Merryman, W. D. *et al.* Correlation between heart valve interstitial cell stiffness and transvalvular pressure: implications for collagen biosynthesis. *Am. J. Physiol. Heart Circ. Physiol.* **290,** H224–31 (2006).

23. Merryman, W. D., Huang, H.-Y. S., Schoen, F. J. & Sacks, M. S. The effects of cellular contraction on aortic valve leaflet flexural stiffness. *J Biomech* **39,** 88–96 (2006).

24. Rabkin-Aikawa, E. *et al.* Clinical pulmonary autograft valves: pathologic evidence of adaptive remodeling in the aortic site. *J. Thorac. Cardiovasc. Surg.* **128,** 552–561 (2004).

25. Chester, A. H. & Taylor, P. M. Molecular and functional characteristics of heart-valve interstitial cells. *Philos. Trans. R. Soc. Lond., B, Biol. Sci.* **362,** 1437–1443 (2007).

26. Gould, S. T., Srigunapalan, S., Simmons, C. A. & Anseth, K. S. Hemodynamic and cellular response feedback in calcific aortic valve disease. *Circ. Res.* **113,** 186–197 (2013).

27. Hinz, B. Formation and function of the myofibroblast during tissue repair. *Journal of Investigative Dermatology* **127,** 526–537 (2007).

28. El-Hamamsy, I. *et al.* Endothelium-dependent regulation of the mechanical properties of aortic valve cusps. *J. Am. Coll. Cardiol.* **53,** 1448–1455 (2009).

29. Walker, G. A., Masters, K. S., Shah, D. N., Anseth, K. S. & Leinwand, L. A. Valvular myofibroblast activation by transforming growth factor-beta: implications for pathological extracellular matrix remodeling in heart valve disease. *Circ. Res.* **95,** 253–260 (2004).

30. Chen, J.-H., Chen, W. L. K., Sider, K. L., Yip, C. Y. Y. & Simmons, C. A. β-catenin mediates mechanically regulated, transforming growth factor-β1-induced myofibroblast differentiation of aortic valve interstitial cells. *Arteriosclerosis, Thrombosis, and Vascular Biology* **31,** 590–597 (2011).

31. Cushing, M. C., Liao, J.-T. & Anseth, K. S. Activation of valvular interstitial cells is mediated by transforming growth factor-β1 interactions with matrix molecules. *Matrix Biology* **24,** 428–437 (2005).

32. Benton, J. A., Kern, H. B. & Anseth, K. S. Substrate properties influence calcification in valvular interstitial cell culture. *J. Heart Valve Dis.* **17,** 689–699 (2008).

33. Gu, X. & Masters, K. S. Regulation of valvular interstitial cell calcification by adhesive peptide sequences. *J Biomed Mater Res A* **9999A,** NA–NA (2010).

34. Pho, M. *et al.* Cofilin is a marker of myofibroblast differentiation in cells from porcine aortic cardiac valves. *... of Physiology-Heart ...* (2008).

35. Kloxin, A. M., Benton, J. A. & Anseth, K. S. In situ elasticity modulation with dynamic substrates to direct cell phenotype. *Biomaterials* **31,** 1–8 (2010).

36. Gould, S. T., Darling, N. J. & Anseth, K. S. Small peptide functionalized thiol-ene hydrogels as culture substrates for understanding valvular interstitial cell activation and de novo tissue deposition. *Acta Biomater* **8,** 3201–3209 (2012).

37. Balachandran, K., Sucosky, P., Jo, H. & Yoganathan, A. P. Elevated cyclic stretch alters matrix remodeling in aortic valve cusps: implications for degenerative aortic valve disease. *Am. J. Physiol. Heart Circ. Physiol.* **296,** H756–64 (2009).

38. Merryman, W. D. *et al.* Synergistic effects of cyclic tension and transforming growth factor-beta1 on the aortic valve myofibroblast. *Cardiovasc. Pathol.* **16,** 268–276 (2007).

39. Thayer, P. *et al.* The effects of combined cyclic stretch and pressure on the aortic valve interstitial cell phenotype. *Ann Biomed Eng* **39,** 1654–1667 (2011).

40. Butcher, J. T. & Nerem, R. M. Valvular endothelial cells regulate the phenotype of interstitial cells in co-culture: effects of steady shear stress. *Tissue Eng.* **12,** 905–915 (2006).

41. Otto, C. M. Calcific aortic valve disease: outflow obstruction is the end stage of a systemic disease process. *European Heart Journal* **30,** 1940–1942 (2009).

42. Beckmann, E., Grau, J. B., Sainger, R., Poggio, P. & Ferrari, G. Insights into the use of biomarkers in calcific aortic valve disease. *J. Heart Valve Dis.* **19,** 441–452 (2010).

43. Cosmi, J. E. *et al.* The risk of the development of aortic stenosis in patients with 'benign' aortic valve thickening. *Arch Intern Med* **162,** 2345–2347 (2002).

44. Faggiano, P. *et al.* Progression of aortic valve sclerosis to aortic stenosis. *Am. J. Cardiol.* **91,** 99–101 (2003).

45. Carabello, B. A. Introduction to aortic stenosis. *Circ. Res.* **113,** 179–185 (2013).

46. Mathers, C. D. & Loncar, D. Projections of global mortality and burden of disease from 2002 to 2030. *PLoS Med.* **3,** e442 (2006).

47. Otto, C. M., Kuusisto, J., Reichenbach, D. D., Gown, A. M. & O'Brien, K. D. Characterization of the early lesion of 'degenerative' valvular aortic stenosis. Histological and immunohistochemical studies. *Circulation* **90,** 844–853 (1994).

48. Olsson, M. *et al.* Accumulation of T lymphocytes and expression of interleukin-2 receptors in nonrheumatic stenotic aortic valves. *J. Am. Coll.*

Cardiol. **23,** 1162–1170 (1994).

49. O'Brien, K. D. *et al.* Apolipoproteins B, (a), and E accumulate in the morphologically early lesion of 'degenerative' valvular aortic stenosis. *Arterioscler. Thromb. Vasc. Biol.* **16,** 523–532 (1996).

50. Olsson, M., Thyberg, J. & Nilsson, J. Presence of oxidized low density lipoprotein in nonrheumatic stenotic aortic valves. *Arterioscler. Thromb. Vasc. Biol.* **19,** 1218–1222 (1999).

51. Wallby, L., Janerot-Sjöberg, B., Steffensen, T. & Broqvist, M. T lymphocyte infiltration in non-rheumatic aortic stenosis: a comparative descriptive study between tricuspid and bicuspid aortic valves. *Heart* **88,** 348–351 (2002).

52. Roger, V. L. *et al.* Heart disease and stroke statistics--2012 update: a report from the American Heart Association. *Circulation* **125,** e2–e220 (2012).

53. Otto, C. M. & D O'BRIEN, K. Why is there discordance between calcific aortic stenosis and coronary artery disease? *Heart* **85,** 601–602 (2001).

54. Tadros, T. M., Klein, M. D. & Shapira, O. M. Ascending Aortic Dilatation Associated With Bicuspid Aortic Valve. *Circulation* (2009).

55. Nistri, S., Basso, C., Marzari, C. & Mormino, P. Frequency of Bicuspid Aortic Valve in Young Male Conscripts by Echocardiogram. *The American journal of ...* (2005).

56. Tutar, E., Ekici, F., Atalay, S. & Nacar, N. The prevalence of bicuspid aortic valve in newborns by echocardiographic screening. *Am. Heart J.* (2005).

57. Somauroo, J. D., Pyatt, J. R., Jackson, M., Perry, R. A. & Ramsdale, D. R. An echocardiographic assessment of cardiac morphology and common ECG findings in teenage professional soccer players: reference ranges for use in screening. *Heart* **85,** 649–654 (2001).

58. Ward, C. Clinical significance of the bicuspid aortic valve. *Heart* **83,** 81–85 (2000).

59. SUBRAMANIAN, R., OLSON, L. J. & EDWARDS, W. D. Surgical pathology of pure aortic stenosis: a study of 374 cases. **59,** 683–690 (1984).

60. Roberts, W. C. & Ko, J. M. Frequency by decades of unicuspid, bicuspid, and tricuspid aortic valves in adults having isolated aortic valve replacement for aortic stenosis, with or without associated aortic regurgitation. *Circulation* **111,** 920–925 (2005).

61. Huntington, K., Hunter, A. G. & Chan, K. L. A prospective study to assess the frequency of familial clustering of congenital bicuspid aortic valve. *JAC* **30,** 1809–1812 (1997).

62. Sabet, H. Y., Edwards, W. D., Tazelaar, H. D. & Daly, R. C. Congenitally bicuspid aortic valves: a surgical pathology study of 542 cases (1991 through 1996) and a literature review of 2,715 additional cases. *Mayo Clin. Proc.* **74,** 14–26 (1999).

63. Sievers, H.-H. & Schmidtke, C. A classification system for the bicuspid aortic valve from 304 surgical specimens. *The Journal of Thoracic and Cardiovascular Surgery* **133,** 1226–1233 (2007).

64. Fernandes, S. M. *et al.* Morphology of bicuspid aortic valve in children and adolescents. *JAC* **44,** 1648–1651 (2004).

65. Aikawa, E. *et al.* Human semilunar cardiac valve remodeling by activated cells from fetus to adult: implications for postnatal adaptation, pathology, and tissue engineering. *Circulation* **113,** 1344–1352 (2006).

66. Sacks, M. S. & Yoganathan, A. P. Heart valve function: a biomechanical perspective. *Philos. Trans. R. Soc. Lond., B, Biol. Sci.* **362,** 1369–1391 (2007).

67. Balachandran, K., Sucosky, P., Jo, H. & Yoganathan, A. P. Elevated cyclic stretch induces aortic valve calcification in a bone morphogenic protein-dependent manner. *Am. J. Pathol.* **177,** 49–57 (2010).

68. Ghaisas, N. K. *et al.* Adhesion molecules in nonrheumatic aortic valve disease:

endothelial expression, serum levels and effects of valve replacement. *JAC* **36,** 2257–2262 (2000).

69. Sorescu, G. P. *et al.* Bone morphogenic protein 4 produced in endothelial cells by oscillatory shear stress stimulates an inflammatory response. *J. Biol. Chem.* **278,** 31128–31135 (2003).

70. Srivatsa, S. S. *et al.* Increased cellular expression of matrix proteins that regulate mineralization is associated with calcification of native human and porcine xenograft bioprosthetic heart valves. *J. Clin. Invest.* **99,** 996–1009 (1997).

71. Mohler, E. R. *et al.* Bone formation and inflammation in cardiac valves. *Circulation* **103,** 1522–1528 (2001).

72. Rajamannan, N. M. *et al.* Human aortic valve calcification is associated with an osteoblast phenotype. *Circulation* **107,** 2181–2184 (2003).

73. Towler, D. A. Molecular and cellular aspects of calcific aortic valve disease. *Circ. Res.* **113,** 198–208 (2013).

74. Miller, J. D., Weiss, R. M. & Heistad, D. D. Calcific aortic valve stenosis: methods, models, and mechanisms. *Circ. Res.* **108,** 1392–1412 (2011).

75. David, L., Feige, J.-J. & Bailly, S. Emerging role of bone morphogenetic proteins in angiogenesis. *Cytokine Growth Factor Rev.* **20,** 203–212 (2009).

76. Shi, Y. & Massagué, J. Mechanisms of TGF-beta signaling from cell membrane to the nucleus. *Cell* **113,** 685–700 (2003).

77. Miyazono, K., Maeda, S. & Imamura, T. BMP receptor signaling: transcriptional targets, regulation of signals, and signaling cross-talk. *Cytokine Growth Factor Rev.* **16,** 251–263 (2005).

78. Rawadi, G., Vayssière, B., Dunn, F., Baron, R. & Roman-Roman, S. BMP-2 controls alkaline phosphatase expression and osteoblast mineralization by a

Wnt autocrine loop. *Journal of Bone and Mineral Research* **18,** 1842–1853 (2003).

79. Baron, R. & Rawadi, G. Wnt signaling and the regulation of bone mass. *Current osteoporosis reports* **5,** 73–80 (2007).

80. Narisawa, S., Yadav, M. C. & Millán, J. L. In Vivo Overexpression of Tissue-Nonspecific Alkaline Phosphatase Increases Skeletal Mineralization and Affects the Phosphorylation Status of Osteopontin. *Journal of Bone and Mineral Research* **28,** 1587–1598 (2013).

81. Harmey, D. *et al.* Concerted regulation of inorganic pyrophosphate and osteopontin by akp2, enpp1, and ank: an integrated model of the pathogenesis of mineralization disorders. *Am. J. Pathol.* **164,** 1199–1209 (2004).

82. Boström, K. I., Rajamannan, N. M. & Towler, D. A. The regulation of valvular and vascular sclerosis by osteogenic morphogens. *Circ. Res.* **109,** 564–577 (2011).

83. Lang, R. M. *et al.* EAE/ASE recommendations for image acquisition and display using three-dimensional echocardiography. *J Am Soc Echocardiogr* **25,** 3–46 (2012).

84. Lindman, B. R., Bonow, R. O. & Otto, C. M. Current management of calcific aortic stenosis. *Circ. Res.* **113,** 223–237 (2013).

85. Baumgartner, H. *et al.* Echocardiographic assessment of valve stenosis: EAE/ASE recommendations for clinical practice. *European Journal of Echocardiography* **10,** 1–25 (2009).

86. Otto, C. M. Why is aortic sclerosis associated with adverse clinical outcomes? *JAC* **43,** 176–178 (2004).

87. Agmon, Y. *et al.* Aortic valve sclerosis and aortic atherosclerosis: different manifestations of the same disease? Insights from a population-based study. *JAC* **38,** 827–834 (2001).

88. Olsson, M., Rosenqvist, M. & Nilsson, J. Expression of HLA-DR antigen and smooth muscle cell differentiation markers by valvular fibroblasts in degenerative aortic stenosis. *JAC* **24,** 1664–1671 (1994).

89. Miller, J. D. *et al.* Dysregulation of antioxidant mechanisms contributes to increased oxidative stress in calcific aortic valvular stenosis in humans. *J. Am. Coll. Cardiol.* **52,** 843–850 (2008).

90. Grau, J. B. *et al.* Analysis of osteopontin levels for the identification of asymptomatic patients with calcific aortic valve disease. *Ann. Thorac. Surg.* **93,** 79–86 (2012).

91. Iung, B. *et al.* A prospective survey of patients with valvular heart disease in Europe: The Euro Heart Survey on Valvular Heart Disease. *Eur. Heart J.* **24,** 1231–1243 (2003).

92. Carabello, B. A. & Paulus, W. J. Aortic stenosis. *Lancet* **373,** 956–966 (2009).

93. Ross, J. J. & Braunwald, E. Aortic stenosis. *Circulation* **38,** 61–67 (1968).

94. Lee, R. *et al.* Fifteen-year outcome trends for valve surgery in North America. *Ann. Thorac. Surg.* **91,** 677–84– discussion p 684 (2011).

95. Brown, J. M. *et al.* Isolated aortic valve replacement in North America comprising 108,687 patients in 10 years: changes in risks, valve types, and outcomes in the Society of Thoracic Surgeons National Database. *J. Thorac. Cardiovasc. Surg.* **137,** 82–90 (2009).

96. Holmes, D. R. & Mack, M. J. Transcatheter valve therapy a professional society overview from the american college of cardiology foundation and the society of thoracic surgeons. *J. Am. Coll. Cardiol.* **58,** 445–455 (2011).

97. Holmes, D. R. *et al.* 2012 ACCF/AATS/SCAI/STS expert consensus document on transcatheter aortic valve replacement. *J. Am. Coll. Cardiol.* **59,** 1200–1254 (2012).

98. Makkar, R. R. *et al.* Transcatheter aortic-valve replacement for inoperable

severe aortic stenosis. *N. Engl. J. Med.* **366,** 1696–1704 (2012).

99. Pibarot, P. & Dumesnil, J. G. Prosthetic Heart Valves: Selection of the Optimal Prosthesis and Long-Term Management. *Circulation* **119,** 1034–1048 (2009).

100. David, T. E. Surgical treatment of aortic valve disease. *Nature Publishing Group* **10,** 375–386 (2013).

101. Ross, D. N. Replacement of aortic and mitral valves with a pulmonary autograft. *Lancet* **2,** 956–958 (1967).

102. Mykén, P. S. U. & Bech-Hansen, O. A 20-year experience of 1712 patients with the Biocor porcine bioprosthesis. *J. Thorac. Cardiovasc. Surg.* **137,** 76–81 (2009).

103. Ali, A. *et al.* Valve failure following homograft aortic valve replacement: does implantation technique have an effect? *European Heart Journal* **29,** 1454–1462 (2008).

104. Lever, C. G. *et al.* Cost-effectiveness and efficacy of an on-site homograft heart-valve bank. *Can J Surg* **38,** 492–496 (1995).

105. Klieverik, L. M. A. *et al.* Surgical treatment of active native aortic valve endocarditis with allografts and mechanical prostheses. *Ann. Thorac. Surg.* **88,** 1814–1821 (2009).

106. Jassar, A. S. *et al.* Graft selection for aortic root replacement in complex active endocarditis: does it matter? *Ann. Thorac. Surg.* **93,** 480–487 (2012).

107. Jamieson, W. R. E. *et al.* Surgical management of valvular heart disease 2004. in *Can J Cardiol* **20 Suppl E,** 7E–120E (2004).

108. Schoen, F. J. & Levy, R. J. Calcification of tissue heart valve substitutes: progress toward understanding and prevention. *Ann. Thorac. Surg.* **79,** 1072–1080 (2005).

109. Manji, R. A. *et al.* Glutaraldehyde-fixed bioprosthetic heart valve conduits

calcify and fail from xenograft rejection. *Circulation* **114,** 318–327 (2006).

110. Stewart, B. F. *et al.* Clinical factors associated with calcific aortic valve disease. Cardiovascular Health Study. *J. Am. Coll. Cardiol.* **29,** 630–634 (1997).

111. O'Brien, K. D. *et al.* Association of angiotensin-converting enzyme with low-density lipoprotein in aortic valvular lesions and in human plasma. *Circulation* **106,** 2224–2230 (2002).

112. Eva Lonn, M. D. Angiotensin-converting enzyme inhibitors and angiotensin receptor blockers in atherosclerosis. *Curr Atheroscler Rep* **4,** 363–372 (2002).

113. Parolari, A. *et al.* Do statins improve outcomes and delay the progression of non-rheumatic calcific aortic stenosis? *Heart* **97,** 523–529 (2011).

114. Hermans, H. *et al.* Statins for calcific aortic valve stenosis: into oblivion after SALTIRE and SEAS? An extensive review from bench to bedside. *Curr Probl Cardiol* **35,** 284–306 (2010).

115. Chan, K. L. *et al.* Effect of Lipid lowering with rosuvastatin on progression of aortic stenosis: results of the aortic stenosis progression observation: measuring effects of rosuvastatin (ASTRONOMER) trial. *Circulation* **121,** 306–314 (2010).

116. Thanassoulis, G. *et al.* Genetic associations with valvular calcification and aortic stenosis. *N. Engl. J. Med.* **368,** 503–512 (2013).

117. Rajamannan, N. M. & Otto, C. M. Targeted therapy to prevent progression of calcific aortic stenosis. *Circulation* **110,** 1180–1182 (2004).

118. Antonini-Canterin, F. *et al.* Stage-related effect of statin treatment on the progression of aortic valve sclerosis and stenosis. *Am. J. Cardiol.* **102,** 738–742 (2008).

119. Dimitrow, P. P., Jawień, M. & Gackowski, A. The influence of statins on levels of calcification biomarkers in patients with aortic sclerosis or mild aortic

stenosis. *J. Heart Valve Dis.* **20,** 18–22 (2011).

120. Ardehali, R., Leeper, N. J., Wilson, A. M. & Heidenreich, P. A. The effect of angiotensin-converting enzyme inhibitors and statins on the progression of aortic sclerosis and mortality. *J. Heart Valve Dis.* **21,** 337–343 (2012).

Chapter 2

Materials and Methods

2.1 Reagents

2.1.1 Media and chemicals

Advanced Dulbecco's Modified Eagle's Medium (DMEM), alpha Minimum Essential Medium (MEM), Medium 200 (M200), Phosphate buffered saline (PBS), and low serum growth supplement (LSGS) (Life Technologies, Carlsbad, CA). Fetal bovine serum (FBS) (Thermo Scientific, Hudson, NH), penicillin, streptomycin, L-glutamine, amphotericin B, sodium deoxycholate, and glutathione sepharose high performance (Life Technologies, Carlsbad, CA). Type II collagenase, hyaluronidase (Worthington Biochemical Corp., Worthington, VA), Trizol (Invitrogen, Carlsbad, CA), platinum *pfx* DNA polymerase (Applied Biosystems, Carlsbad, CA), and Fast SYBR Green Master Mix (Life Technologies, Carlsbad, CA). Hydrogen peroxide (H_2O_2), methanol, ethanol, xylene, formalin buffered solution, chloridric acid (HCl), sodium hydroxide (NaOH), diethyl pyrocarbonate (DEPC), ascorbic acid, dexamethasone, β-glycerophosphate, Alizarin red S, Hematoxylin and Eosin (H&E), proteinase K, UO126, and pravastatin (Sigma-Aldrich, St. Louis, MO). Fast red (Vector Laboratories, Burlingame, CA), streptavidin-HRP solution, 3,3′-diaminobenzidine (Life Technologies, Carlsbad, CA), Proteoprep Blue Albumin and IgG depletion kit (Sigma-Aldrich, St. Louis, MO), and BCA protein assay (Thermo Scientific, Waltham, MA).

2.1.2 Antibodies and Proteins

Neutralizing antibody anti-osteopontin (NAb OPN), neutralizing antibody anti-vascular endothelial growth factor (NAb VEGF) (R&D systems, Minneapolis, MN), antibody anti-phospho-extracellular signal-related kinase 1/2 (Ab pERK1/2), antibody anti-platelet endothelial cell adhesion molecule (Ab PECAM1), antibody anti-protein kinase B (Ab Akt), and antibody anti-phospho-Akt (Ab pAkt) (Cell Signal, Beverly, MA). Neutralizing antibody anti-αvβ3 (Ab αvβ3) (Millipore, Billerica, MA), Neutralizing antibody anti-cluster of differentiation 44 (CD44) (Ab CD44) (Ancell, Bayport, MN), antibody anti-ERK (Ab ERK), secondary antibody goat anti-rabbit/mouse horseradish peroxidase-conjugated (HRP) (Santa Cruz Biotechnology,

SantaCruz, CA), antibody anti-rabbit Alexa Fluor 488-conjugated, and antibody anti-mouse Alexa Fluor 568-conjugated (Life Technologies, Carlsbad, CA).

Type I collagen (BD Biosciences, Sparks, MD), recombinant bone morphogenetic protein 4 (BMP4), recombinant Noggin (NOG), recombinant VEGF, and recombinant OPN (Peprotech, Rocky Hill, NJ).

2.2 Tissues and Cells

2.2.1 Echocardiography evaluation

A certified echocardiographer evaluated all patients enrolled by M-mode, two-dimensional and Color Doppler echocardiographic assessment. All measurements were performed according to the American Society of echocardiography recommendations. A single cardiologist assessed the aortic valve calcification assigning a calcium score: 1 - no calcification; 2 - mildly calcified (small isolated spots); 3 - moderately calcified (multiple larger spots); 4 - severely calcified (extensive thickening and calcification of all cusps).

2.2.2 Aortic valve collection

Aortic valves from control and aortic sclerosis patients were obtained through collaborations with The Gift of Life Donor Program and the heart transplant research program at the University of Pennsylvania Perelman School of Medicine. Stenotic aortic valves were collected through the University of Pennsylvania Perelman School of Medicine Surgery Department. All patients were enrolled in the protocol #80934 following Institutional Review Board (IRB) approved guidelines. For each patient informed consent was obtained and all the clinical information were collected by patient interview and chart review.

The exclusion criteria used for the study are the following: presence of bicuspid

aortic valve, premature menopause and/or osteoporosis, prior aortic valve surgery, rheumatic heart disease, endocarditis, active malignancy, chronic liver failure, calcium regulation disorders (hyperparathyroidism, hyperthyroidism, and hypothyroidism), serum creatinine ≥ 1.5 mg/dl, and chronic or acute inflammatory states (sepsis, autoimmune disease, and inflammatory bowel disease).

2.2.3 Valve endothelial cell and valve interstitial cell isolation

Aortic valve endothelial and interstitial cells were isolated by mechanical disruption and enzymatic digestion. After the explant the leaflets were placed in complete DMEM containing 10% FBS, 100 U/ml penicillin, 100 μg/ml streptomycin, 4 mM L-glutamine, 1 μg/ml amphotericin B, and 0.82 μg/ml sodium deoxycholate. Within 6 hours the leaflets were washed in 1X PBS, then placed in a tube containing complete DMEM with 2 mg/ml type II collagenase and incubated in a shaker for 20 minutes at 37°C. The valve endothelial cells (VEC) were collected by wiping the leaflet surfaces with sterile cotton swabs and plating them in complete M200. After removing the endothelial layer the specimens were finely minced and place over night at 37°C in a tube containing complete DMEM with 1 mg/ml type II collagenase and 100 U/ml hyaluronidase. The resulting valve interstitial cells (VIC) were seeded in tissue culture plates in complete DMEM and maintained at 37°C and 5% CO_2. All the experiments were performed on cultured cells between the second and sixth passage. All the cells were tested for PECAM1 presence to confirming the purity or absence of endothelial cells.

2.4 Molecular Biology Techniques

2.4.1 RNA isolation

Extraction of RNA was performed using the RNeasy Fibrous tissue kit (QIAGEN, Valencia, CA) homogenizing the entire aortic valve leaflets and Trizol

reagent for cultured cells. RNA concentrations were measured spectrophotometrically at 260 nm with NanoDrop 2000 (Thermo Scientific, Wilmington, DE). Only high quality (absorbance ratio A260/A280 > 1.8) was utilized for two steps PCR amplification or stored at -80°C for further analysis.

2.4.2 Reverse Transcription and Real Time Polymerase Chain Reaction

Reverse transcriptase polymerase chain reaction (RT-PCR) kit (Applied Biosystems, Carlsbad, CA) was used to synthesize the complementary DNA from total RNA samples. PCR was performed using platinum *pfx* DNA polymerase (Applied Biosystems, Carlsbad, CA) to evaluate the presence or absence of CD44 variants. Real Time PCR (qPCR) (Fast SYBR Green Master Mix) was used to calculate the relative expression of genes and dissociation curves were generated after each run to control proper primer behavior. 18S gene expression was used for normalization. The primers used for the analysis are listed in the Appendix A (Table 1).

Complementary DNA was also analyzed with the RT^2 Profiler PCR Array (SABioscience, Valencia, CA) for the detection of the expression of 84 human extracellular matrix and adhesion molecules (Appendix A, Table 2) following the manufacturer's instructions.

2.4.3 Immunohistochemistry

Immunohistochemistry analyses of the aortic valve tissues were perform using standard protocols from the Pathology Laboratory of the University Of Pennsylvania Perelman School of Medicine. The structure of the leaflets was checked by H&E and modified Movat pentachrome staining (dark red – nuclei; dark violet – elastic fiber; yellow – collagen fibers; blue – proteoglycans). Alizarin Red staining was performed to visualize the amount of calcium present on the aortic valves. Histological staining for specific antibody (dilution 1:50 – 1:200) was carried out using standard protocols and paraffin embedded section were stained using the detection kit from DAKO (Glostrup,

Denmark).

2.4.4 Immunofluorescence

Immunofluorescence staining were used to evaluate protein expression in tissues and cells using a standard protocol. The primary antibodies were specific for the interested proteins with a dilution ranging from 1:50 to 1:2000 and the secondary antibody Alexa Fluor dye-conjugated with a dilution of 1:200. Confocal microscope Olympus Fluoview 1000 was used to capture the images and the software ImageJ (National Institute of Health) was use to quantify the staining.

2.4.5 Western blot

Western blot analysis was carried out to assess protein expression using specific primary antibody (dilution 1:500 – 1:200) and secondary antibody HRP-conjugated (dilution 1:5000) following a standard protocol. The autoradiography films were developed with a Kodak M35 X-Omat processor and the images were analyzed using the software ImageJ.

2.4.6 TUNEL assay

Terminal deoxynucleotidyl transferase dUTP nick end labeling (TUNEL) was used to determine apoptotic cells. Paraffin-embedded tissue sections were dewaxed in xylene, and then rehydrated through a graded series of ethanol and distilled water. Sections were then permeabilized by proteinase K treatment and subsequently incubated with TUNEL reaction mixture (Promega, Madison, WI) in a humidified chamber. The blocking was performed in 0.3% H_2O_2 in methanol followed by incubation with streptavidin-HRP solution, 3,3′-diaminobenzidine solution, and HRP-coupled anti-mouse IgG staining. A negative control using all reagents except terminal transferase was performed in parallel. Confocal microscope Olympus Fluoview 1000

was used to capture the images and the software ImageJ was use to quantify the staining.

2.4.7 In situ hybridization

Total OPN and its isoforms mRNA was visualized by *in situ* mRNA hybridization method using probes purchased from Exiqon (Woburn, MA). *In situ* hybridization kit from Biochain (Hayward, CA) was used to perform the detection steps. Paraffin-embedded sections were deparaffinazed by xylene washes and rehydration was obtained through graded ethanol solutions. The sections were fixed with 4% formalin buffered solution in DEPC-PBS and proteinase K (10 μg/ml) was used for the permeabilization of the tissue sections. After several washes with DEPC-PBS the sections were incubated with pre-hybridization solution and then hybridize with hybridization solution + digoxigenin labeled probe (5 μg/ml). For the detection AP-conjugates anti-digoxigenin antibodies were used and the developing solution (NTB and CIP into Alkaline Phosphatase Buffer) allowed us to visualize were the probes hybridized with the targeted mRNA sequence. Fast red counterstaining was used to visualize the nuclei.

2.4.8 ELISA assay

Blood samples were collected from the subjects before they underwent surgical intervention and plasma was separated through centrifugation. Plasma analyses were carried out using ELISA method kit to evaluate OPN (R&D, Minneapolis, MN), Fetuin A (Biovendor Research & Diagnostic Products, Chandlier, NC), NT-proBNP (Phoenix Pharmaceuticals, Burlingame, CA), Parathyroid hormone (IBL America, Minneapolis, MN), ADMA (ALPCO Diagnostics, Salem, NH). Estimation of tissue OPN was carried out using ELISA kit purchased from Biovendor LLC (Candler, NC). The manufacturer's protocols were followed to process and analyze the samples, absorbance was measured using the ELx 808 Ultra Micro plate reader (Bio Tek Instruments Inc.,

USA) and the concentrations were calculated using the 4-parameter logarithm using the KC Junior software (Bio Tek Instruments Inc., Winooski, VT).

2.4.9 In Situ Proximity Ligation Assay

In situ proximity ligation assay (PLA) kit was purchased from Olink Bioscience (Uppsala, Sweeden). The assay was performed following manufacturer instructions. Briefly, cells were grown on glass coverslips until ≈80% confluence, then were treated with 100 ng/ml BMP4 in presence or absence of 5 ng/ml neutralizing antibody anti CD44 (NAb CD44). At the end of the treatments the cells were fixed with cold methanol. The cells were then incubated with isoform-specific antibodies anti CD44 together with antibody anti OPN overnight at 4°C with gentle agitation. After primary antibody incubation cells were rinse and PLUS / MINUS secondary PLA probes against rabbit and mouse IgG were added and incubated at 37°C for 1 hour with gentle agitation. In the end of the incubation with secondary antibodies cells were incubated with ligation mixture for 30 minutes at 37°C, following amplification mixture was applied for 100 minutes at 37°C. Finally, coverslips were mounted on microscope slides with Doulink Mounting Medium and the cells were photographed and analyzed using confocal microscope Olympus Fluoview 1000 and the software ImageJ.

2.5 Tensile Stretch Bioreactor

2.5.1 Bioreactor design and tissue preparation

Two chambers and one moving piston compose the bioreactor; each chamber has 8 media baths and each bath has one stationary pin press-fit into the bottom for tissue anchorage. The moving arm is connected to the other pin and to the central motorized piston.

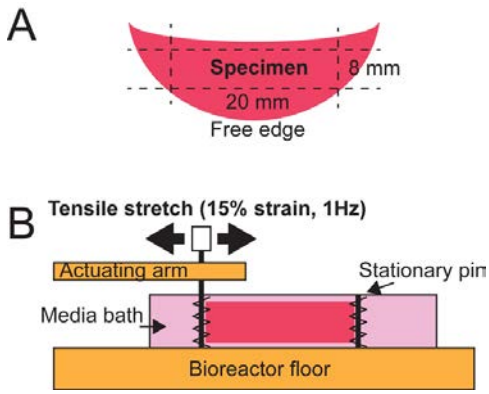

Figure 2.1. Tensile stretch bioreactor design.

(A) Preparation of leaflet tissue strips. (B) Configuration of testing sample in tension bioreactor.

Adapted from: Poggio, P. *et al.* Noggin attenuates the osteogenic activation of human valve interstitial cells in aortic valve sclerosis. *Cardiovasc. Res.* **98,** 402–410 (2013).

The aortic valve leaflets were collected in the operating room and place immediately in complete DMEM. Each leaflet was trimmed to form a strip, measuring 20 mm circumferentially and 8 mm radially. The endothelial layer was preserve limiting the tissue handling to the edges. Two springs were threaded at the short extremities of each tissue strip and then inserted in the tension bioreactor. The experiments had duration of 6 days and 5 ml of osteogenic media (OS) (DMEM/F12 containing 10% FBS, 100 U/ml penicillin, 100 μg/ml streptomycin, 4 mM L-glutamine, 1 μg/ml amphotericin B, and 0.82 μg/ml sodium deoxycholate, 284 mM ascorbic acid, 10 nm Dexamethasone, and 10 mM β-glycerophosphate) ± BMP4 (100 ng/ml) ± NOG (500 ng/ml) were added fresh every 3 days. As internal control we used leaflet place in the bioreactor but without activating the motorized piston. At the end of the experiment the tissues strips were removed and divided in two pieces, one embedded in OCT for preparing frozen sections and the other for RNA isolation.

2.5.1 Aortic valve tissue engineering

Porcine Aortic valve leaflets were a gift from the Gorman Cardiovascular Research Group at University of Pennsylvania. The leaflets were collected in saline

solution for transportation and treated with antibiotic (10 KU/ml penicillin and 10 mg/ml streptomycin) for 48 hours for sterilization. Decellularization of the leaflets was carried put by incubation with 0.25% trypsin for 24 hours at 37°C. The decellularized porcine scaffold were then seeded with VICs isolated from aortic sclerosis patients at a density of 500,000 cells/cm2 and grown for 3 days, then flipped and seeding was repeated on the other side of the leaflets. The final recellularized leaflets were then used in static and dynamic conditions in the tension bioreactor as described for the human aortic valves.

2.6 *In vitro* assays

2.6.1 Calcification assay

The ability to form hydroxyapatite crystal was tested in smooth muscle cells (SMC) and VIC derived from control, sclerotic and stenotic aortic valves. Cells were plated and grown in complete DMEM until they reached ~80% confluency. During the calcification assay the cells were cultured in complete alpha MEM supplemented with 3 mM phosphate buffer and the media was replaced every other day. At the endpoint the cells were washed briefly in 1X PBS and incubated overnight in 0.6 M HCL at 4°C. Calcium levels were estimated with a colorimetric assay using ELx 808 Ultra Micro plate reader with a absorbance wavelength at 575 nm. Normalization of total calcium content was carried out harvesting the cells in 1 M NaOH and estimating the total proteins with the BCA protein assay. Final amount of calcium was expressed as mg of calcium over mg of total proteins. Moreover, pictures of each well at different time points were taken using an inverted microscope (Hitech Instruments, Inc., Broomall, CA).

2.6.3 Wound healing assay

Migration ability was tested on human umbilical vein endothelial cells (HUVEC) in complete M200 with 10% LSGS in combination with different proteins

and molecules. A wound was created in confluent plates by using a sterile 200 ml tip and the complete M200 was replaced with M200 containing low FBS (0.5%). Wound closure was monitored in the presence or absence of 50 ng/ml OPN, 50 ng/ml (p)OPN, Neutralizing 10 mg/ml Ab anti-αvβ3, 10 mg/ml NAb anti-CD44 or 10 nM UO126. After wounding, cell migration was estimated by image analysis using an inverted Olympus CK2 microscope and the wound closure was determined, with ImageJ analysis, as the difference between the wound width at 0 and 24 hours.

2.6.4 Angiogenesis assay

The ability to form new vessel was tested on excised human aortic valve in a 3 dimensional (3D) collagen structure under 30 ng/ml VEGF, 50 ng/ml OPN, 50 ng/ml (p)OPN, 10 mM UO126, 10 mg/ml NAb CD44, 10 mg/ml NAb αvβ3, 10 mg/ml NAb OPN, or 10 mg/ml NAb VEGF. Type I collagen was suspended in DMEM and 0.01 mM NaOH and the resulting solution was titrated with 0.1 M NaOH to pH 7.4. The excised tissues (1 mm^2) were embedded in type I collagen solution and allowed to polymerize in an incubator at 37°C. Complete M200 was added after the complete collagen polymerization, the media was changed every other day and photos were taken with an inverted microscope every 3 days until the end of the experiments.

2.7 Osteopontin preparation and analysis

2.7.1 Recombinant osteopontin preparation

Three vector pDEST490 containing the OPN isoforms a, b and c were purchased from Addgene (Cambridge, MA). The open reading frame coding for OPN isoforms was excised from the pDEST490 vectors using restriction enzymes (BamHI and SmaI, Cell Signal, Beverly, MA) and ligated into the pGEX-5x-2 vector (GE healthcare; Piscataway, NJ). The pGEX vector was chosen because contain the FLAG tag and the Glutathione *S*-transferase (GST) tag. The pGEx vectors were transformed into

BL21(DE3) competent E. Coli (Life Technologies, Carlsbad, CA) to express large amount of OPN isoform. Using the GST tag the OPN isoforms were purified with glutathione sepharose following the manufacturer's instructions.

2.7.2 Circulating osteopontin purification

Purification of osteopontin from plasma samples was achieved by a two-step purification protocol. The first step was the removal of the large amount of human serum albumin (HAS) and the major subclasses of gamma globulin (IgG) from the plasma. The Proteoprep Blue Albumin and IgG depletion kit was used twice on each plasma sample. After HSA/IgG removal, plasma samples were incubated with Ab OPN and then incubated with protein A agarose beads to immunoprecipitate the protein of interest. Purchased recombinant OPN and non immune-IgG were used as controls.

2.8 Statistical analysis

The statistical analysis was performed using the SPSS 21 and Prism 6 software. Continuous variables were expressed as mean ± standard deviation or mean ± standard error of mean. Pearson chi-square and t test was used to evaluate categorical variables and Mann Whitney test was used for continuous variables. Comparisons between more than two groups were performed using ANOVA test and Kruskal-Wallis test. A value of $p < 0.05$ was considered to be statistically significant.

Chapter 3

Osteopontin Levels Correlate With The Progression Of Calcific Aortic Valve Disease

Part of this chapter has been published as[1,2]:

Paolo Poggio*, Juan B. Grau*, Rachana Sainger, William J. Vernick, William F. Seefried, Emanuela Branchetti, Benjamin C. Field, Joseph E. Bavaria, Michael A. Acker, and Giovanni Ferrari. Analysis of Osteopontin levels for the identification of asymptomatic patients with calcific aortic valve disease. *The Annals of Thoracic Surgery* **93**, 79–86 (2012). * These authors contributed equally to this work.

Rachana Sainger, Juan B. Grau, **Paolo Poggio**, Emanuela Branchetti, Joseph E. Bavaria, Joseph H. Gorman III, Robert C. Gorman, and Giovanni Ferrari. Dephosphorylation of circulation human Osteopontin correlates with severe valvular calcification in patients with calcific aortic valve disease. *Biomarkers* **17**, 111–118 (2012).

3.1 Introduction

Aortic valve sclerosis (AVSc) is related to thickening of the aortic leaflets without obstruction of the left ventricular outflow. However, the presence of AVSc has been associated with a higher risk of cardiovascular events, including increased mortality[3-5]. Therefore, identifying asymptomatic patients that express markers associated with calcification will allow us to label them as at high risk to have a rapid evolution of calcific aortic valve disease (CAVD). In addition, the identification of high-risk patients at early stages of degeneration will open new perspectives for the appropriate timing of therapeutic intervention on future clinical trials.

Osteopontin (OPN) is a multifunctional glycol-phospho-protein that is known for its regulatory function in bone remodeling. OPN is involved in a myriad of processes, including inflammation and in the inhibition of biomineralization of dystrophic and ectopic sites[6]. OPN, also named secreted phosphoprotein-1 (SPP1), is encoded by the *SPP1* gene, which is transcribed into three splicing variants, OPN-a, -b, and -c. The presence of a fourth splicing variant, called OPN-d, has recently been reported, however no details have been provided yet, and therefore it was not included in this study[7]. OPN-a encodes the full-length protein, whereas isoforms b and c result from alternative splicing[7]. The 5' canonical translation start codon generates a protein that includes an N-terminal signal sequence that diverts it to the secretory vesicles, whereas a downstream start codon generates a shorter protein that localizes to the cytoplasm.

It has been previously reported that circulating OPN levels are elevated in aortic valve stenosis (AVS) patients when compared to healthy controls[6]. Since the biological function of OPN is to regulate calcium deposition[8], it has been proposed that the increasing levels of OPN in diseased tissue reflects a compensatory mechanism linked to loss of function due to transcriptional / post-translational changes or protein-protein interactions. We hypothesized that plasma and tissue OPN levels were elevated in AVSc patients, before signs of aortic valve calcification and before aortic valve area changes. We evaluated the expression of tissue and plasma OPN levels in control, AVSc and AVS patients. Furthermore, we analyzed the OPN isoforms differential

expression and OPN post-translational modifications. By correlating OPN levels and progression of CAVD we aimed to provide a novel tool for the identification of asymptomatic patients.

3.2 Results

3.2.1 Baseline patient characteristic

The analysis was carried out with 56 controls, 50 AVSc and 51 AVS patients. Controls and AVSc patients had no significant difference in age, while AVS patients were significantly older. All the clinical details regarding the patient population used for this part of the study are summarized in Table 3.1.

Table 3.1 Patient demographics and Clinical details.

Demographics	Controls N-56	Aortic sclerosis N=50	Aortic stenosis N=51
Age (in years)	62.8 ± 2.2	64.6 ± 1.4	76.16 ± 8.26
Male	29 (51.7%)	30 (60.0%)	29 (56.9%)
Smokers	19 (33.9%)	20 (40.0%)	20 (39.2%)
Diabetes	15 (26.8%)	09 (18.0%)	15 (29.4%)
Hypertension	39 (69.6%)	23 (46.0%)	38 (74.5%)
Cerebral Vascular Accident	1 (1.6%))	1 (1.96%)	01 (2.0%)
Peripheral vascular disease	4 (7.1%)	4 (7.8%)	04 (8.0%)
Hyperlipidemia	29 (51.8%)	16 (31.4%)	28 (54.9%)
Coronary artery disease	17 (35.6%)	15 (29.4%)	17 (29.4%)

Adapted from[1]: Grau, J. B. *et al.* Analysis of osteopontin levels for the identification of asymptomatic patients with calcific aortic valve disease. *Ann. Thorac. Surg.* **93,** 79–86 (2012).

3.2.2 Tissue osteopontin levels correlate with the progression of calcific aortic valve disease

We analyzed the expression level of OPN in the tissue of patients with AVSc and AVS compared to healthy controls. The tissue histology analysis confirmed the thickening of the aortic leaflets in the pathological stages and the presence of calcification only in AVS patients (Figure 3.1A). We notice that OPN expression increased from control to aortic sclerosis to aortic stenosis (Figure 3.1A). Notably, the highest levels of OPN were noted surrounding the areas of highest calcification, on the aortic side of the leaflets. To evaluate the correlation between early stages of valve degeneration with increasing OPN levels, we performed qPCR and Elisa analyses on the tissue of our three cohorts of patients (Figure 3.1B). We were able to confirm the correlation between the pathological stages of CAVD and the levels of OPN.

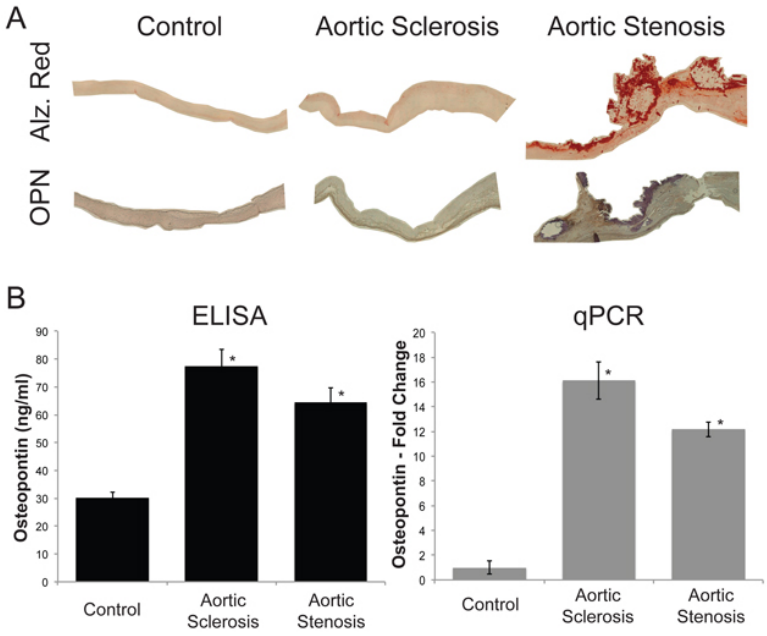

Figure 3.1. Osteopontin levels correlate with the progression of calcific aortic valve disease.

(A) Longitudinal sections of human aortic valve leaflet stained with alizarin red (Alz. Red) and immunostaining for OPN (10x magnification). (B) Bar graphs representing quantification of osteopontin analyzed by ELISA and qPCR. For qPCR analysis, OPN levels were normalized against the control level. * $p < 0.05$. Adapted from[1]: Grau, J. B. *et al.* Analysis of osteopontin levels for the identification of asymptomatic patients with calcific aortic valve disease. *Ann. Thorac. Surg.* **93,** 79–86 (2012).

3.2.3 Plasma osteopontin levels correlate with the progression of calcific aortic valve disease

Patients with signs of AVSc are at higher risk of developing AVS and other cardiovascular complications[3-5]. Thus, there is the necessity to identify a series of molecular markers able to label asymptomatic patients before the disease proceed to the final stage. We therefore analyzed the OPN levels in the blood of our cohorts of patients in correlation with the presence or absence of signs of biomineralization detectable with Transesophageal echocardiography (TEE) reading. A calcium score was assigned to each patient on a scale of 1 to 4 based on the method described by Rosenhek *et al.*[9], where 1 is absence of calcium, 2, 3 and 4 correspond to mild, moderate and severe calcification, respectively (Chapter 2). OPN levels correlated with the presence of calcium deposition on the aortic leaflets (Figure 3.2A). Interestingly, all the patients evaluated with calcium score 3 or 4 had non-functional valves and were classified as having AVS. Patients with mild calcification were classified as having AVSc due to the normal function of the aortic valve measured by peak velocity and aortic valve area. It is important to note that the group labeled with calcium score 1 included both the controls and the AVSc patients with no calcium appearance. This group is of the most importance since it generates the question if OPN levels in AVSc patients, with no signs of biomineralization, were higher then in the control group. We therefore conducted a comparative analysis between five groups: controls with calcium score 1, AVSc with calcium score 1 and 2, and AVS with calcium score 3 and 4. Remarkably, OPN levels were elevated in asymptomatic AVSc patients with no appearance of calcification detected during TEE evaluation (Figure 3.2B). These results suggest that OPN could be used as an early marker of CAVD, since its circulating and tissue levels are elevated in AVSc asymptomatic patient even before signs of biomineralization are detectable by TEE reading.

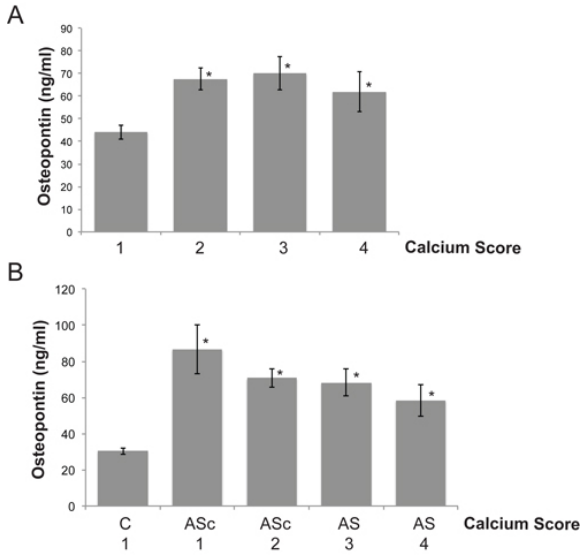

Figure 3.2. Comparison between echocardiographic evaluation and osteopontin levels in patients with calcific aortic valve disease.

(A) Bar graph representing absolute OPN levels, measured by ELISA, in the plasma of patients with different calcium scores. (B) Bar graph representing absolute OPN levels, measured by ELISA, in the plasma of control group (calcium score 1) and patients (calcium score 1 to 4). (C = control; ASc = aortic sclerosis; AS = aortic stenosis). * $p < 0.05$. Adapted from[1]: Grau, J. B. *et al.* Analysis of osteopontin levels for the identification of asymptomatic patients with calcific aortic valve disease. *Ann. Thorac. Surg.* **93,** 79–86 (2012).

3.2.4 Differential expression of osteopontin splicing variant in calcific aortic valve disease

In the attempt to better characterize OPN as a biomarker for the early stage of CAVD, we investigated the OPN splicing variants in the aortic valve tissue (Figure 3.3A). We therefore analyzed by qPCR the differential expression of OPN splicing variants in the controls, the AVSc, and the AVS patients. OPN splicing variants -a, -b and -c were overexpressed in the pathological stages (both AVSc and AVS). Interestingly, the expression profiles of the three isoforms were different in AVSc compared to AVS: OPN-a was increased significantly only at early stages of the disease; OPN-b was increased progressively from AVSc to AVS; while OPN-c labeled

both of the pathological stages. Due to the overall small group of patients, we cannot conclude that the splicing variants profile could be use a biomarker itself, however the analysis prompts us to further investigate the tissue localization and biological function of the OPN splicing variants. OPN-a, -b, and -c *in situ* hybridization experiments with specific probes for the isoforms confirm increasing levels of OPN mRNAs in the aortic valve tissue of control, AVSc and AVS. These results show a differential pattern expression of OPN splicing variants in human CAVD tissues.

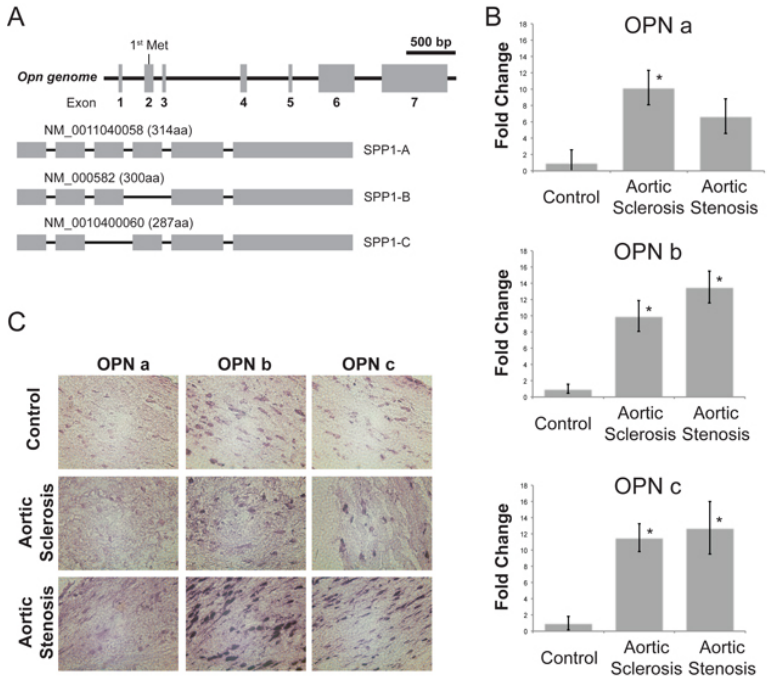

Figure 3.3. Differential expression of osteopontin splicing variant in calcific aortic valve disease.

(A) Graphic representation of OPN splicing variants. (B) Relative quantification of OPN-a, OPN-b, OPN-c by qPCR. * $p < 0.05$. (C) Tissue distribution of OPN isoforms detected by *in situ* hybridization (100x magnification). Adapted from[1]: Grau, J. B. *et al.* Analysis of osteopontin levels for the identification of asymptomatic patients with calcific aortic valve disease. *Ann. Thorac. Surg.* **93,** 79–86 (2012).

3.2.5 Purification of osteopontin from human plasma

To better characterize the circulating OPN, we decided to purify the OPN from control and end stage patient blood for consecutive post-translational modification analysis. Because of large excess of human serum albumin (HSA) and other proteins in plasma, OPN analysis were carried out implementing immunoprecipitation techniques and subsequent evaluation by Western blot (Figure 3.4A). We performed two-step purification: the first step removed HSA and IgG; the second step was the immunoprecipitation of OPN. The purified protein was eluted from the beads in different fractions using acid elution buffer (Figure 3.4B). The same purification protocol was used for plasma derived from controls and AVS patients (Figure 3.4C). Western blot analysis of purified OPN reviled two bands from plasma of AVS patients. This different pattern could be explained by a differential post-translational modification of the protein in AVS patients.

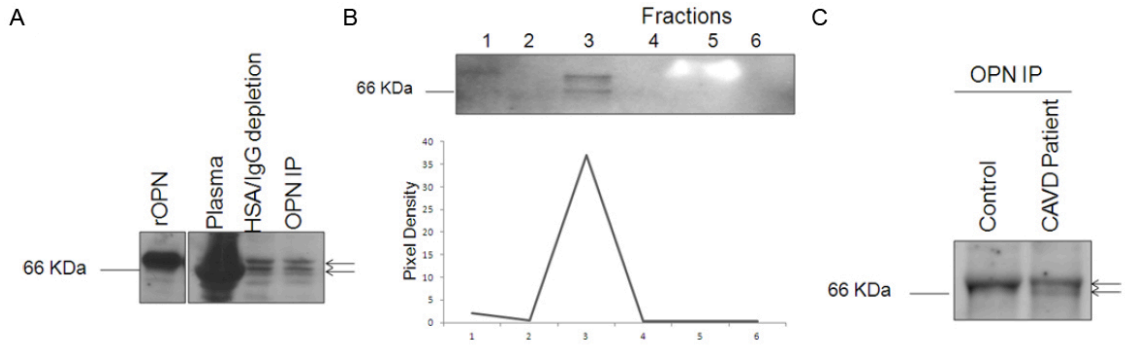

Figure 3.4 Circulating OPN purification.

(A) Representative pattern for osteopontin purification from CAVD patients and healthy controls. 50 ng of recombinant OPN was used as a positive control (Lane 1). Total plasma (Lane 2) was depleted of HSA and IgG using ProteoSeek Albumin/IgG Removal Kit (Lane 3) and then used for OPN Immunoprecipitation with a specific OPN antibody (Lane 4). (E) Western blot showing different fractions collected during sample elution. (F) Western blot of purified OPN from CAVD patients and controls. Arrows indicates double bands. Adapted from[2]: Sainger, R. *et al.* Dephosphorylation of circulating human osteopontin correlates with severe valvular calcification in patients with calcific aortic valve disease. *Biomarkers* **17,** 111–118 (2012).

3.2.6 Phosphorylated osteopontin labels healthy controls

Since we noticed a different pattern in the Western blot analysis from AVS compared to controls, we decided to investigate the phosphorylation status of OPN. We evaluated the possible phosphorylation sites using Netphos 2.0 Software, which predicted 34 serine, 2 threonine and 2 tyrosine on the OPN sequence (Figure 3.5A). Currently there are no specific antibodies that recognize the phosphorylation sites of OPN. We evaluate OPN post-translational modification by Western blot using antibodies anti phospho-serine, -threonine and -tyrosine on the immunoprecipitated OPN. Circulating OPN from controls was phosphorylated in serine, threonine and tyrosine, while OPN purified from AVS patients showed a lack of phosphorylation in tyrosine (Figure 3.5B and C). Serine and threonine phosphorylation levels where comparable between the two groups.

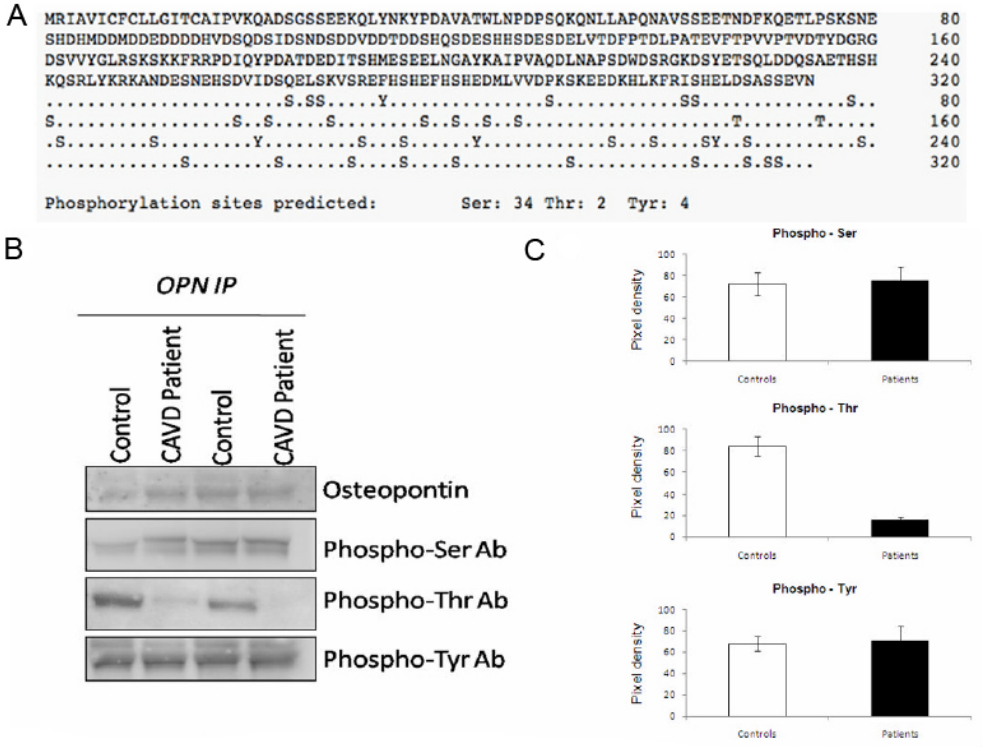

Figure 3.5. Differential post-translational modification of human circulating osteopontin from controls and calcific aortic valve disease patients.

(A) Analysis of osteopontin protein using NetPhos 2.0 Server to predict serine, threonine and tyrosine phosphorylation sites. (B) Representative Western blots of phospho-serine, phospho-tyrosine and phospho-threonine on purified OPN from controls and CAVD patients. (B) Densitometry of Western

blots of phospho-serine, phospho-tyrosine and phospho-threonine on purified OPN from controls and CAVD patients. Adapted from[2]: Sainger, R. *et al.* Dephosphorylation of circulating human osteopontin correlates with severe valvular calcification in patients with calcific aortic valve disease. *Biomarkers* **17,** 111–118 (2012).

3.3 Discussion

The presence of AVSc has been suggested as a marker of increased cardiovascular risk[10]. Based on this hypothesis, the presence of AVSc may prompt clinicians towards more aggressive prevention strategies, although this approach has not been tested in a larger prospective clinical trial. In this chapter it is presented a translational, interdisciplinary research study aimed to correlate echocardiographic evaluation with the differential expression of OPN levels for the identification of patients with asymptomatic AVSc. Overall our experiments provided several novel messages for the identification of asymptomatic patients with CAVD: patients with AVS and AVSc had higher OPN levels compared with controls. OPN level was elevated in asymptomatic AVSc patients with no appearance of calcification (bright echoes) during TEE evaluation. Moreover, OPN splicing variants -a, -b, and -c were differentially expressed during CAVD progression. Interestingly, plasma OPN isolated from AVS patients was characterized by a loss of phosphorylation in tyrosine, suggesting that not only the levels could be associated with the progression of CAVD.

As a future clinical implication, the analysis of the differential expression of OPN splicing variants during CAVD may help in developing diagnostic strategies to follow the progression of asymptomatic aortic valve degeneration. A molecular tool for the early detection of AVSc patients could therefore implement the choice of the ideal timing for therapeutic intervention either using statins or other drugs.

3.4 References

1. Grau, J. B. *et al.* Analysis of osteopontin levels for the identification of asymptomatic patients with calcific aortic valve disease. *Ann. Thorac. Surg.* **93,** 79–86 (2012).

2. Sainger, R. *et al.* Dephosphorylation of circulating human osteopontin correlates with severe valvular calcification in patients with calcific aortic valve disease. *Biomarkers* **17,** 111–118 (2012).

3. Cosmi, J. E. *et al.* The risk of the development of aortic stenosis in patients with 'benign' aortic valve thickening. *Arch Intern Med* **162,** 2345–2347 (2002).

4. Faggiano, P. *et al.* Progression of aortic valve sclerosis to aortic stenosis. *Am. J. Cardiol.* **91,** 99–101 (2003).

5. Roger, V. L. *et al.* Heart disease and stroke statistics--2012 update: a report from the American Heart Association. *Circulation* **125,** e2–e220 (2012).

6. Yu, P.-J. *et al.* Correlation between plasma osteopontin levels and aortic valve calcification: potential insights into the pathogenesis of aortic valve calcification and stenosis. *J. Thorac. Cardiovasc. Surg.* **138,** 196–199 (2009).

7. Ivanov, S. V. *et al.* Tumorigenic properties of alternative osteopontin isoforms in mesothelioma. *Biochem. Biophys. Res. Commun.* **382,** 514–518 (2009).

8. Steitz, S. A. *et al.* Osteopontin inhibits mineral deposition and promotes regression of ectopic calcification. *Am. J. Pathol.* **161,** 2035–2046 (2002).

9. Rosenhek, R. *et al.* Predictors of outcome in severe, asymptomatic aortic stenosis. *N. Engl. J. Med.* **343,** 611–617 (2000).

10. Gharacholou, S. M., Karon, B. L., Shub, C. & Pellikka, P. A. Aortic valve sclerosis and clinical outcomes: moving toward a definition. *Am. J. Med.* **124,** 103–110 (2011).

Chapter 4

Role Of Osteopontin In Endothelial Cell Migration

Part of this chapter has been published as[1]:

Paolo Poggio, Juan B. Grau, Benjamin C. Field, Rachana Sainger, William F. Seefried, Flavio Rizzolio, and Giovanni Ferrari. Osteopontin controls endothelial cell migration *in vitro* and in excised human valve tissue from patients with calcific aortic stenosis and controls. *Journal of Cellular Physiology* **226**, 2139–2149 (2011).

4.1 Introduction

Degenerative lesions in human valves are characterized by endothelial cell (EC) disruption, increased cellularity and extracellular matrix deposition, accumulation of oxidized lipoproteins, non-foam cell and foam cell macrophages, and occasional T cells within the valve interstitium[2,3]. These histological findings resemble early sclerotic lesions of the vasculature, and together with the shared risk factors, suggest that, as in atherosclerosis, the initiation of aortic valve sclerosis involves chronic inflammatory and neo-angiogenesis processes potentiated by systemic factors.

Multiple biologic pathways are responsible for aortic valve degeneration. EC activation and neo-vascularization of the leaflets characterize the valve degeneration process since the aortic sclerosis phase. Pro-angiogenic factors are still detectable in the valve tissue when leaflet motion is impaired by calcium deposition[4]. The angiogenic process starts concomitantly with EC disruption, inflammation and lipid deposition[5]. Therefore, in the pathogenesis of calcific aortic valve disease (CAVD), injury to the endothelium is an important initial step causing thickening of the valve as a consequence of abnormal deposition of extracellular matrix, and thus preventing oxygen supply by diffusion. Decreased oxygen tension is a strong initiator of the angiogenic response through the induction of vascular endothelial growth factor (VEGF) gene expression[6,7]. The over-expression of VEGF receptors, Flk-1 and Flt-1, also increase with tissue hypoxia further supporting the importance of angiogenesis in the initiation and progression of CAVD. The endothelium lining the surface of valve leaflets is presumed to be involved in valve homeostasis and pathology. AVS leaflets show a stronger angiogenic response than control valve leaflets[4,8-10].

In this chapter, it is analyzed the role of osteopontin (OPN) in the regulation of EC activation *in vitro* and its role on excised tissues from AVS patients and controls. Studying the process of EC activation could bring to light important insights in the molecular mechanisms that drive the process of valve degeneration and help in the development of a therapeutic target before the calcification process occurs and surgical intervention becomes inevitable.

4.2 Results

4.2.1 Baseline patients characteristics

On the total of 7 subjects, 43% were male. Their age was 61.3 ± 21.7 years. For the patients with AVS, the initial AVA was 0.8 ± 0.2, two had systemic hypertension, three had significant coronary artery disease and one was a current smoker. All patients had a comprehensive echocardiographic assessment including, M-mode, two-dimensional and color Doppler echocardiography. Table 4.1 further characterizes the study groups. Aortic valve calcification score was 3.5 ± 0.59 in AVS patients and 1.3 ± 0.49 in controls ($p < 0.001$).

Table 4.1. Patient demographics and Clinical details.

Demographics	**Controls N=4**	**Aortic sclerosis N=3**
Age (years)	48 ± 16	78.7 ± 14.8
Male	1 (25.0%)	2 (66.7%)
Smokers	0 (0.0%)	1 (33.3%)
Hypertension	1 (25.0%)	2 (66.7%)
Diabetes Mellitus	0 (0.0%)	0 (0.0%)
Coronary Artery Disease	0 (0.0%)	3 (100.0%)
Hyperlipidemia	1 (33.3 %)	0 (0.0%)

Adapted from[11]: Poggio, P. *et al.* Osteopontin controls endothelial cell migration in vitro and in excised human valvular tissue from patients with calcific aortic stenosis and controls. *J. Cell. Physiol.* **226,** 2139–2149 (2011).

4.2.2 Osteopontin promotes endothelial cell migration

Since the endothelium is one of the primary targets during valve degeneration, we decided to characterize the EC response and to analyze the intracellular signaling pathway activated by *in vitro* OPN treatments. For the experiments we used human umbilical vein endothelial cells (HUVEC) due to the similarity to valve endothelial cells (VEC), in particular because the difficulty to obtain a homogeneous culture of VECs.

To test the effect that OPN has on ECs, we implemented wound healing assays. After the confluent layer of ECs was scratch with a pipet tip to create the wound OPN was added to the media and plates were incubated at 37C. Differences in EC migration could be observed after 4 hours of treatment (not shown) and were evident after 24 hours of treatment (Figure 4.1). As positive control 10% FBS was added to the media. These experiments confirmed that OPN had an active role in promoting EC migration *in vitro*.

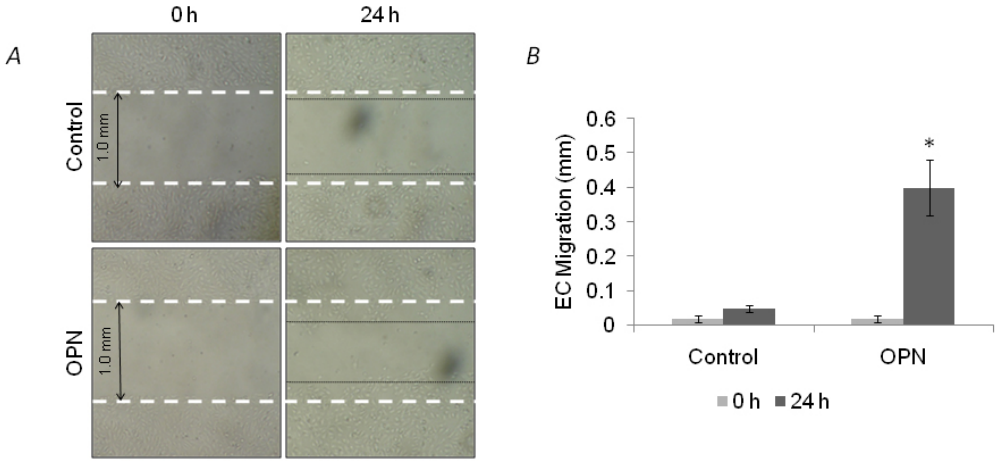

Figure 4.1. OPN induces in vitro endothelial cell migration.

(A) Wound healing assay of confluent HUVECs in the presence or absence of recombinant OPN (50 ng/ml) analyzed after 24 hours. Magnification 4x. (B) Bar graph representation of endothelial cell migration. * $p < 0.01$. Adapted from[11]: Poggio, P. *et al.* Osteopontin controls endothelial cell migration in vitro and in excised human valvular tissue from patients with calcific aortic stenosis and controls. *J. Cell. Physiol.* **226,** 2139–2149 (2011).

4.2.3 Endothelial cell migration induced by OPN require Erk1/2 phosphorylation

It has been reported that the positive effect of OPN on neovascularization is mediated by PI3K–Erk1/2 intracellular signaling pathway *in vivo*[12]. To test the intracellular signaling pathway that mediates EC migration, we first analyzed the MAPK activation in the presence or absence of recombinant OPN. The MAPK profile array shows significant phosphorylation of Erk1/2 (Figure 4.2A). To confirm this result, ECs were treated for 5', 15' 30', and 60' with recombinant OPN and then analyzed by Western blot with phospho-specific Erk1/2 antibodies (Figure 4.2B). Since this experiment show the activation of Erk1/2 intracellular signaling after OPN treatment, we used a common Erk1/2 chemical inhibitor (UO126) to test if Erk1/2 mediated EC migration *in vitro*. The analysis of wound closure after 24 hours of OPN treatment in presence of UO126 showed the abolishment of EC migration (Figure 4.2C and D).

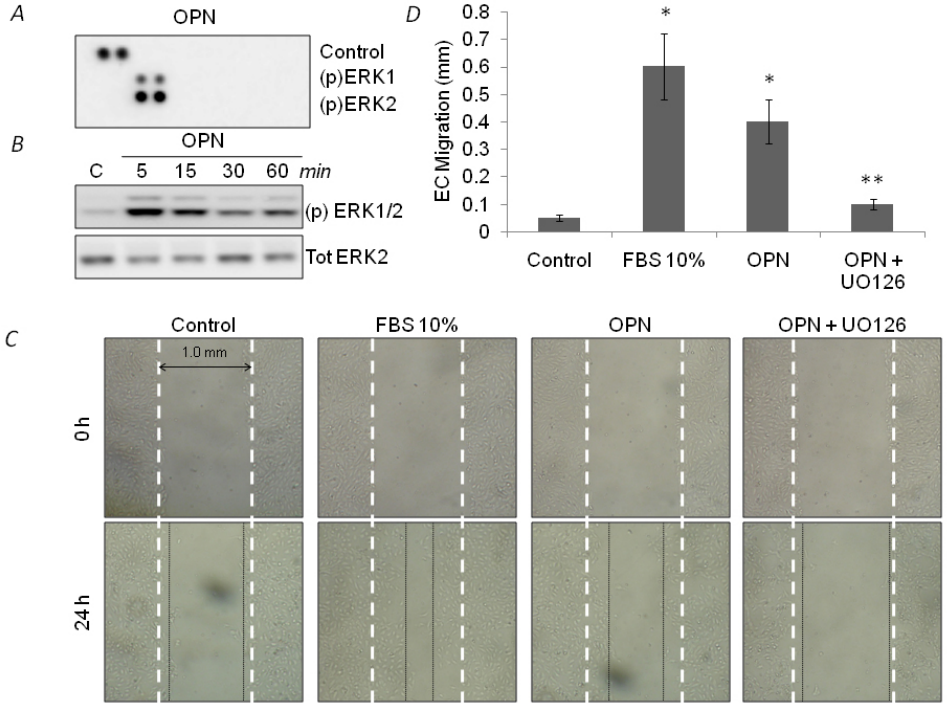

Figure 4.2. OPN promotes *in vitro* endothelial cell migration through Erk1/2 phosphorylation.

(A) Phospho-MAP kinase profile array of HUVECs treated with recombinant OPN (50 ng/ml) showing (p)ERK 1/2 activation. (B) Western blot for (p)ERK 1/2 of OPN-treated HUVECs. Tot ERK2 was used

to normalize the results and as a loading control. (C) Wound healing assay of confluent HUVECs treated with FBS10% as a positive control, and OPN (50 ng/ml) in the presence or absence of ERK1/2 chemical inhibitor UO126 (10 mM). Endothelial cell migration was photographed after 24 h at 4x magnification. (D) Bar graph representation of endothelial cell migration. * $p < 0.01$ and ** $p < 0.01$ *vs.* OPN treated. Adapted from[11]: Poggio, P. *et al.* Osteopontin controls endothelial cell migration in vitro and in excised human valvular tissue from patients with calcific aortic stenosis and controls. *J. Cell. Physiol.* **226,** 2139–2149 (2011).

4.2.4 OPN biological activity is controlled by its phosphorylation status in endothelial cells

To further characterize the role of OPN on the regulation of EC migration, we considered the effects of OPN post-translational modifications. Recombinant OPN was phosphorylated *in vitro* using casein kinase II (CKII) (Figure 4.3A).

We treated EC for 24 hours and analyze wound healing in presence or absence of phosphorylated OPN and non-phosphorylated OPN. The results of this experiment demonstrated that phospho-OPN did not activate EC migration *in vitro*, whereas, dephosphorylated OPN promoted EC migration (Figure 4.3B and C).

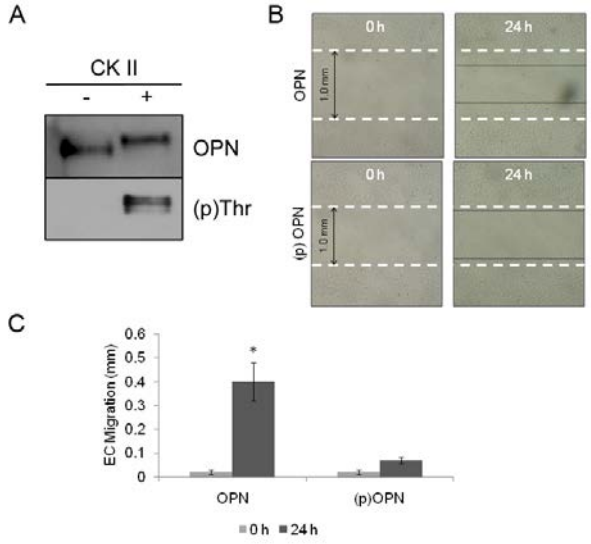

Figure 4.3. OPN phosphorylation status controls *in vitro* endothelial cell migration.

(A) Representative Western blot for OPN and phospho-threonine in the phosphorylated and non-phosphorylated OPN recombinant used for the in vitro analysis. (B) Wound healing assay of confluent HUVECs in the presence or absence of recombinant OPN (50 ng/ml) or phosphorylated OPN (50 ng/ml) analyzed after 24 h. Magnification 4x. (B) Bar graph representation of endothelial cell migration. * $p < 0.01$. Adapted from[11]: Poggio, P. *et al.* Osteopontin controls endothelial cell migration in vitro and in excised human valvular tissue from patients with calcific aortic stenosis and controls. *J. Cell. Physiol.* **226,** 2139–2149 (2011).

4.2.5 Osteopontin, CD44 and αVβ3 interaction is essential for endothelial cell migration

The primary receptors for OPN are those integrins that bind the central integrins attachment motif RGD. Since no specific OPN receptors have been identified so far, integrin αVβ3 was established as a primary receptor for OPN. In addition to the integrin binding, OPN also binds with a hyaluronic acid receptor, CD44 in an RGD-independent manner[13,14].

Since both CD44 and αVβ3 can mediate the biologic activities of OPN, we first analyzed the role of OPN on Erk1/2 activation in ECs in the presence or absence of neutralizing antibodies anti CD44 and αVβ3. We demonstrated that both neutralizing antibodies (CD44 and αVβ3) blocked Erk1/2 phosphorylation induced by OPN or phospho-OPN (Figure 4.4A). Then, we characterized the biological effects of these two neutralizing antibodies on EC migration. We performed wound healing assays on ECs under OPN treatment in presence or absence of neutralizing antibodies for CD44 and αVβ3. The neutralization of either CD44 or αVβ3 inhibited OPN effects on EC migration (Figure 4.4B and C). These results allowed us to demonstrate that dephosphorylated OPN induced EC migration through CD44 and αVβ3 activating the Erk1/2.

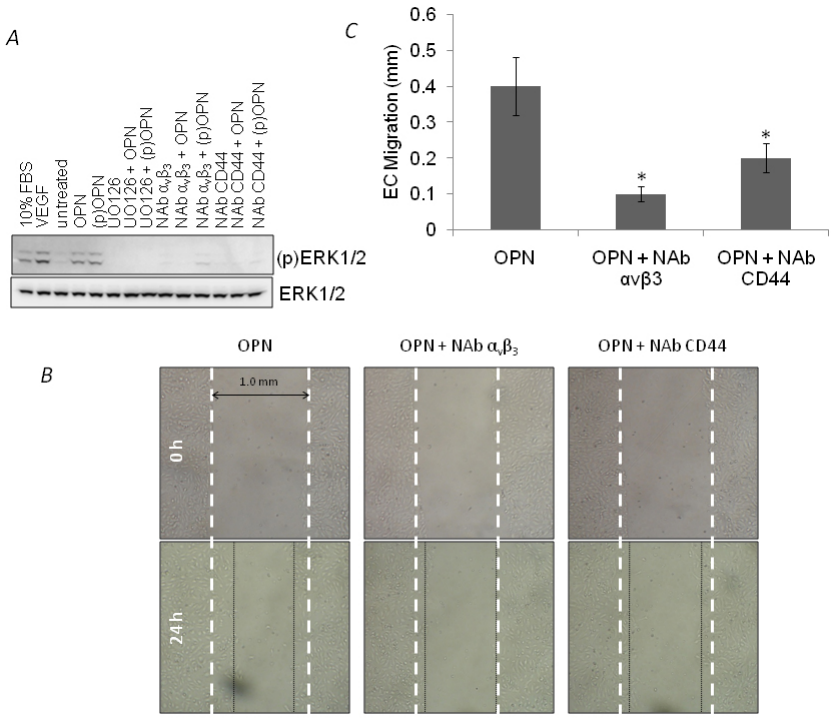

Figure 4.4. αvβ3 and CD44 are necessary for OPN-induced endothelial cell migration.

(A) Western blot of total protein extract of HUVECs to test ERK1/2 phosphorylation under different treatments. From left to right: FBS10%, VEGF (30 ng/ml), untreated, OPN (50 ng/ml), (p)OPN (50 ng/ml), UO126 (10 mM) in the presence of OPN or (p)OPN, neutralizing antibody for αvβ3 (10 mg/ml) in the presence or absence of OPN or (p)OPN and neutralizing antibody for CD44 (10 mg/ml) in the presence or absence of OPN or (p)OPN. (B) Wound healing assay of confluent HUVECs treated with OPN (50 ng/ml) in the presence of neutralizing antibody for CD44 or αvβ3. Endothelial cell migration was photographed after 24 hours at 4x magnification. (C) Bar graph representation of endothelial cell migration. * $p < 0.01$. Adapted from[11]: Poggio, P. *et al.* Osteopontin controls endothelial cell migration in vitro and in excised human valvular tissue from patients with calcific aortic stenosis and controls. *J. Cell. Physiol.* **226,** 2139–2149 (2011).

4.2.6 OPN controls endothelial cell migration of excised aortic valve through Erk1/2

Angiogenesis is a key step in the remodeling of the aortic valve and the development of progressive valve calcification and degeneration. We decided to

investigate the response of excised aortic valve treated with OPN and its intracellular signaling pathways. To evaluate the ability of VECs to migrate and form tubular-like structures without any exogenous stimuli, leaflets derived from AVS patients and healthy controls were embedded in a 3D collagen type I matrix for 14 days. At day 14, formation of tubular-like structures was evaluated with a phase contrast microscope. From cultures of control leaflets, the endothelial migrating cells formed a monolayer around the valve tissue with few tubular-like structures. AVS-derived leaflets showed extensive tubular-like structures (Fig. 4.5A and B).

To test if OPN has a similar effect on VECs embedded in 3D collagen, we repeated the cell sprouting assay in the presence or absence of OPN and we measured the cell number, migration distance and the formation of tubular-like structures of VECs derived from both AVS and control tissues. OPN promoted migration and tubular-like formation in our 3D assay, confirming the similarity between HUVECs and VECs. We then tested the effect of OPN on valve tissue to analyze the Erk1/2 mediate of the effects of OPN on VEC migration. OPN enhanced VEC migration into the 3D collagen matrix and UO126 blocked such migration. Together, these results suggest that both HUVECs and VECs were activated by OPN and that the activation is mediated by Erk1/2 intracellular signaling pathway.

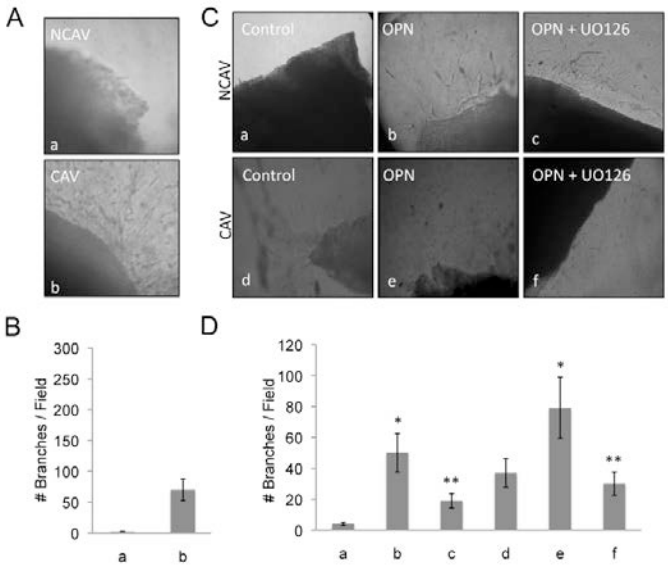

Figure 4.5. OPN induces in vitro angiogenesis of excised human aortic valve tissues through ERK1/2.

(A) *In vitro* angiogenesis assay of excised tissue from calcified (CAV) and non-calcified aortic valve (NCAV). (B) Bar graph representation of the *in vitro* angiogenesis assay. The number of tubular-like structures was counted as a number of branches per field. Pictures were taken at 10x magnification. (C) Non-calcified and calcified tissue embedded in collagen and treated with OPN in the presence or absence of UO126 (10 mM). (D) Bar graph representation of the in vitro angiogenesis assay. The number of tubular-like structures was counted as a number of branches per field. Pictures were taken at 10x magnification. * $p < 0.01$ and ** $p < 0.01$ *vs.* OPN treated. Adapted from[11]: Poggio, P. *et al.* Osteopontin controls endothelial cell migration in vitro and in excised human valvular tissue from patients with calcific aortic stenosis and controls. *J. Cell. Physiol.* **226,** 2139–2149 (2011).

4.2.7 CD44 and αVβ3 receptors controls endothelial cell migration of excised aortic valve

Finally, we tested the role of both CD44 and αVβ3 on the formation of tubular-like structures on aortic valve derived tissues. In accord with our *in vitro* experiments, both CD44 and αVβ3 are necessary for EC migration and collagen sprouting. With the 3D assay we were able to demonstrate that the neutralization of either CD44 or αVβ3 blocked the cellular reorganization into the collagen matrix when aortic valve leaflets were treated with OPN, and confirmed the inability to promote any VEC migration by the phosphorylated form of OPN (Figure4.6).

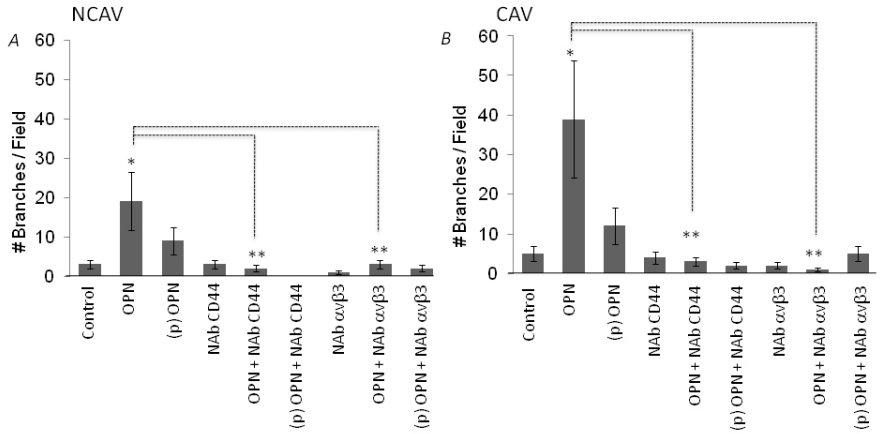

Figure 4.6. αvβ3 and CD44 are necessary for OPN-induced *in vitro* angiogenesis of excised human aortic valve tissues.

(A) Bar graph representation of the *in vitro* angiogenesis assay on control tissues (NCAV). The number of tubular-like structures was counted as the number of branches per field. Pictures were taken at 10x magnification. (B) Bar graph representation of the *in vitro* angiogenesis assay on aortic stenosis tissues (CAV). The number of tubular-like structures was counted as the number of branches per field. Pictures were taken at 10x magnification. * $p < 0.01$ and ** $p < 0.01$ *vs.* OPN treated. Adapted from[11]: Poggio, P. *et al.* Osteopontin controls endothelial cell migration in vitro and in excised human valvular tissue from patients with calcific aortic stenosis and controls. *J. Cell. Physiol.* **226,** 2139–2149 (2011).

4.3 Discussion

OPN is a phosphorylated, acidic, RGD-containing glycoprotein that binds certain CD44 variants and integrin receptors, including $\alpha V\beta 3$[15]. OPN acts as a cytokine, playing important roles in the migration and invasion of several tumor cells[16,17]. In addition, OPN is regarded to be an important angiogenic factor in several pathologies. In this chapter it is described the biological effects of OPN *in vitro* and in excised aortic valve tissues. The results, combined with previously reported studies, confirm that the biological function of OPN on aortic valve degeneration plays an important role on VECs.

Calcified aortic valve leaflets have also been shown to express neo-angiogenesis factors[18]. Although angiogenesis is considered to be part of the early stages of calcification, pro-angiogenic factors are expressed even when the valve is completely calcified, suggesting that this mechanism is still present and active during the entire degeneration process.

Correspondingly, it has been shown that ECs of stenotic but not those of non-stenotic valves exhibit CEACAM1, a cell adhesion molecule expressed in angiogenic, but not in quiescent ECs[9,19,20]. Chalajour *et al.*[9] have demonstrated that the formation of angiogenic sprouts from calcified valves occurs significantly faster than from non-calcified valves. Immunoreactivity of CD44 and vWF has been demonstrated in the tubular-like structures[9]. We reported the analysis on the role of OPN on cultured

endothelial cells due to their physiological implication on the aortic valve leaflets. The comparison of the effects of OPN on aortic valve derived tissues form AVS patients and controls demonstrated that OPN activated the same intracellular signaling pathways in HUVECs and VEC from excised aortic valve tissues.

Based on the presented results, EC migration of both HUVEC and aortic valve derived cells is dependent on CD44 and αVβ3 and results in Erk1/2 phosphorylation. Moreover, the OPN post-translational modifications are important in the ability to promote EC migration. These data provide new insights into the cellular and molecular mechanisms involving endothelial cells in stenotic aortic valve tissues. These results could bring new potential perspectives to the development of future preventive treatments for this condition.

4.4 References

1. Poggio, P. *et al.* Osteopontin controls endothelial cell migration in vitro and in excised human valvular tissue from patients with calcific aortic stenosis and controls. *J. Cell. Physiol.* **226,** 2139–2149 (2011).

2. O'Brien, K. D. *et al.* Apolipoproteins B, (a), and E accumulate in the morphologically early lesion of 'degenerative' valvular aortic stenosis. *Arterioscler. Thromb. Vasc. Biol.* **16,** 523–532 (1996).

3. Olsson, M., Thyberg, J. & Nilsson, J. Presence of oxidized low density lipoprotein in nonrheumatic stenotic aortic valves. *Arterioscler. Thromb. Vasc. Biol.* **19,** 1218–1222 (1999).

4. Collett, G. D. M. & Canfield, A. E. Angiogenesis and pericytes in the initiation of ectopic calcification. *Circ. Res.* **96,** 930–938 (2005).

5. Pastor-Pérez, F. & Marín, F. Hypertension, aortic sclerosis and the prothrombotic state: understanding the complex interaction. *J Hum Hypertens* **23,** 287–288 (2009).

6. Ferrara, N. & Davis-Smyth, T. The biology of vascular endothelial growth factor. *Endocr. Rev.* **18,** 4–25 (1997).

7. Ferrara, N. Molecular and biological properties of vascular endothelial growth factor. *J. Mol. Med.* **77,** 527–543 (1999).

8. Soini, Y., Salo, T. & Satta, J. Angiogenesis is involved in the pathogenesis of nonrheumatic aortic valve stenosis. *Hum. Pathol.* **34,** 756–763 (2003).

9. Chalajour, F. *et al.* Angiogenic activation of valvular endothelial cells in aortic valve stenosis. *Exp. Cell Res.* **298,** 455–464 (2004).

10. Chalajour, F. *et al.* Identification and characterization of cells with high angiogenic potential and transitional phenotype in calcific aortic valve. *Exp. Cell Res.* **313,** 2326–2335 (2007).

11. Poggio, P. *et al.* Noggin attenuates the osteogenic activation of human valve interstitial cells in aortic valve sclerosis. *Cardiovasc. Res.* **98,** 402–410 (2013).

12. Dai, J. *et al.* Osteopontin induces angiogenesis through activation of PI3K/AKT and ERK1/2 in endothelial cells. *Oncogene* **28,** 3412–3422 (2009).

13. Okamoto, H. Osteopontin and cardiovascular system. *Mol. Cell. Biochem.* **300,** 1–7 (2007).

14. Katagiri, Y. U. *et al.* CD44 variants but not CD44s cooperate with beta1-containing integrins to permit cells to bind to osteopontin independently of arginine-glycine-aspartic acid, thereby stimulating cell motility and chemotaxis. *Cancer Res.* **59,** 219–226 (1999).

15. Denhardt, D. T., Noda, M., O'Regan, A. W., Pavlin, D. & Berman, J. S. Osteopontin as a means to cope with environmental insults: regulation of inflammation, tissue remodeling, and cell survival. *J. Clin. Invest.* **107,** 1055–1061 (2001).

16. Rittling, S. R. & Chambers, A. F. Role of osteopontin in tumour progression. *Br J Cancer* **90,** 1877–1881 (2004).

17. Tuck, A. B., Chambers, A. F. & Allan, A. L. Osteopontin overexpression in breast cancer: knowledge gained and possible implications for clinical management. *J. Cell. Biochem.* **102,** 859–868 (2007).

18. Rajamannan, N. M. Calcific aortic stenosis: medical and surgical management in the elderly. *Curr Treat Options Cardiovasc Med* **7,** 437–442 (2005).

19. Ergun, S. *et al.* CEA-related cell adhesion molecule 1: a potent angiogenic factor and a major effector of vascular endothelial growth factor. *Mol Cell* **5,** 311–320 (2000).

20. Yetkin, E. & Waltenberger, J. Molecular and cellular mechanisms of aortic stenosis. *Int. J. Cardiol.* **135,** 4–13 (2009).

Chapter 5

Role Of Osteopontin In Valve Interstitial Cell Activation And Calcification

Part of this chapter has been published as[1,2]**:**

Paolo Poggio, Juan B. Grau, Benjamin C. Field, Rachana Sainger, William F. Seefried, Flavio Rizzolio, and Giovanni Ferrari. Osteopontin controls endothelial cell migration *in vitro* and in excised human valvular tissue from patients with calcific aortic stenosis and controls. *Journal of Cellular Physiology* **226**, 2139–2149 (2011).

Paolo Poggio*, Juan B. Grau*, Rachana Sainger, William J. Vernick, William F. Seefried, Emanuela Branchetti, Benjamin C. Field, Joseph E. Bavaria, Michael A. Acker, and Giovanni Ferrari. Analysis of Osteopontin levels for the identification of asymptomatic patients with calcific aortic valve disease. *The Annals of Thoracic Surgery* **93**, 79–86 (2012). * These authors contributed equally to this work.

5.1 Introduction

The valve interstitial cells (VIC), a heterogeneous population, represent the majority of the cells within the valve leaflets. To further characterize the calcific aortic valve disease (CAVD), the role of osteopontin (OPN) has been analyzed in human derived aortic valve interstitial cells. The primary receptors for OPN, as previously discuss, are those integrins that present the central integrin binding motif RGD[3]. In addition to the integrin, the C-terminal fragment of OPN binds directly to CD44v6 in an RGD-independent manner[3], inducing cell migration[4,5]. This receptor consists of 20 exons, where the first five and the last five exons are constant and the others are present only in the variants. Exons 1 to 16 encode for the extracellular domain, exon 17 encodes for the transmembrane domain and the exons 18 and 19 encode for the cytoplasmic domain (Figure 5.1). The ten exons located between 5a to 14 are subjected to alternative splicing, resulting in the generation of CD44 variants. CD44 is a multifunctional receptor which plays a role in cell adhesion, cell traffic, presentation of chemokine and growth factors, transmission of growth signals and signals mediating hematopoiesis and apoptosis[5].

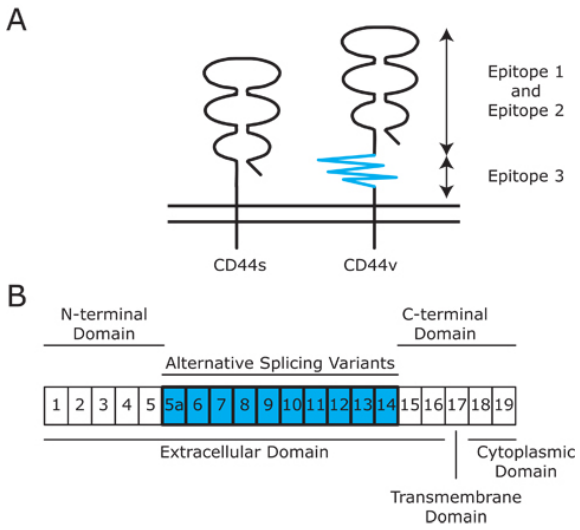

Figure 5.1. CD44 splicing variants.

(A) Schematic structure of CD44s and CD44v that has an additional longer stem, which contains the variant exon(s). (B) CD44 gene consists of 20 exons, exons 1-5 (N-terminal domain) and exons 15-19 (C-terminal domain). Exons 5a-14 (v1 to v10) generate CD44 variants through alternative splicing.

This chapter investigates, *ex vivo* and *in vitro*, the role of OPN-CD44 functional interaction in the formation of calcium nodules in relation to the progression of CAVD. This part of the study was carried out using human derived smooth muscle cells (SMC), VICs and excised aortic valve leaflets, obtained through the heart transplant program and the cardiovascular surgery department. The preliminary experiments were tested on SMCs rather then VICs, since these two cell type share many molecular and physiological characteristics (Table 5.1).

Table 5.1. Similarities between valve interstitial cells and smooth muscle cells.

	VIC / SMC
Morphology	Resemble fibroblasts in morphology, being elongated and forming an orthogonal pattern of overgrowth post-confluence. Long cytoplasmic extensions, prominent adhesion and gap junctions, an incomplete basal lamina, and close association with the extracellular matrix[6,7]
Markers expressed	α-SMA[8]
	Vimentin[9]

Adapted from[1]: Poggio, P. *et al.* Osteopontin controls endothelial cell migration in vitro and in excised human valvular tissue from patients with calcific aortic stenosis and controls. *J. Cell. Physiol.* **226,** 2139–2149 (2011).

5.2 Results

5.2.1 OPN biological activity is controlled by its phosphorylation status in smooth muscle cells

To characterize the role of OPN on the regulation of VIC calcification, we implemented a calcification assay in combination with phospho-OPN or OPN not phosphorylated. *In vitro* inorganic phosphate (Pi) calcification assay has been

extensively used as a model to test the biological activity of proteins involved in the calcium deposition[10,11], we tuned our calcification assay on SMCs. Recombinant OPN was phosphorylated *in vitro* using casein kinase II (Figure 5.2A) and its ability to control calcium deposition tested. Dephosphorylated recombinant OPN did not inhibit SMC biomineralization, while phosphorylated recombinant OPN inhibited calcium deposition *in vitro* (Figure 5.2B and C). These experiments confirm that the phosphorylation status controls the ability of OPN to inhibit biomineralization.

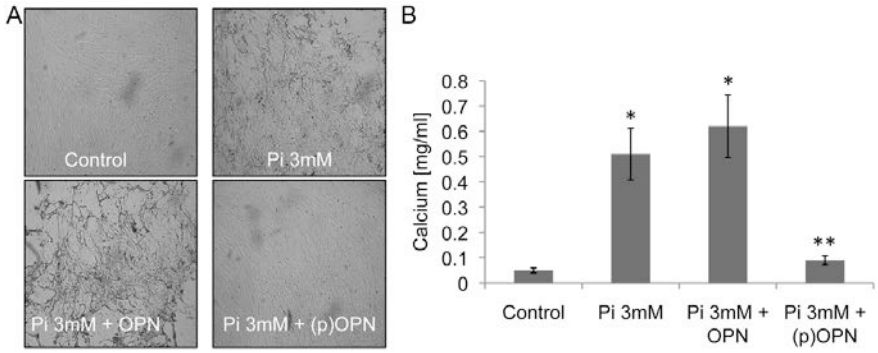

Figure 5.2. OPN phosphorylation status controls *in vitro* smooth muscle cell calcification.

(A) *In vitro* calcification of confluent smooth muscle cells treated with calcification medium (MEM containing 3 mM phosphate buffer) in the presence or absence of OPN (50 ng/ml) or (p)OPN (50 ng/ml). (B) Bar graph representation of total calcium expressed as calcium mg/ml of medium. * $p < 0.01$ and ** $p < 0.01$ *vs.* OPN treated. Adapted from[1]: Poggio, P. *et al.* Osteopontin controls endothelial cell migration in vitro and in excised human valvular tissue from patients with calcific aortic stenosis and controls. *J. Cell. Physiol.* **226,** 2139–2149 (2011).

5.2.2 OPN-a, -b and -c inhibit biomineralization

OPN can be present in different isoforms and we decided to investigate the role of the three OPN isoforms -a, -b, and -c on a SMC in presence of Pi. Since OPN isoforms were not available for purchase, we cloned the three OPN isoforms in a bacterial expression plasmid (PGEX-5). Chimeric GST-Flag-tagged OPN isoforms were generated and purified (Chapter 2) (Figure 5.2A and B). *In vitro* calcification assay was performed when the cells were confluent in presence or absence of non-

phosphorylated and phosphorylated OPN-a, -b and -c. All OPN splicing variants -a, -b, and -c were able to control *in vitro* biomineralization, inhibiting calcium deposition on SMCs surface only when they were in the phosphorylated form (Figure 5.3C and D). These results indicate that all the phosphorylated OPN splicing variants tested maintain the *in vitro* ability to inhibit calcium deposition induced by Pi treatments. Since the results between the three OPN isoforms are comparable we decided to use for the subsequent analysis the full-length recombinant OPN (OPN a).

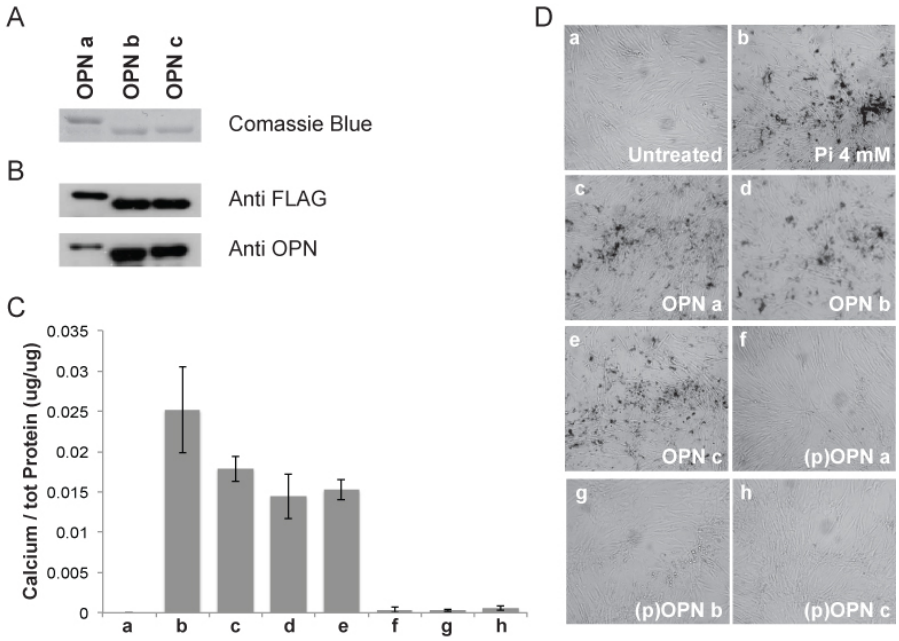

Figure 5.3 Osteopontin splicing variants and their role in cells biomineralization.

(A) OPN splicing variant production and detection with Commassie blue staining. (B) OPN-a, OPN-b, and OPN-c expression detected by Western blot using anti-FLAG and anti-OPN antibodies. (C) Bar graph representative of calcium formed on vascular smooth muscle cells (SMC). (D) Calcification assay performed using OPN isoforms: (a, b) calcium accumulation on SMC cultured in normal media and in calcification media; (c, d, e) calcium deposition on SMC treated with calcification media in the presence of OPN isoforms non-phosphorylated; (f, g, h) calcium deposition on SMC treated with calcification media in the presence of phosphorylated OPN isoforms. Calcium accumulation was quantified and normalized against protein content. Adapted from[2]: Grau, J. B. *et al.* Analysis of osteopontin levels for the identification of asymptomatic patients with calcific aortic valve disease. *Ann. Thorac. Surg.* **93,** 79–86 (2012).

5.2.3 OPN controls smooth muscle cell calcification through CD44 and not αVβ3

Since both CD44 and αVβ3 can mediate the biologic activities of OPN, in particular both receptor are required for ECs migration, we decided to further analyze the OPN interactions with CD44 and αVβ3 in SMCs and the intracellular signaling activated.

Based on the previous results and to complete the *in vitro* characterization of OPN biological activity, we tested the protective biological activity of OPN using the same *in vitro* calcification assay in the presence or absence of UO126, and the neutralizing antibodies anti CD44 and αVβ3. The inhibition of Erk1/2 with the chemical inhibitor UO126 did not disrupt the protective effect of phospho-OPN in the *in vitro* calcification assay. We notice similar results by blocking the activity of αVβ3 (Fig. 5.4). On the contrary, a neutralizing antibody anti CD44 was able to revert the inhibitory effects of OPN and allowed calcium deposition on the surface of cultured SMCs (Fig. 5.4). These experiments suggest that the protective effect of phosphorylated OPN was independent of Erk1/2 and mainly mediated by the activity of CD44.

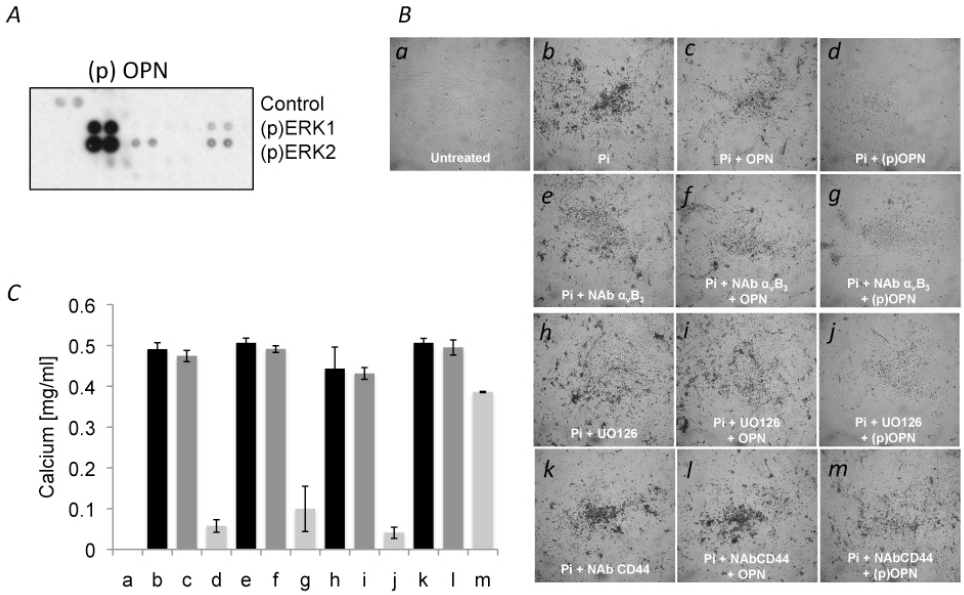

Figure 5.4. CD44 but not αvβ3 regulated (p)OPN-induced smooth muscle cell biomineralization.

(A) Phospho-MAP kinase profile array of human smooth muscle cells (SMC) treated with recombinant OPN (50 ng/ml) showing (p)ERK 1/2 activation. (B) *In vitro* calcification of confluent SMC treated with calcification medium (MEM containing 3 mM phosphate buffer) in the presence of the indicated treatments. (C) At day 8 of treatment, calcium was estimated using the calcium assay reagent. Amount of total calcium is expressed as calcium mg/ml of medium. Pictures were taken at 4x magnification. Adapted from[1]: Poggio, P. *et al.* Osteopontin controls endothelial cell migration in vitro and in excised human valvular tissue from patients with calcific aortic stenosis and controls. *J. Cell. Physiol.* **226,** 2139–2149 (2011).

5.2.4 OPN-CD44 functional interaction as a hallmark of early stages of calcific aortic valve disease

Based on the previous results we decide to better understanding the OPN-CD44 interaction in human tissue and human isolated valve interstitial cells derived from healthy controls, AVSc and AVS patients.

Upon informed consent, 27 patients were selected from our cardiac bioregistry. Four controls and 18 aortic valve sclerotic tissues were obtained through the heart transplant research program at the University of Pennsylvania Perelman School of Medicine. Five aortic valve stenotic tissues were collected during aortic valve replacement (AVR) procedures from patients with end-stage CAVD (Table 5.2).

Table 5.2. Patient demographics and Clinical details.

	Controls		Aortic Sclerosis		Aortic Stenosis	
Demographics	N =	4	N =	18	N =	5
Age	33.8	± 12.2	58.8	± 9.1	80.2	± 7.0
Male subjects	25%	(1)	50%	(9)	20%	(1)
Diabetes	25%	(1)	28%	(5)	20%	(1)
Hypertension	25%	(1)	50%	(9)	100%	(5)
Cerebral vascular accident	25%	(1)	17%	(3)	0%	(0)
Coronary artery disease	0%	(0)	39%	(7)	40%	(2)
Congestive heart failure	0%	(0)	33%	(6)	20%	(1)
Hyperlipidemia	0%	(0)	33%	(6)	80%	(4)

In control aortic valves, both OPN and CD44 expressions were barely detectable throughout the entire leaflets (Figure 5.5A and B). In contrast, in sclerotic and stenotic aortic valves the expression of both proteins was higher when compared to healthy controls. Moreover, the stenotic tissues had a uniform expression, while the sclerotic ones had a major concentration of OPN and CD44 in the ventricularis region (Figure 5.5A and B). To test *ex vivo* functional interaction, between OPN and CD44, Proximity Ligation Assay (PLA) was performed as described in Chapter 2. Reaction products (red dots), representing the direct binding between OPN and CD44, showed the functional interaction of these two proteins in both sclerotic and stenotic tissues. This particular interaction had approximately 10-fold increment, when compared to control aortic valves (Figure 5.5C and D).

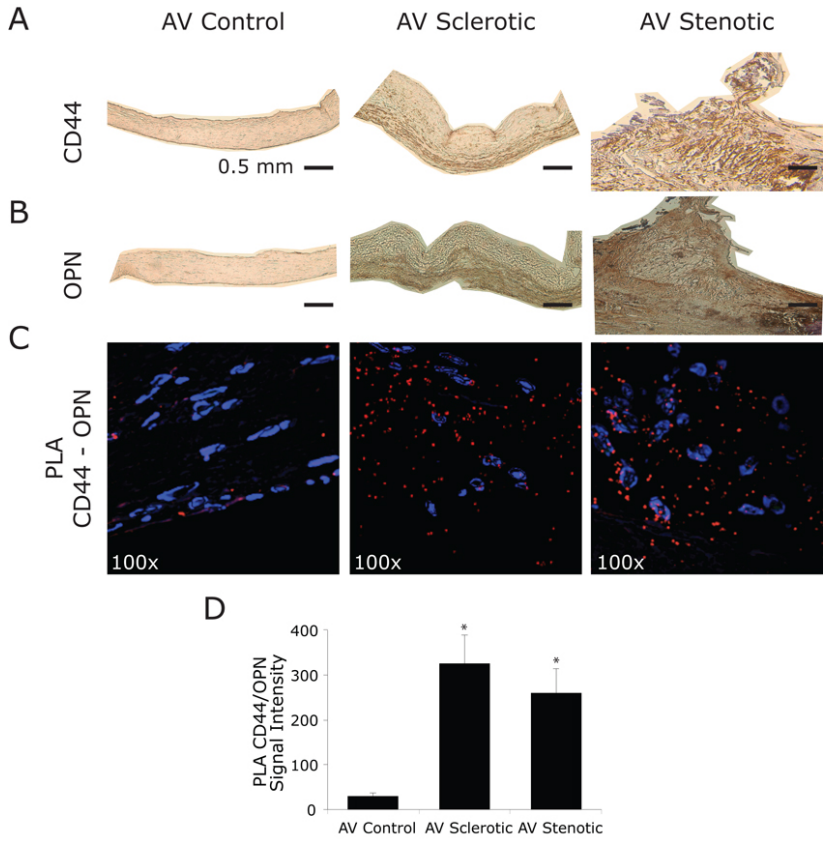

Figure 5.5. CD44-OPN functional interaction as a hallmark of early stages of calcific aortic valve disease.

(A-B) Representative images showing histological analysis of human aortic valves (control, sclerotic and stenotic). Immunohistochemistry staining for CD44 and OPN. Bar represents 0.5 mm. (C) Proximity Ligation Assay (PLA), red fluorescence dots indicate reaction product showing extracellular binding

between CD44 and OPN. Magnification 100x. (D) Bar graph representing PLA quantification in control, sclerotic and stenotic aortic valves. * p value <0.05.

Since bone morphogenetic protein 4 (BMP4) is known to be potent osteogenic morphogens present in ossified valves and directly affects osteogenic marker expression[12,13], and mechanical stimulation is an important component of valve degeneration[14-16], we decided to test whether OPN-CD44 binding was regulated by biomechanical stimulation. We therefore applied 15% stretch at 1Hz in the presence or absence of BMP4, using a tensile bioreactor to mimic the stress on the valve during the cardiac cycle (Chapter 2). As an internal control, native tissues were treated statically in the presence or absence of BMP4. Cyclic stretch of the leaflets did not damage leaflet morphology and maintains native ECM structure and cellular composition[17,18]. OPN-CD44 binding was influenced only by BMP4, independently of the mechanical stimuli (Figure 5.6).

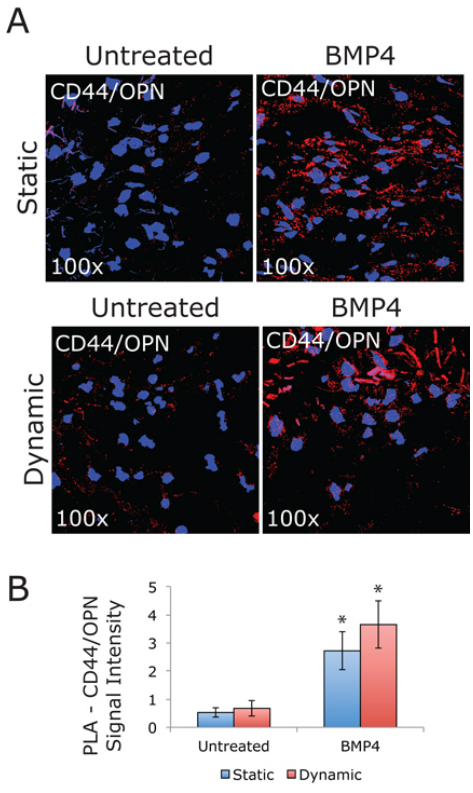

Figure 5.6. CD44-OPN functional interaction in aortic valve sclerosis tissue under biomechanical stretch.

(A) PLA showing CD44/OPN binding in aortic valve sclerotic tissue at 6 days under static or dynamic (15% stretch at 1 Hz) conditions ± BMP4 (100 ng/ml). (B) Bar graph represents PLA quantification. * p value <0.05.

5.2.5 BMP4 induces OPN and CD44 binding in aortic valve sclerosis-derived valve interstitial cells

Since BMP4 alone was able to increase OPN-CD44 interaction, we tested the role of this interaction in the regulation of VIC osteogenic-like transdifferentiation and calcification deposition. We isolated primary interstitial cells from 10 patients (2 controls, 4 sclerotic and 4 stenotic) according to the method described in Chapter 2. Phenotypic stability was assessed after isolation and isolated VICs were used between passage 2 and 4. It has been shown that OPN binds only the variants 3 and 6 of CD44 (CD44v3 and CD44v6). We therefore tested whether these variants were present in aortic valve-derived VICs in our three cohorts of patients. All tested human isolated-VICs expressed CD44v6 isoform, independently of the progression of the disease and no CD44v3 was detectable (Figure 5.7).

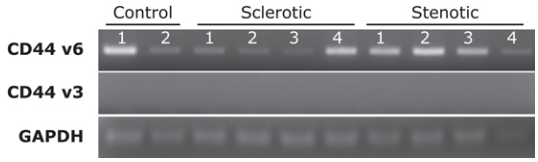

Figure 5.7. CD44 variant expression in human isolated valve interstitial cells.
PCR product obtained using primers for CD44v6 and CD44v3 on human isolated valve interstitial cells (VIC), 2 control, 4 sclerotic and 4 stenotic patients. GAPDH was used as internal control.

In a time course experiment, we showed that in AVSc-derived VICs, the binding between OPN and CD44 is highly increased in response to BMP4 treatment. The PLA products (red dots), representing the interaction between the extracellular portion of the transmembrane receptor CD44 and OPN, increased after 4 hours of BMP4 treatment and persisted up to 6 days. A neutralizing antibody anti CD44 (NAb-CD44),

recognizing the epitope 2 (conserved region in the extracellular domain), compete with the OPN binding site to CD44 and could prevent the OPN-CD44 interaction (Figure 5.8).

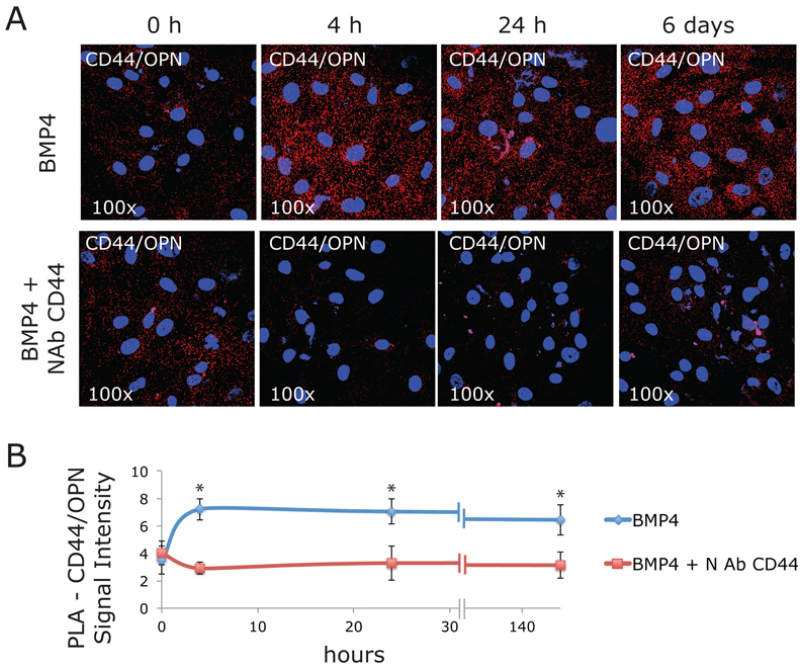

Figure 5.8. CD44-OPN interaction on isolated VICs from asymptomatic AVSc patients.

(A) Proximity Ligation Assay (PLA) showing CD44/OPN binding in aortic valve sclerotic valve interstitial cells (VIC) at 0h, 4h, 24h and 6 days after in vitro BMP4 treatments (100 ng/ml) ± NAb CD44 (5 ug/ml). Magnification 100x. (B) Line graph represents PLA quantification * p value <0.05.

5.2.6 OPN and CD44 interaction protects sclerotic valve interstitial cells from calcification induced by BMP4

To link the OPN-CD44 interaction with calcium deposition, we treated isolated sclerotic VICs for 12 days in the presence or absence of BMP4. Using qPCR analysis, we evaluated the expression of OPN and ALP under BMP4 treatment to demonstrate its role in controlling the VIC activation towards an osteogenic-like phenotype. We noticed a significant up regulation of OPN by 3.3 ± 0.3 fold and ALP 2.2 ± 0.2 fold (p value <

0.05). To demonstrate the active role of endogenous OPN in protecting VICs from calcification, we checked presence of calcium deposition in AVSc-derived VICs treated with BMP4 for 12 days. Despite the increased level of ALP, AVSc-derived VICs did not show any sign of calcium accumulation. However, blocking OPN-CD44 interaction (by neutralizing antibody against either CD44 or OPN) induced calcium deposition, 3.4 ± 0.9 and 1.9 ± 0.2 fold increase, respectively when compared to BMP4 treatment alone (Figure 5.9). These results suggest the direct role of the functional interaction between OPN-CD44 in preventing calcium accumulation in AVSc-derived VICs.

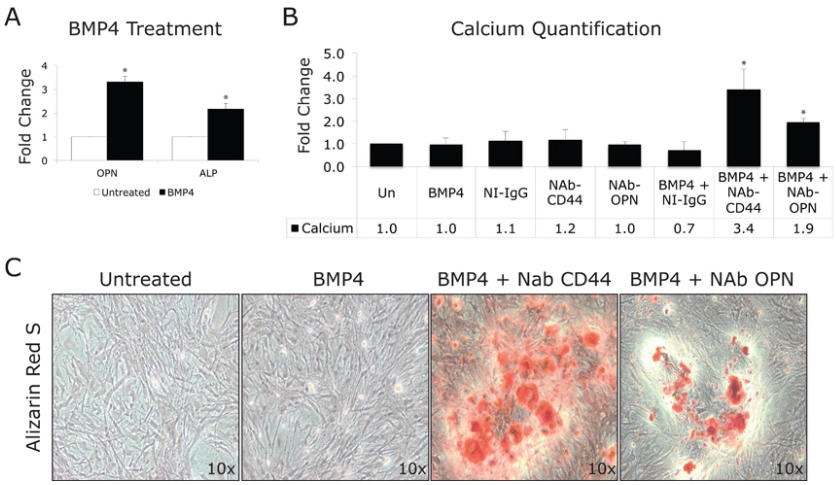

Figure 5.9. CD44 and OPN protect human sclerotic valve interstitial cells from calcification induced by BMP4.

(A) Bar graphs represent fold change gene expression of OPN and ALP in aortic valve sclerotic valve interstitial cells (VIC) after 12 days in vitro treatment in the presence or absence of BMP4 (100 ng/ml). (B) Bar graph represents calcium deposition on aortic valve sclerotic VICs after 12 days treatment with BMP4 (100 ng/ml), NAb CD44 (5 ug/ml), NAb OPN (5 ug/ml), NI-IgG (5 mg/ml) and their combinations. * p value <0.05. (C) Alizarin red staining representing calcium deposition (red) on VICs after 12 days treatment with BMP4 (100 ng/ml), NAb CD44 (5 ug/ml), NAb OPN (5 ug/ml) and their combinations.

5.2.7 Akt phosphorylation induced by OPN-CD44 is required to protect sclerotic valve interstitial cells from calcium deposition

Since the previous experiments on Erk1/2 did not show any link with calcium deposition, we investigated another intracellular signaling pathway activated OPN-CD44 in human-derived VICs. Extensive work has reported a direct activation of MAPK signaling pathway by OPN in different cell lines[4,19,20]. We therefore decided to analyze Akt activation. Phosphorylation of SMAD1/5/8 was also tested as an independent signaling pathway activated by BMP4. In our experiment phospho-Akt is seen by Western blot after 15', 4h and 24h of BMP4 and OPN treatments, however Akt phosphorylation is prevented by pre-treatment with a neutralizing antibody against CD44 (NAb-CD44). Furthermore, the phosphorylation of SMAD1/5/8 is BMP4 dependent and the presence of NAb-CD44 does not affect SMAD phosphorylation (Figure 5.10).

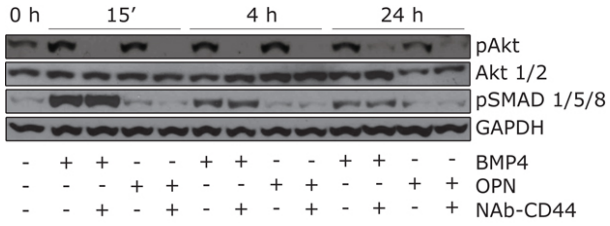

Figure 5.10. Akt phosphorylation induced by CD44/OPN.

Western blot of pAkt, Akt 1/2, pSMAD 1/5/8 and GAPDH at 0h, 15', 4h and 24h after BMP4 (100 ng/ml) in combination with NAb CD44 (5 mg/ml) or NAb OPN (5 mg/ml).

Since Akt was phosphorylated after BMP4 treatments, we evaluated the role of this phosphorylation, on regulating calcium deposition of VICs derived from AVSc patients. We therefore treated AVSc-derived VICs with BMP4 in the presence or absence of Wortmannin, a known phosphoinositide-3-kinase (PI3K)/Akt cascade inhibitor. The combination of BMP4 and Wortmannin resulted in an increment of calcium deposits measured by colorimetric assay by 2.7 ± 0.2 fold and by Alizarin red staining (Figure 5.11). These results suggest that Akt phosphorylation induced by OPN-CD44 is required to protect human sclerotic valve interstitial cells from calcium deposition.

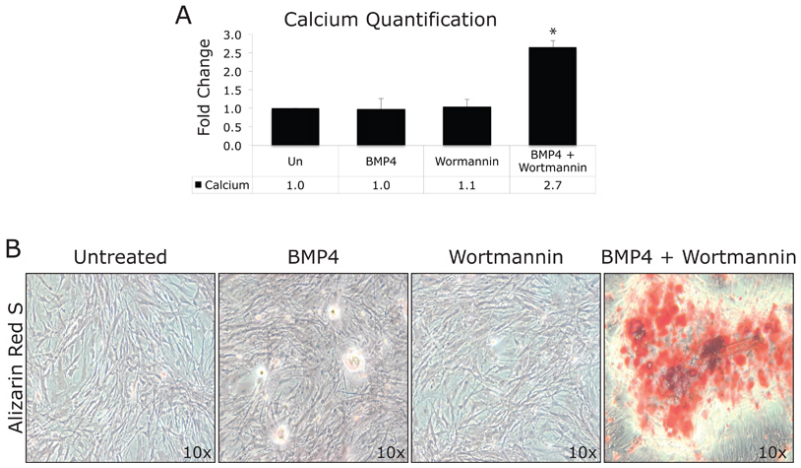

Figure 5.11. Akt phosphorylation is required to protect human sclerotic valve interstitial cells from calcium deposition.

(A) Bar graph represents calcium deposition on aortic valve sclerotic VICs after 12 days treatment with BMP4 (100 ng/ml) ± Wortmannin (0.2 mM). * p value <0.05. (B) Alizarin red staining representing calcium deposition (red) on VICs after 12 days treatment with BMP4 (100 ng/ml) ± Wortmannin (0.2 mM).

5.3 Discussion

Due to its asymptomatic presentation, little is known about the molecular mechanisms underlying tissue remodeling and VIC activation in aortic valve sclerosis patients. Here, we unveil the specific functional association of OPN with CD44v6 and the intracellular signaling mechanisms controlling calcium deposition on VIC derived from non-calcified AV tissues.

High levels of OPN in native human calcified aortic valves from patients undergoing aortic valve replacements have been shown by immunohistochemistry, reverse transcription–polymerase chain reaction (RT-PCR), Western blotting, and in situ hybridization analyses[4,19]. In addition to native valves, increased OPN levels were also found by immunohistochemistry in calcified valve allografts and in areas of calcification in glutaraldehyde-pretreated bioprosthetic porcine valves[21,22]. Elevated circulating OPN levels are also reported in other cardiovascular diseases, such as

atherosclerosis, ischemic heart disease, heart failure, and rheumatic mitral stenosis[4].Osteopontin is of special interest for CAVD, since it is the only described biomarker directly involved in the ectopic and dystrophic calcification phenomenon that occurs during native and bio-prosthetic valve degeneration. Interestingly, circulating levels of OPN are also elevated in patients with signs of AVSc, suggesting that OPN could also be used as biomarker to label patients at risk to develop severe stenosis[23].

This chapter provides several new insights into the specific interaction of OPN with CD44 and the intracellular signaling controlling calcium deposition in human sclerotic-derived VICs. Tissue from early stages of AVSc is extremely difficult to obtain since these valves are mechanically functional and are not indicated for repair or replacement. However, our collaborations with the Gift of Life program and with the heart transplant program allow us to rely on this unique collection of human specimens. Using this major resource we demonstrated a specific OPN-CD44 functional interaction in early asymptomatic stage of CAVD. We then show, *in vitro*, that preventing OPN-CD44 interaction result in calcium accumulation of VIC obtained from non-calcified AVSc patients after treatments with BMP4. Finally, using neutralizing antibodies and general inhibitors of intracellular signaling pathways we unveil that Akt phosphorylation induced by OPN-CD44 is required to protect human sclerotic valve interstitial cells from calcium deposition. The model depicted in Figure 5.12 provides novel insights into the intracellular mechanisms controlling OPN, and in general VIC activation and calcification, in human AVSc-derived cells.

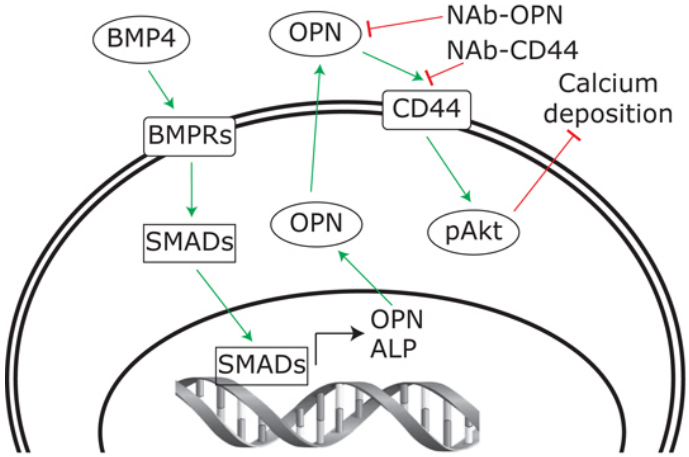

Figure 5.12. Summary scheme.

5.4 References

1. Poggio, P. *et al.* Osteopontin controls endothelial cell migration in vitro and in excised human valvular tissue from patients with calcific aortic stenosis and controls. *J. Cell. Physiol.* **226,** 2139–2149 (2011).

2. Grau, J. B. *et al.* Analysis of osteopontin levels for the identification of asymptomatic patients with calcific aortic valve disease. *Ann. Thorac. Surg.* **93,** 79–86 (2012).

3. Rangaswami, H., Bulbule, A. & Kundu, G. C. Osteopontin: role in cell signaling and cancer progression. *Trends Cell Biol.* **16,** 79–87 (2006).

4. Okamoto, H. Osteopontin and cardiovascular system. *Mol. Cell. Biochem.* **300,** 1–7 (2007).

5. Zhao, L. *et al.* CD44 regulates vascular gene expression in a proatherogenic environment. *Arteriosclerosis, Thrombosis, and Vascular Biology* **27,** 886–892 (2007).

6. Filip, D. A., Radu, A. & Simionescu, M. Interstitial cells of the heart valves possess characteristics similar to smooth muscle cells. *Circ. Res.* **59,** 310–320 (1986).

7. Diane L Mulholland & Gotlieb, A. I. Cardiac Valve Interstitial Cells: Regulator of Valve Structure and Function. *Cardiovascular Pathology* **6,** 167–174 (1997).

8. Taylor, P. M., Batten, P., Brand, N. J., Thomas, P. S. & Yacoub, M. H. The cardiac valve interstitial cell. *Int. J. Biochem. Cell Biol.* **35,** 113–118 (2003).

9. Liu, A. C., Joag, V. R. & Gotlieb, A. I. The emerging role of valve interstitial cell phenotypes in regulating heart valve pathobiology. *Am. J. Pathol.* **171,** 1407–1418 (2007).

10. Gericke, A. *et al.* Importance of phosphorylation for osteopontin regulation of biomineralization. *Calcif Tissue Int* **77,** 45–54 (2005).

11. Speer, M. Y. *et al.* Smooth muscle cells deficient in osteopontin have enhanced susceptibility to calcification in vitro. *Cardiovasc. Res.* **66,** 324–333 (2005).

12. Rabkin, E., Hoerstrup, S. P., Aikawa, M., Mayer, J. E. & Schoen, F. J. Evolution of cell phenotype and extracellular matrix in tissue-engineered heart valves during in-vitro maturation and in-vivo remodeling. *J. Heart Valve Dis.* **11,** 308–14; discussion 314 (2002).

13. Rabkin-Aikawa, E., Farber, M., Aikawa, M. & Schoen, F. J. Dynamic and reversible changes of interstitial cell phenotype during remodeling of cardiac valves. *J. Heart Valve Dis.* **13,** 841–847 (2004).

14. Balachandran, K., Sucosky, P., Jo, H. & Yoganathan, A. P. Elevated cyclic stretch alters matrix remodeling in aortic valve cusps: implications for degenerative aortic valve disease. *Am. J. Physiol. Heart Circ. Physiol.* **296,** H756–64 (2009).

15. Mikhaylova, L., Malmquist, J. & Nurminskaya, M. Regulation of in vitro vascular calcification by BMP4, VEGF and Wnt3a. *Calcif Tissue Int* **81,** 372–381 (2007).

16. Sucosky, P., Balachandran, K., Elhammali, A., Jo, H. & Yoganathan, A. P. Altered shear stress stimulates upregulation of endothelial VCAM-1 and ICAM-1 in a BMP-4- and TGF-beta1-dependent pathway. *Arterioscler. Thromb. Vasc. Biol.* **29,** 254–260 (2009).

17. Merryman, W. D. *et al.* Synergistic effects of cyclic tension and transforming growth factor-beta1 on the aortic valve myofibroblast. *Cardiovasc. Pathol.* **16,** 268–276 (2007).

18. Allison, D. D., Drazba, J. A., Vesely, I., Kader, K. N. & Grande-Allen, K. J. Cell viability mapping within long-term heart valve organ cultures. *J. Heart Valve Dis.* **13,** 290–296 (2004).

19. Scatena, M., Liaw, L. & Giachelli, C. M. Osteopontin: A Multifunctional Molecule Regulating Chronic Inflammation and Vascular Disease.

Arteriosclerosis, Thrombosis, and Vascular Biology **27,** 2302–2309 (2007).

20. Dai, J. *et al.* Osteopontin induces angiogenesis through activation of PI3K/AKT and ERK1/2 in endothelial cells. *Oncogene* **28,** 3412–3422 (2009).

21. Shen, M. *et al.* Osteopontin is associated with bioprosthetic heart valve calcification in humans. *C. R. Acad. Sci. III, Sci. Vie* **320,** 49–57 (1997).

22. Shen, M. *et al.* Protein adsorption of calcified and noncalcified valvular bioprostheses after human implantation. *Ann. Thorac. Surg.* **71,** S406–7 (2001).

23. Sainger, R. *et al.* Comparison of transesophageal echocardiographic analysis and circulating biomarker expression profile in calcific aortic valve disease. *J. Heart Valve Dis.* **22,** 156–165 (2013).

Chapter 6

Osteogenic-like Activation Of Human Aortic Valve Interstitial Cells

Part of this chapter has been published as[1]:

Paolo Poggio, Rachana Sainger, Emanuela Branchetti, Juan B. Grau, Eric K. Lai, Robert C. Gorman, Michael S. Sacks, Alessandro Parolari, Joseph E. Bavaria, and Giovanni Ferrari. Noggin attenuates the osteogenic activation of human valve interstitial cells in aortic valve sclerosis. *Cardiovascular Research* **98**, 402–410 (2013).

6.1 Introduction

The aortic valve leaflets are a highly specialized structure consisting mostly of VICs and complex extracellular matrix (ECM) structures[2-4]. The leaflet is divided into three functionally specific layers. The fibrosa layer, facing the aorta, is primarily composed of type I collagen fibers with a strong preferred circumferential orientation. The ventricularis, facing the left ventricle, mainly consists of elastin and collagen. The spongiosa, located between the fibrosa and the ventricularis, is largely composed of glycosaminoglycans[5]. It has been speculated than valve interstitial cells (VIC) maintain valve tissue homeostasis through regulated ECM biosynthesis[3]. VICs appear to be phenotypically plastic as they transdifferentiate during valve development, disease and remodeling from a quiescent to an osteogenic-like phenotype[6,7]. The activation of VICs results in the expression of specific markers such as osteopontin (OPN), osteonectin (ON), runt-related transcription factor 2 (RUNX2), *a*-smooth muscle actin (SMA), osteocalcin (OCN) and alkaline phosphatase (ALP). Furthermore, activated VICs express and actively remodel fibronectin (FN), which is a major component of the insoluble ECM[8]. Bone Morphogenic Protein 2 and 4 (BMP2 and BMP4) are known to be potent osteogenic morphogens and to be present in ossified valves and directly affects osteogenic marker expression[6,7,9-11]. Furthermore, aortic valve leaflets are exposed to large cyclical stresses. During each cardiac cycle, the normally functioning aortic valve interacts closely with the surrounding environment and it is exposed to a myriad of mechanical forces such as transvalvular pressure, axial, shear and bending stresses, and cyclic flexure[3,12-16]. While normal hemodynamic forces have been shown to cause constant tissue renewal, altered mechanical forces are believed to induce changes in aortic valve biology that could possibly lead to valve disease[2-4,17,18].

Over the last decade, several clinical trials have been performed to try to halt the progression of calcific AVS. Early enthusiastic findings, documenting a reduction in the progression of the disorder, have been questioned by later randomized studies, which show substantial equivalence between treatments and placebo[19-23]. It has been proposed that the therapy may have been initiated too late in the course of the disease to be effective[5,12,24].

In this chapter, it is investigated the mechanisms of human VIC activation in the very early stage of the disease using surgically resected aortic valve tissues and patient matched derived cells. Moreover, it is investigate the effect of HMG-CoA reductase inhibitor (pravastatin) on VIC osteogenic-like activation and calcium deposition.

6.2 Results

6.2.1 Patient population

Fourteen controls, 32 AVSc, and 48 AVS patients were enrolled for this part of the study. After echocardiographic and exclusion criteria evaluations, described in Chapter 2, 14 controls, 17 AVSc and 29 AVS were further analyzed. Patient demographics and echocardiographic data are described in Table 6.1 and Table 6.2.

Table 6.1 Patient demographics.

Demographics	Controls N = 14		Aortic sclerosis N = 32		Aortic stenosis N = 48	
Age	38.8	± 15.8	57.8	± 12.3	75.8	± 7.9
Male subjects	7	(58.3%)	13	(76.5%)	14	(48.3%)
Smokers	4	(33.3%)	8	(47.1%)	14	(48.3%)
Diabetes	..		3	(17.6%)	7	(24.1%)
Hypertension	2	(16.7%)	9	(52.9%)	23	(79.3%)
Cerebral vascular accident	..		..		1	(3.4%)
Coronary artery disease	1	(8.3%)	2	(11.8%)	7	(24.1%)
Congestive heart failure	..		12	(70.6%)	4	(13.8%)
Hyperlipidemia	1	(8.3%)	6	(35.3%)	18	(62.1%)

Adapted from[1]: Poggio, P. *et al.* Noggin attenuates the osteogenic activation of human valve interstitial cells in aortic valve sclerosis. *Cardiovasc. Res.* **98,** 402–410 (2013).

Table 6.2 Echocardiographic measurements

	Controls	Aortic Sclerosis	Aortic Stenosis	
Demographic				p value
Aortic Valve Area (cm^2)	> 2	> 2	0.77 ± 0.24	< 0.01
Doppler Velocity (m/s)	< 2	< 2	3.9 ± 0.71	< 0.01
Calcium Score	1	1	3.4 ± 0.53	< 0.01

Adapted from[1]: Poggio, P. *et al.* Noggin attenuates the osteogenic activation of human valve interstitial cells in aortic valve sclerosis. *Cardiovasc. Res.* **98,** 402–410 (2013).

6.2.2 Analysis of aortic valve leaflet microstructure and extracellular matrix composition

The histological analysis on 5 controls, 5 AVSc, and 5 AVS patients allowed us to measure the thickness of the leaflets, the number of cells and the extracellular matrix components (ECM) in the three different cohorts.

In controls aortic valves the microstructure of the leaflets was defined in a distinctly organized tri-layered architecture (fibrosa, spongiosa and ventricularis). Sclerotic aortic valves had a partially modified tri-layer structure compered to the controls and AVSc leaflet thickness was significantly increased. Moreover, a slight reduction in the total number of cells was notice in AVSc tissue when compared to controls. In contrast to controls and AVSc, the AVS leaflet structure was completely disarrayed and a large loss of cells was observed (Figure 6.1A). Modified Movat's Pentachrome staining was used to evaluate the ECM components, proteoglycan (bluish green), collagen (yellow), and elastin (dark violet). AVSc leaflets showed an increased ECM deposition; in particular we notice elastin deposition in the ventricularis layer of the leaflets. Tissues from AVS patients showed increased deposition of collagen, proteoglycan, and elastin fiber compared to controls and AVSc leaflets (Figure 6.1B).

We then investigated the presence of calcium deposits with Alizarin red staining. In controls and AVSc leaflets the staining was negative and the presence of calcium was comparable between the two groups. In contrast, in all the leaflets analyzed from aortic stenotic valves, calcium deposits were largely present and the distribution was mostly in the fibrosa layer (Figure 6.1C).

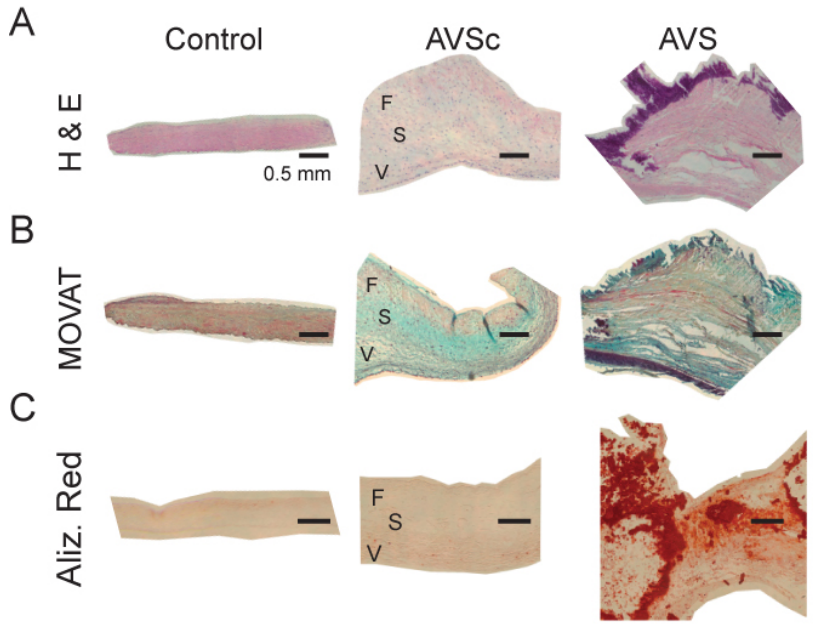

Figure 6.1. Analysis of aortic valve sclerosis microstructure.

(A, B, C) Representative images (n=5/group) for control, aortic valve sclerosis (AVSc), and aortic valve senosis (AVS) tissues: H&E staining; Movat's Pentachrome staining: ECM components are distinguished as proteoglycan (bluish green), collagen (yellow), and elastin (dark violet); VIC nuclei are stained dark red. Alizarin red was used to visualize calcium content. F: fibrosa; S: spongiosa and V: ventricularis. Bar represents 0.5mm. Adapted from[1]: Poggio, P. *et al.* Noggin attenuates the osteogenic activation of human valve interstitial cells in aortic valve sclerosis. *Cardiovasc. Res.* **98,** 402–410 (2013).

To better evaluate the ECM components among the three groups, we quantify type I collagen and two proteoglycans, decorin (DCN) and biglycan (BGN), by Real Time PCR (qPCR). Collagen type I was up regulated 7.5 ± 0.1 fold in AVSc *vs.* controls and 12.2 ± 0.1 fold in AVS *vs.* controls. Decorin was up regulated 17.8 ± 1.1 fold in AVSc *vs.* controls and 19.3 ± 0.9 fold in AVS *vs.* controls. Biglycan was up regulated 18.1 ± 1.9 fold in AVSc *vs.* controls and 22.9 ± 1.2 fold in AVS *vs.* controls.

All the comparison were statistically different with a value $p < 0.01$ (Figure 6.2).

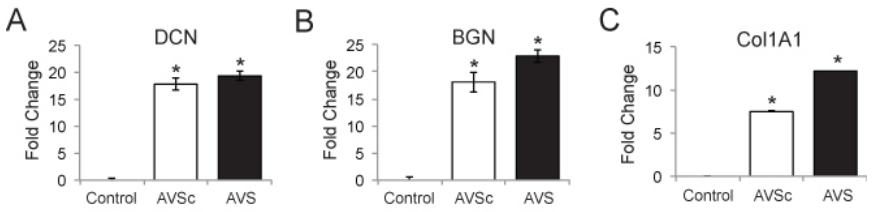

Figure 6.2. Analysis of aortic valve sclerosis extracellular matrix.

(D, E, F) Bar graph shows fold change gene expression of Decorin (DCN), Biglycan (BGN) and Collagen Type I (Col1A1) transcripts by RT-qPCR, respectively. Data were normalized against 18S gene expression and represented as fold change ± dCt SE. * $p < 0.01$. Adapted from[1]: Poggio, P. *et al.* Noggin attenuates the osteogenic activation of human valve interstitial cells in aortic valve sclerosis. *Cardiovasc. Res.* **98,** 402–410 (2013).

6.2.3 Osteogenic-like gene expression in aortic valve sclerosis tissues

To better characterize the three cohorts we analyses 84 genes by RT^2 PCR Array. The evaluated genes were related to ECM and cell adhesion molecules (CAM) and the complete list is reported in the Appendix A (Table 2). Among the genes up regulated more than two-fold, we validated the differential expression of 5 specific genes involved in the osteogenic-like transdifferentiation of valve interstitial cells (VIC) in 24 patients (8 controls, 8 AVSc, and 8 AVS).

The relative expressions, in AVSc tissues compared to controls, were 10.5 ± 3.5 fold for osteopontin (OPN), 11.9 ± 1.8 fold for osteonectin (ON), 10.6 ± 0.7 for fold thrombospondin 1 (THBS1), and 16.4 ± 1.1 fold for thrombospondin 2 (THBS2). AVS had a similar trend with a relative expression of 12.4 ± 4.1 fold for osteopontin (OPN), 12.6 ± 2.1 fold for osteonectin (ON), 12.3 ± 0.9 for fold thrombospondin 1 (THBS1), and 20.6 ± 0.5 fold for thrombospondin 2 (THBS2), when compered to healthy controls. Runt-related transcription factor 2 (RUNX2) was diverging in AVSc and AVS tissues; in AVSc the expression was -2.5 ± 0.5 fold while in AVS was 3.8 ± 0.4 fold, when compared to controls. All the comparison were statistically different with a value $p <$

0.01 (Figure 6.3). We assessed by immunofluorescence RUNX2 levels to confirm the qPCR results. Comparable with the gene analysis, RUNX2 expression was detectable only in AVS tissues in all the three layers. (Figure 6.3)

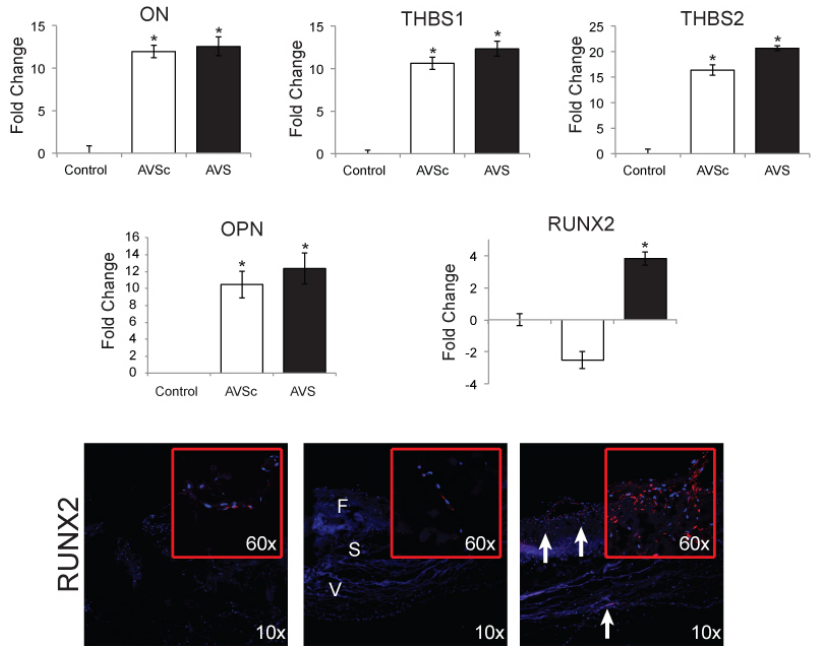

Figure 6.3. Osteogenic-like markers are up regulated in asymptomatic aortic valve sclerosis-derived tissues.

Bar graphs show fold change gene expression of Osteonectin (ON), Thrombospondin 1 (THBS1), Thrombospondin 2 (THBS2), Osteopontin (OPN), and Runt-related Transcription Factor 2 (RUNX2). All RT-qPCR were normalized against 18S gene expression and represented as fold change ± dCt SE. * $p < 0.01$. Lower panels represent immunofluorescence staining of RUNX2 on aortic valve tissues (red). Adapted from[1]: Poggio, P. *et al.* Noggin attenuates the osteogenic activation of human valve interstitial cells in aortic valve sclerosis. *Cardiovasc. Res.* **98,** 402–410 (2013).

We also check for biosynthetically active VIC presence, the expression of alpha-smooth muscle actin (SMA) was used as a marker of activated VICs. Western blot and immunofluorescence revealed an increased number of SMA positive VICs in the fibrosa layer of both AVSc and AVS leaflets (Figure 6.4).

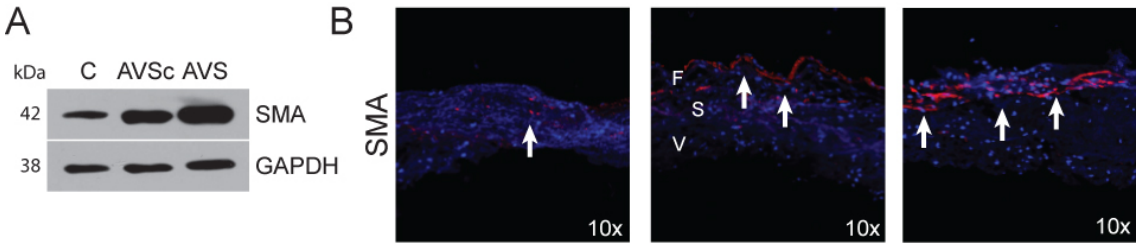

Figure 6.4. Activated valve interstitial cells aortic valve sclerosis tissues.

(A) Western blot of α-smooth muscle actin (SMA). (B) Immunofluorescence of SMA on aortic valve tissues. Adapted from[1]: Poggio, P. *et al.* Noggin attenuates the osteogenic activation of human valve interstitial cells in aortic valve sclerosis. *Cardiovasc. Res.* **98,** 402–410 (2013).

Finally, since BMP4 is an inducer of osteoblastic differentiation, we tested whether BMP4 was also present and up regulated in our AVSc and AVS cohorts. Immunofluorescence and qPCR showed a significant up regulation in both AVSc and AVS tissues, 9.0 ± 0.9 fold and 12.4 ± 0.6 fold, respectively ($p < 0.01$). Interestingly, we notice a compelling BMP4 side-specific over expression correlating with the fibrosa susceptibility to form calcium deposits, typical of the late stage disease (Figure 6.5).

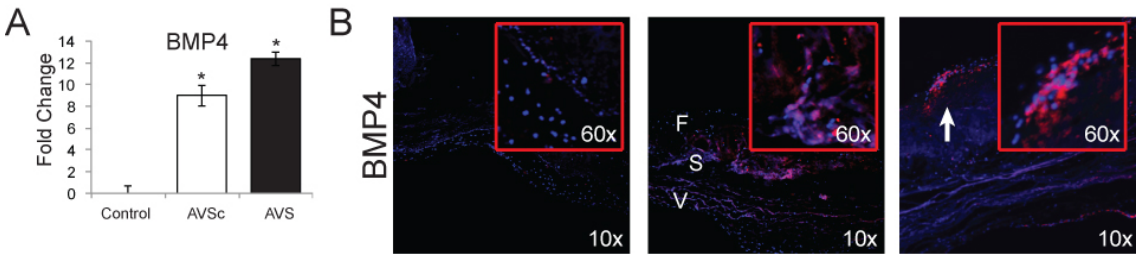

Figure 6.5. BMP4 is up regulated in aortic valve sclerosis tissues.

(A) Bar graph shows fold change gene expression of BMP4. RT-qPCR were normalized against 18S gene expression and represented as fold change ± dCt SE. * $p < 0.01$. (B) Immunofluorescence of BMP4 on aortic valve tissues. Adapted from[1]: Poggio, P. *et al.* Noggin attenuates the osteogenic activation of human valve interstitial cells in aortic valve sclerosis. *Cardiovasc. Res.* **98,** 402–410 (2013).

5.2.4 Role of BMP4 in osteogenic-like transdifferentiation of aortic valve sclerosis tissues

Based on the obtained results, we decide to carry out *in vitro* and *ex vivo* experiments to determine the role of BMP4 in the osteogenic-like transdifferentiation of human aortic valve sclerosis-derived valve interstitial cells.

To test the impact of BMP4 on AVSc-derived tissues we used a tensile bioreactor, to mimic the stress on the valve during the cardiac cycle we applied 15% stretch at 1 Hz. Since, Cyclic stretch does not damage leaflet morphology and maintains native ECM structure and cellular composition[25,26], we tested VIC survival within the leaflets from controls, AVSc and AVS patients. TUNEL assay was used to evaluate the apoptotic VICs within the leaflets inserted in the bioreactor under static or dynamic conditions for 6 days. The stretch did not affect the controls and affected minimally AVSc- derived VICs. In contrast, a large number of VICs, within the leaflets excised from AVS patients and exposed to cyclic stretch, were found fluorescin positive, indicating the apoptotic nuclei (Figure 6.6). Due to the high apoptotic rate in AVS-derived VICs and the relatively low access to control tissues we focus our analysis on aortic valve sclerosis-derived tissues and VICs.

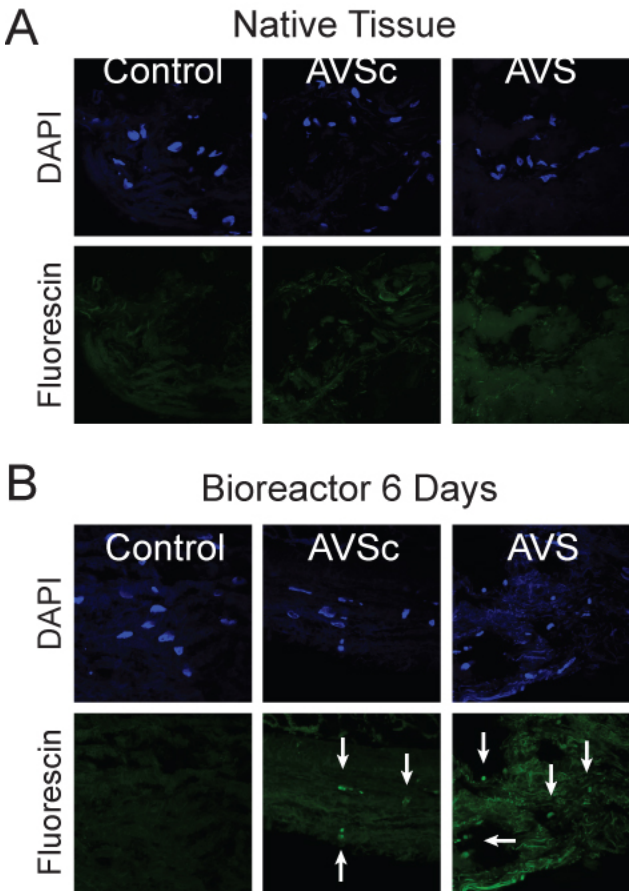

Figure 6.6. Detection of apoptotic cells in aortic valve tissues exposed to tensile stretch.

(A) TUNEL assay using native tissue analyzed after the excision of the tissue. (B) TUNEL assay using native tissue incubated in the bioreactor under dynamic condition after 6 days. Adapted from[1]: Poggio, P. *et al.* Noggin attenuates the osteogenic activation of human valve interstitial cells in aortic valve sclerosis. *Cardiovasc. Res.* **98,** 402–410 (2013).

To evaluate VIC osteogenic-like transdifferentiation we measured the expression of alkaline phosphatase (ALP) by qPCR and the presence of calcium nodules by histological staining (Alizarin red). Interestingly, we found that only the combination of mechanical (15% stretch at 1 Hz) and biological (100 ng/ml BMP4) stimuli was able to stimulate ALP and calcium accumulation. ALP was up regulated by 26.9 ± 0.7 fold ($p < 0.01$) in the native tissue under dynamic condition in the presence of BMP4, when compared to the tissue exposed to dynamic condition only (Figure 6.7).

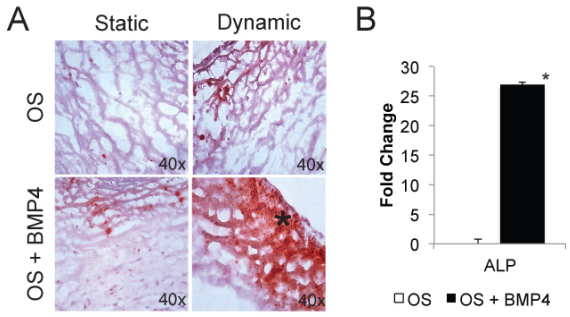

Figure 6.7. BMP4 induces biomineralization of human aortic valve sclerosis tissue.

(A) Immunohistochemistry staining with Alizarin red (to visualize calcium content) in aortic valve sclerosis (AVSc) tissue cultured in static and dynamic conditions in presence of osteogenic media (OS) ± BMP4 (100 ng/ml). * Represent the location of the fibrosa layer. (B) Alkaline Phosphatase (ALP) expression by RT-qPCR in native tissue cultured under dynamic condition in presence of OS ± BMP4 (100 ng/ml). Data were normalized against 18S gene expression and represented as fold change ± dCt SE. * $p < 0.05$. Adapted from[1]: Poggio, P. *et al.* Noggin attenuates the osteogenic activation of human valve interstitial cells in aortic valve sclerosis. *Cardiovasc. Res.* **98,** 402–410 (2013).

To further characterize the impact of BMP4 and mechanical stretch on the VIC activation, we tested the expression of SMA, FN, OPN, and ON. Protein expression revealed by immunofluorescence revealed a consistent overexpression of all the osteogenic markers tested. As control and to provide supporting evidence for a direct functional role of BMP4 in inducing osteogenic-like activation of AVSc-derived VICs, we tested noggin (NOG), a known inhibitor of BMP4, in relation of VIC activation. NOG was able to reduce BMP4-mediated up regulation of ALP and OPN by 44.4% and 64.3%, respectively ($p < 0.05$). Notably, we observed a NOG-related reduction of SMA and FN by 117% and 163%, respectively ($p < 0.05$) (Figure 6.8).

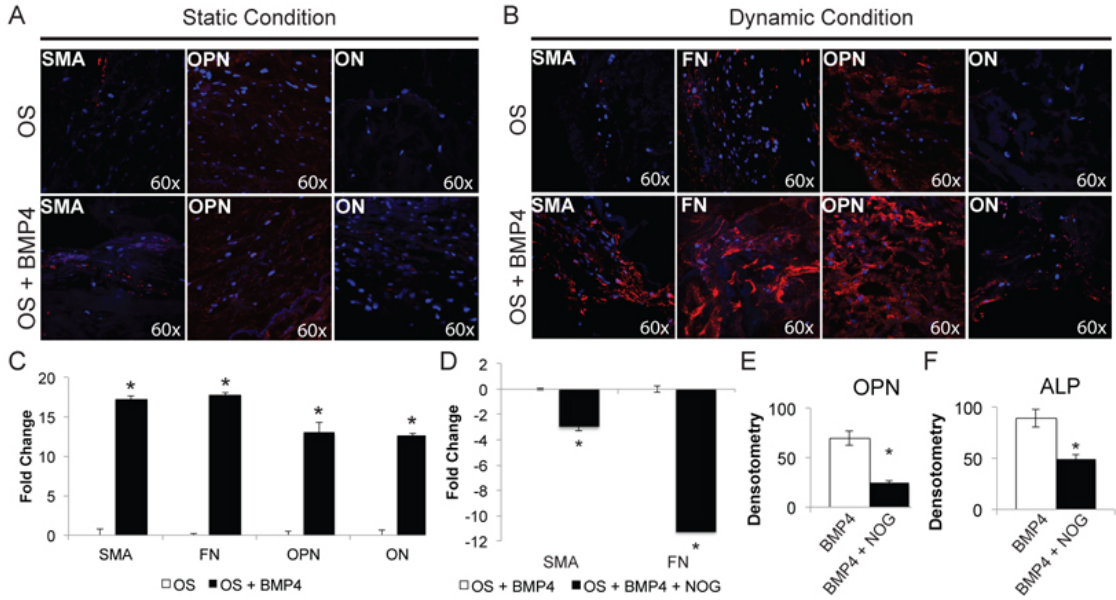

Figure 6.8. BMP 4 induces osteogenic markers expression in human aortic valve sclerosis tissue.

(A) Immunofluorescence staining showing expression of α-Smooth Muscle Actin (SMA), Osteopontin (OPN), and Osteonectin (ON) in aortic sclerosis tissue cultured in static condition in presence of osteogenic media (OS) ± BMP4 (100 ng/ml). (B) Immunofluorescence staining showing expression SMA, Fibronectin (FN), OPN, and ON in AVSc tissue cultured in dynamic conditions in presence of OS ± BMP4 (100 ng/ml). (C) SMA and FN expression by RT-qPCR in native tissue cultured under dynamic condition in presence of OS ± BMP4 ± Noggin (NOG) (500 ng/ml) *p<0.05. (D, E) Densitometry of OPN and Alkaline Phosphatase (ALP) expression by RT-qPCR in native tissue cultured under dynamic condition in presence of OS ± BMP4 (100 ng/ml) ± Noggin (NOG) (500 ng/ml). * p < 0.05. All RT-qPCR analysis were normalized against 18S gene expression and represented as fold change ± dCt SE. OS was used to calculate the basal gene levels. Adapted from[1]: Poggio, P. *et al.* Noggin attenuates the osteogenic activation of human valve interstitial cells in aortic valve sclerosis. *Cardiovasc. Res.* **98,** 402–410 (2013).

5.2.5 Activation of isolated valve interstitial cells by BMP4

Our results, on tissues from asymptomatic patients with aortic sclerosis, showed that we could induce osteogenic-like transdifferentiation of VICs. To better understand the VIC activation, we sought to test isolated patient-derived cells and we conducted the

experiment using collagen type I-coated plates. BMP4 treatment in OS media showed up regulation of OPN, RUNX2, and ON only in control-derived VICs by 7.63 ± 0.6, by 5.36 ± 0.6, and by 3.44 ± 0.2 fold, respectively ($P < 0.05$), and NOG was able to counteract the BMP4 effect. Contrarily, AVSc- and AVS-derived VICs showed no significant up regulation in RUNX2 and ON. OPN was upregulated by 2.1 ± 0.2 in AVSc-derived VICs but not in AVS-derived VICs (Figure 6.9). As previously discuss in chapter 5, treatment with BMP4 were not able to induce any calcium accumulation during the timeframe of the experiments.

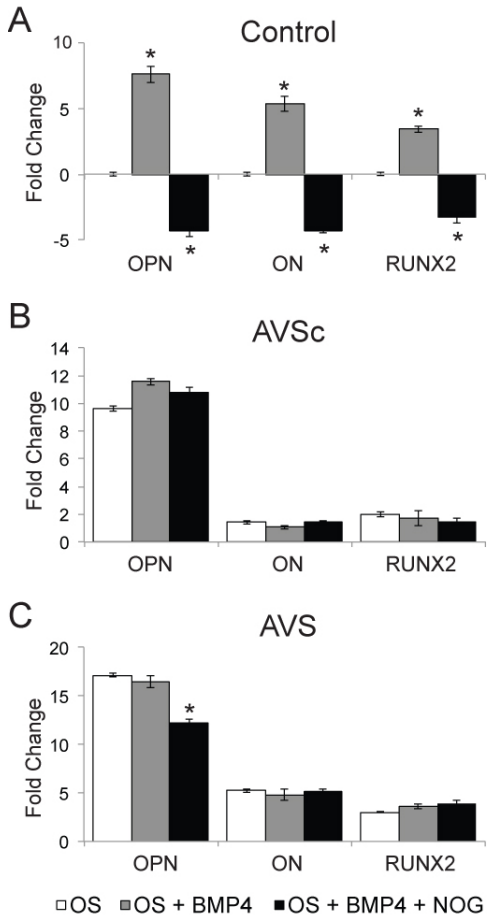

Figure 6.9. Activation of valve interstitial cells after BMP4 treatments.

(A, B, C) Bar graphs represent fold change gene expression of Osteopontin (OPN), Runt-related transcription factor 2 (RUNX2) and Osteonectin (ON) *in vitro* treatment in presence of osteogenic media (OS) ± Bone Morphogenetic Protein 4 (BMP4) (100 ng/ml) ± Noggin (NOG) (500 ng/ml) in control, aortic valve sclerosis (AVSc) and Aortic Valve Stenosis (AVS) derived VICs plated on collagen type I. * $p < 0.05$. Adapted from[1]: Poggio, P. *et al.* Noggin attenuates the osteogenic activation of human valve interstitial cells in aortic valve sclerosis. *Cardiovasc. Res.* **98,** 402–410 (2013).

In order to discern the progression of aortic valve sclerosis to stenosis, we implemented a tissue engineered (TE) model to test the impact of the combinatory effect of BMP4 and mechanical stimulation on isolated VICs derived from AVSc patients. VICs derived from AVSc patients were seeded on the TE model based on a decellularized porcine aortic valve. TE aortic valves were placed in the tensile stretch bioreactor and exposed to mechanical stretch in presence or absence of BMP4 or in presence of a combination of BMP4 and NOG for 6 days. In contrast to the VIC cultured in plated, the AVSc-derived VICs embedded in the TE valves exhibited a significantly up regulation of the osteogenic markers analyzed. SMA, OPN, ON, and RUNX2 were up regulated by 1.94 ± 0.1, by 2.28 ± 0.3, by 3.17 ± 0.3, and by 3.22 ± 0.2 fold, respectively ($P < 0.05$). NOG treatments completely reverted SMA, ON, and RUNX up regulation, furthermore NOG reduced the expression of OPN by -4.11 ± 0.2 folds ($P < 0.05$) (Figure 6.10).

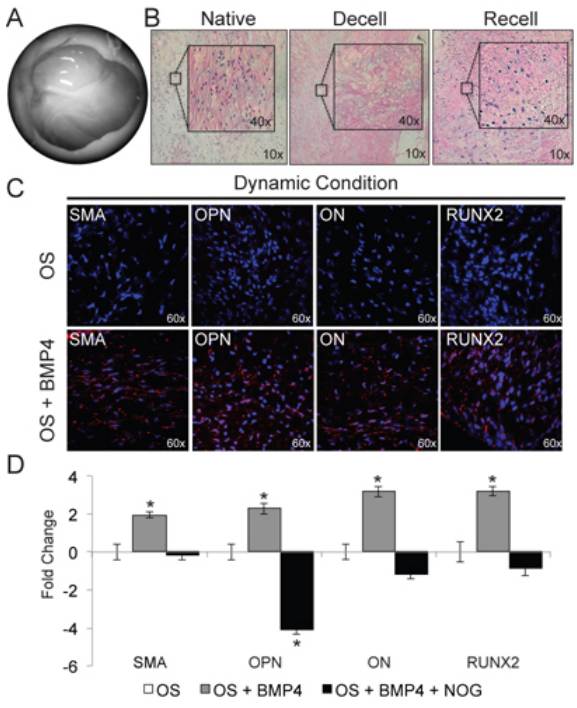

Figure 6.10. Noggin attenuates BMP4-induced activation of human valve interstitial cell in asymptomatic aortic valve sclerosis.

(A) Decellularized porcine Aortic Valve (AV) scaffold. (B) H&E staining showing the presence or absence of Valve Interstitial Cells (VIC) in the native porcine aortic valve (Native), after decellularization (Decell) and after reseeding of human VICs (Recell). (C) Immunofluorescence staining showing

expression of α-Smooth Muscle Actin (SMA), OPN, ON and RUNX2 in AVSc tissue cultured in dynamic conditions in presence of OS ± BMP4 (100 ng/ml). (D) SMA, OPN, ON and RUNX2 expression by RT-qPCR in tissue engineering tissue cultured under dynamic condition in presence of OS ± BMP4 (100 ng/ml) ± Noggin (NOG) (500 ng/ml). All RT-qPCR analysis were normalized against 18S gene expression and represented as fold change ± dCt SE. * $p < 0.05$. OS was used to calculate the basal gene levels. Adapted from[1]: Poggio, P. *et al.* Noggin attenuates the osteogenic activation of human valve interstitial cells in aortic valve sclerosis. *Cardiovasc. Res.* **98,** 402–410 (2013).

6.2.6 Valve interstitial cells phenotypic changes induced by Pravastatin

Since we demonstrated that AVSc-derived tissues and cells show over expression of osteogenic markers compared to healthy controls, we tested the effect of pravastatin on VIC phenotype changes. *Ex vivo* tissues derived from AVSc patients were placed in the bioreactor and subjected to tensile stretch in presence or absence of 100 μM pravastatin. After 6 days of treatments, qPCR analysis showed a down regulation of SMA, OPN, ON, and RUNX2 by -4.49 ± 1.2, by -1.83 ± 0.9, -4.72 ± 0.4, and by -4.44 ± 0.2, respectively ($p < 0.05$) (Figure 6.11).

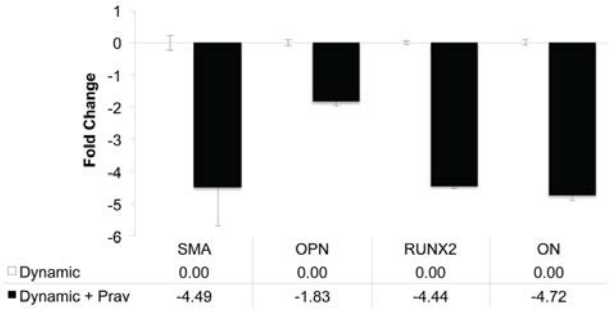

Figure 6.11. Statin treatment of aortic valve sclerosis tissue.

Bar graphs show fold change gene expression of SMA, OPN, RUNX2, and ON. All RT-qPCR were normalized against 18S gene expression and represented as fold change ± dCt SE. * $p < 0.01$.

To further investigate the effect of pravastatin, we treated isolated VICs from controls, AVSc and AVS patients. We noticed a different response in the three groups,

VICs derived from healthy controls were unresponsive to pravastatin, while AVSc- and AVS-derived VICs had opposite results. VICs isolated from AVSc patients showed a significant down regulation of SMA, RUNX2, ON, and OCN by -2.3 ± 0.4, by -1.3 ± 0.4, by -2.2 ± 0.2, and by -1.7 ± 0.3 fold, respectively ($p < 0.05$). Interestingly, we notice a significant up regulation of osteogenic markers in AVS-derived VICs after pravastatin treatments, SMA by 2.7 ± 0.4 fold, RUNX2 by 3.2 ± 0.3 fold, ON by 2.9 ± 0.4 fold, and OCN by 3.1 ± 0.4 fold ($p < 0.05$) (Figure 6.12).

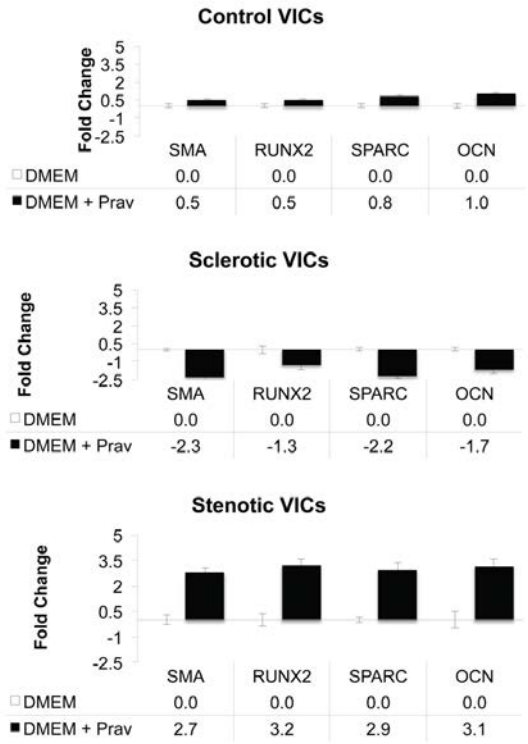

Figure 6.12 Statin treatment of isolated valve interstitial cells.

Bar graphs show fold change gene expression of SMA, OPN, RUNX2, and ON. All RT-qPCR were normalized against 18S gene expression and represented as fold change ± dCt SE.

6.3 Discussion

To impact the progression of calcific aortic valve disease (CAVD), we need to understand the earliest stages of this pathology in order to measure the effects of

targeted therapy on the microscopic processes in the valve leaflets. Despite recent efforts, progress to understand, diagnose, and treat calcific aortic valve stenosis (AVS) have been hindered by our inability to resolve the cellular mechanisms leading VIC activation towards an osteogenic-like phenotype[24,27,28]. We performed an analysis of aortic valve leaflets and patient-matched derived VICs using control, AVSc, and AVS patients. Notably, the valve mechanical functions of aortic sclerosis are largely unaffected; patients with aortic sclerosis have similar aortic valve area (AVA) and Doppler velocity values when compared with controls. Accordingly, aortic sclerosis patients are largely asymptomatic and are not indicated for aortic valve replacement (AVR). Therefore, we established collaboration with the heart transplant program that allowed us the use of either hearts of donors that were not used for transplantation or from recipients that, although transplanted, had a normally functioning aortic valve.

Our study provides several new insights into the early pathogenesis and the progression of AVSc. First, our data show that aortic valve leaflets form AVSc patient shows extensive ECM remodeling even in the absence of biomineralization. These events are associated with activation of VICs towards an osteogenic-like phenotype associated with up regulation of BMP4. Taken together, these results show that aortic sclerosis could be considered, from the cellular and molecular point of view, a pathological stage. Secondly, the results demonstrate that non-calcified aortic valve leaflets from asymptomatic patients can be induced to express markers of osteogenic transdifferentiation under the combinatory effect of biological (BMP4) and mechanical (tensile stretch) forces. Recent studies on aortic valve disease have described the expression of developmental genes in areas of valve calcification; thereby supporting the idea that valve calcification is not a passive deposition of calcium, but is actively regulated by a hierarchy of signaling pathways and transcription factors. Among these, BMPs signaling is important for valvulogenesis and osteogenesis and it is increased during AVS[29,30]. Recent manuscripts suggest a regulatory mechanisms of the BMP family in controlling osteogenic phenotype under mechanotrasduction stimulation[31-33]. BMP4 is essential in the osteochondrogenic gene program associated with vascular and valve calcification[34,35]. However, the factors that regulate mineralization in aortic diseases are poorly understood. Here, we reported the up regulation of SMA, OPN, RUNX2, and ON during the progression of calcific AVS. Furthermore, we observe the

fibrosa-layer susceptibility of non-calcified aortic sclerosis tissue to undergo biomineralization similarly to the natural course of the pathology. The deposition of calcium on the aortic side of aortic sclerosis tissue is likely due to the presence of nucleation centers, which provide the starting point for calcium nodule formation[36]. Notably, VIC transdifferentiation towards an osteogenic-like phenotype characterized by SMA, FN, OPN, and ALP overexpression are reduced by BMP4 antagonist NOG. We also implemented a TE model to demonstrate that human isolated VICs could be seeded in 3D scaffold and the biomechanical stimuli induced the transdifferentiation of the seeded VICs. This model allowed the used of human VIC in a controlled 3D environment and could be used to further characterize the osteogenic-like transdifferentiation. Of note, when using the TE model, we do not see calcium accumulation, which could be explained by the short duration (6 days) of the experiment and by the lacking of center of nucleation.

Despite the high prevalence of CAVD, no pharmacological treatment has been found to halt the progression of this degenerative pathology[19,21,23]. It has been hypothesized that the therapy has been initiated too late in the course of the disease[5]. Our results showed that statins were able to reduce the activation of VIC derived from aortic valve sclerosis patients. Additionally, this reduction was more pronounced using our *ex vivo* model based on AVSc excised tissues. In conclusion, our data support the hypothesis that statin treatments could be beneficial for patients in the early asymptomatic phase of CAVD. Therefore, new clinical trials should be designed to test the impact of lowering lipid therapy to halt the progression of this disease in its earliest phase.

6.4 References

1. Poggio, P. *et al.* Noggin attenuates the osteogenic activation of human valve interstitial cells in aortic valve sclerosis. *Cardiovasc. Res.* **98,** 402–410 (2013).

2. Mulholland, D. L. & Gotlieb, A. I. Cell biology of valvular interstitial cells. *Can J Cardiol* **12,** 231–236 (1996).

3. Merryman, W. D. *et al.* Correlation between heart valve interstitial cell stiffness and transvalvular pressure: implications for collagen biosynthesis. *Am. J. Physiol. Heart Circ. Physiol.* **290,** H224–31 (2006).

4. Blevins, T. L., Carroll, J. L., Raza, A. M. & Grande-Allen, K. J. Phenotypic characterization of isolated valvular interstitial cell subpopulations. *J. Heart Valve Dis.* **15,** 815–822 (2006).

5. Rajamannan, N. M. *et al.* Calcific Aortic Valve Disease: Not Simply a Degenerative Process: A Review and Agenda for Research From the National Heart and Lung and Blood Institute Aortic Stenosis Working Group * Executive Summary: Calcific Aortic Valve Disease - 2011 Update. *Circulation* **124,** 1783–1791 (2011).

6. Rabkin-Aikawa, E., Farber, M., Aikawa, M. & Schoen, F. J. Dynamic and reversible changes of interstitial cell phenotype during remodeling of cardiac valves. *J. Heart Valve Dis.* **13,** 841–847 (2004).

7. Rabkin, E., Hoerstrup, S. P., Aikawa, M., Mayer, J. E. & Schoen, F. J. Evolution of cell phenotype and extracellular matrix in tissue-engineered heart valves during in-vitro maturation and in-vivo remodeling. *J. Heart Valve Dis.* **11,** 308–14; discussion 314 (2002).

8. Moursi, A. M. *et al.* Fibronectin regulates calvarial osteoblast differentiation. *J. Cell. Sci.* **109 (Pt 6),** 1369–1380 (1996).

9. Balachandran, K., Sucosky, P., Jo, H. & Yoganathan, A. P. Elevated cyclic stretch alters matrix remodeling in aortic valve cusps: implications for

degenerative aortic valve disease. *Am. J. Physiol. Heart Circ. Physiol.* **296,** H756–64 (2009).

10. Mikhaylova, L., Malmquist, J. & Nurminskaya, M. Regulation of in vitro vascular calcification by BMP4, VEGF and Wnt3a. *Calcif Tissue Int* **81,** 372–381 (2007).

11. Sucosky, P., Balachandran, K., Elhammali, A., Jo, H. & Yoganathan, A. P. Altered shear stress stimulates upregulation of endothelial VCAM-1 and ICAM-1 in a BMP-4- and TGF-beta1-dependent pathway. *Arterioscler. Thromb. Vasc. Biol.* **29,** 254–260 (2009).

12. Otto, C. M., Kuusisto, J., Reichenbach, D. D., Gown, A. M. & O'Brien, K. D. Characterization of the early lesion of 'degenerative' valvular aortic stenosis. Histological and immunohistochemical studies. *Circulation* **90,** 844–853 (1994).

13. Rosenhek, R. *et al.* Mild and moderate aortic stenosis. Natural history and risk stratification by echocardiography. *Eur. Heart J.* **25,** 199–205 (2004).

14. Sacks, M. S., David Merryman, W. & Schmidt, D. E. On the biomechanics of heart valve function. *J Biomech* **42,** 1804–1824 (2009).

15. Rosenhek, R. *et al.* ESC Working Group on Valvular Heart Disease Position Paper: assessing the risk of interventions in patients with valvular heart disease. *European Heart Journal* **33,** 822–8– 828a– 828b (2012).

16. Baumgartner, H. & Otto, C. M. Aortic stenosis severity: do we need a new concept? *J. Am. Coll. Cardiol.* **54,** 1012–1013 (2009).

17. Balachandran, K., Sucosky, P. & Yoganathan, A. P. Hemodynamics and mechanobiology of aortic valve inflammation and calcification. *Int J Inflam* **2011,** 263870 (2011).

18. Thayer, P. *et al.* The effects of combined cyclic stretch and pressure on the aortic valve interstitial cell phenotype. *Ann Biomed Eng* **39,** 1654–1667 (2011).

19. Parolari, A. *et al.* Nonrheumatic calcific aortic stenosis: an overview from basic

science to pharmacological prevention. *Eur J Cardiothorac Surg* **35,** 493–504 (2009).

20. Moura, L. M. *et al.* Rosuvastatin affecting aortic valve endothelium to slow the progression of aortic stenosis. *J. Am. Coll. Cardiol.* **49,** 554–561 (2007).

21. Cowell, S. J. *et al.* A randomized trial of intensive lipid-lowering therapy in calcific aortic stenosis. *N. Engl. J. Med.* **352,** 2389–2397 (2005).

22. Benton, J. A., Kern, H. B., Leinwand, L. A., Mariner, P. D. & Anseth, K. S. Statins block calcific nodule formation of valvular interstitial cells by inhibiting alpha-smooth muscle actin expression. *Arteriosclerosis, Thrombosis, and Vascular Biology* **29,** 1950–1957 (2009).

23. Rossebø, A. B. *et al.* Intensive lipid lowering with simvastatin and ezetimibe in aortic stenosis. *N. Engl. J. Med.* **359,** 1343–1356 (2008).

24. Otto, C. M. Calcific aortic valve disease: new concepts. *Semin. Thorac. Cardiovasc. Surg.* **22,** 276–284 (2010).

25. Merryman, W. D. *et al.* Synergistic effects of cyclic tension and transforming growth factor-beta1 on the aortic valve myofibroblast. *Cardiovasc. Pathol.* **16,** 268–276 (2007).

26. Allison, D. D., Drazba, J. A., Vesely, I., Kader, K. N. & Grande-Allen, K. J. Cell viability mapping within long-term heart valve organ cultures. *J. Heart Valve Dis.* **13,** 290–296 (2004).

27. Aikawa, E. & Otto, C. M. Look more closely at the valve: imaging calcific aortic valve disease. *Circulation* **125,** 9–11 (2012).

28. Kurtz, C. E. & Otto, C. M. Aortic stenosis: clinical aspects of diagnosis and management, with 10 illustrative case reports from a 25-year experience. *Medicine* **89,** 349–379 (2010).

29. Kaden, J. J. *et al.* Expression of bone sialoprotein and bone morphogenetic protein-2 in calcific aortic stenosis. *J. Heart Valve Dis.* **13,** 560–566 (2004).

30. Pohjolainen, V. *et al.* Noncollagenous bone matrix proteins as a part of calcific aortic valve disease regulation. *Hum. Pathol.* **39,** 1695–1701 (2008).

31. Osman, L., Yacoub, M. H., Latif, N., Amrani, M. & Chester, A. H. Role of human valve interstitial cells in valve calcification and their response to atorvastatin. *Circulation* **114,** I–547–I–552 (2006).

32. Yang, X. *et al.* Pro-osteogenic phenotype of human aortic valve interstitial cells is associated with higher levels of Toll-like receptors 2 and 4 and enhanced expression of bone morphogenetic protein 2. *J. Am. Coll. Cardiol.* **53,** 491–500 (2009).

33. Balachandran, K., Sucosky, P., Jo, H. & Yoganathan, A. P. Elevated cyclic stretch induces aortic valve calcification in a bone morphogenic protein-dependent manner. *Am. J. Pathol.* **177,** 49–57 (2010).

34. Shao, E. S., Lin, L., Yao, Y. & Boström, K. I. Expression of vascular endothelial growth factor is coordinately regulated by the activin-like kinase receptors 1 and 5 in endothelial cells. *Blood* **114,** 2197–2206 (2009).

35. Yip, C. Y. Y. & Simmons, C. A. The aortic valve microenvironment and its role in calcific aortic valve disease. *Cardiovasc. Pathol.* **20,** 177–182 (2011).

36. Fokin, V. M., Yuritsyn, N. S. & Zanotto, E. D. *Nucleation Theory and Applications*. 74–125 (Wiley-VCH Verlag GmbH & Co. KGaA, 2005). doi:10.1002/3527604790.ch4

Chapter 7

Conclusion

7.1 Calcific aortic valve disease

Calcific aortic valve disease (CAVD) is the most common heart valve disease with a prevalence of ≈ 30% in adults over 65 years in the sub-clinical asymptomatic form, called aortic valve sclerosis (AVSc)[1]. Importantly, between 16% and 33% of patients with AVSc will progress to aortic valve stenosis (AVS)[2,3], the most common cause of sudden death among valve heart diseases[4]. Moreover, the incidence of CAVD continues to rise due to the aging population[5], as such, calcific aortic valve disease has a serious impact on general health. AVSc is characterized by thickening of the leaflets with none or marginal effect on the mechanical properties of the valve, making its presentation largely asymptomatic[6]. Almost 10% of these patients will progress to AVS, the end stage disease, which is associated with impaired leaflet motion and resistances to blood flow[1]. At the onset of mild symptoms of AVS, survival deviates considerably from the event-free curve, with a dramatic decline with severe AVS[7,8]. Therapeutic strategies able to reduce or halt the progression of CAVD are needed, but currently no pharmacological therapies has been successful leaving aortic valve replacement (AVR) the treatment of choice.

1. Could osteopontin be used as biomarker for early detection of calcific aortic valve disease?

Since the presence of AVSc has been associated with a higher risk of cardiovascular events, early identification of these patients will open new perspectives for early therapeutic intervention. It has been previously reported that circulating OPN levels are elevated in aortic valve stenosis (AVS) patients when compared to healthy controls[9]. Since the biological function of OPN is to regulate calcium deposition[10], it has been proposed that the increasing levels of OPN in diseased tissue and blood reflects a compensatory mechanism. We confirmed that OPN expression increased from control to AVSc and AVS derived tissues. We demonstrated an up regulation of plasma OPN levels derived from AVSc patients with no signs of aortic calcification compared

to healthy controls. Moreover, in the plasma of end-stage disease patients we found increased levels of OPN, which showed reduced phosphorylation at two tyrosine residues. Finally, OPN splicing variants -a, -b, and -c were differentially expressed during CAVD progression. These data indicate the possible use of OPN and its translational/post-translational modifications as possible biomarker for the identification of early phase of CAVD, in patients with no chronic inflammation or active malignancy.

2. Which is the role of osteopontin in valve endothelial cell migration?

Early aortic lesions seem to be initiated by increased mechanical or decreased shear stress, in combination with endothelial dysfunction, which is followed by lipids deposition[11]. Valve endothelial cell (VEC) activation and neo-vascularization of the leaflets characterize the valve degeneration process beginning in the aortic sclerosis phase[11]. Since OPN is overexpressed in CAVD patients and the endothelium is one of the primary targets during valve degeneration, we decided to characterize the VEC intracellular signaling pathway activated by OPN, using *in vitro* and *ex vivo* approaches. The experiments performed have demonstrated that OPN is able to regulate the EC migration through Erk1/2 phosphorylation. Moreover, we had shown the involvement of the both αvβ3 and CD44, two major OPN receptors, in the wound healing process. Interestingly, we noticed that dephosphorylated OPN but not the phosphorylated form, was able to stimulate EC migration. To further analyze the role of OPN in neo-vascularization we implemented a 3D system, where excised human aortic valve tissues were embedded in collagen. AVS-derived tissues were more prone to develop new tubular-like structure than healthy valves. Non-phosphorylated OPN was able to further increase the sprout of tubular-like structure from AVS-derived tissues through αvβ3 and CD44 and subsequent Erk1/2 phosphorylation.

3. What is the role of osteopontin in valve interstitial cell osteogenic-like activation and biomineralization?

Considering that valve interstitial cells (VIC) represent the majority of the cells within the valve leaflets and that VIC are prone to calcification when activated, we decided to evaluate the role of OPN on VIC osteoblastic-like activation and biomineralization. First of all, we characterize which form of OPN was involved in calcium deposition. We demonstrated that all of the splicing variants tested were able to inhibit calcium accumulation only when they were phosphorylated. Moreover, the protective effect of phosphorylated OPN was independent of αvβ3 and Erk1/2 activation. The OPN protective effect was mainly mediated by the activation of CD44 and the phosphorylation of Akt. To further analyze the cause of VIC activation and subsequent calcification, we investigated the BMP4 signaling pathway. With this set of experiments, we were able to demonstrate that BMP4 was responsible for the osteogenic-like transdifferentiation. Furthermore, the OPN-CD44 functional interaction was able to prevent biomineralization induced by BMP4.

Significantly, OPN post-translational modification and interaction with different receptors are able to activate different signaling pathways on different cell population. Non-phosphorylated OPN induces VEC migration through αvβ3 and CD44 engagement and phospho-Erk1/2, while phosphorylated OPN inhibits VIC calcium accumulation through CD44v6 activation and phospho-Akt.

4. Is it possible to analyze cell behavior while preserving the specialized aortic leaflet architecture?

The aortic valve has a highly specialized architecture with a complex extracellular matrix (ECM)[12-14]. In controls aortic valves the microstructure of the leaflets was defined in a distinctly organized tri-layered architecture, while the AVSc leaflets had a

partially modified tri-layer structure. Notably, the thickness of AVSc leaflets was significantly increased. Moreover, AVS leaflet structure was completely disarrayed, a large loss of cells was observed and massive calcium deposits were found. Interestingly, a significant up regulation of BMP4 and SMA was found in AVSc- and AVS-derived tissues. We also noticed SMA positive VIC presence only in the aortic side and the fibrosa layer, which is more prone to develop calcium accumulation. Taken together, these results indicate a side specific osteogenic-like activation in the early phase of CAVD. Furthermore, aortic valve leaflets are exposed to large cyclical stresses. During each cardiac cycle, the normally functioning aortic valve interacts closely with the surrounding environment and it is exposed different mechanical forces[13,15-17]. To better understand the complexity of the disease, we implemented a tensile stretch bioreactor able to maintain the integrity of the leaflet structure. The bioreactor allowed us to test biological stimuli in combination with mechanical forces. We were able to test excised tissues derived from controls, AVSc and AVS patients, but we further analyzed only AVSc tissues because of the rarity of control tissues and because AVS tissues were not suitable to be adapted to the tensile bioreactor. Implementing this *ex vivo* model, we were able to demonstrate that AVSc tissues could be induced to express advanced osteogenic marker and furthermore, these tissues developed calcium accumulation in the fibrosa layer. We also implemented a tissue engineering (TE) model to demonstrate that isolated human VICs could be genetically manipulated and subsequently seeded in a 3D scaffold. Finally, the combination of biological and mechanical stimuli induced the osteogenic-like transdifferentiation of the seeded VICs.

5. Can statins be effective on the early stage of calcific aortic valve disease?

Over the last decade several clinical trials, mostly extensions of atherosclerosis-related studies (collectively referred as “statin trials”), have been performed in order to study the impact on the progression of calcific aortic valve disease (CAVD) but generated contradictory results. The early enthusiastic findings documenting a reduction in the progression of CAVD have been questioned by more recent randomized studies,

which showed substantial equivalence between treatments and placebo[18-22]. It has been suggested that CAVD therapy in these trials may have been initiated too late in the course of the disease to be effective[16,23-25]. In addition, human aortic sclerotic tissues are generally not available to investigators since these valves are not surgically replaced until moderate to severe aortic stenosis occurs[26-30]. We now understand that AVS is just the end-stage of a disease that progresses from the microscopic early changes of aortic sclerosis to, in a subset of patients, asymptomatic and then symptomatic severe calcific stenosis. *In vitro* and *in vivo* studies have shown that valve calcification is an active process controlled by inflammatory mediators and regulators of osteogenic-like differentiation of VIC in the fibrosa layer of leaflets. Here, we have investigated the early asymptomatic stage of CAVD using a human bio-registry of tissue and VIC-derived cells[6,31-33]. Furthermore, we studied the effect of pravastatin on human isolated VICs derived from controls, AVSc and AVS patients and finally we tested the effect of pravastatin on AVSc excised tissues under mechanical stretch. Our results indicate that statin treatments are able to reduce the activation of VIC derived from aortic valve sclerosis patients. This reduction was more pronounced using our *ex vivo* model based on AVSc excised tissues. Interestingly, VICs isolated from healthy controls were unresponsive to the statin treatments; while VICs derived from AVS patients had an even greater increase in osteogenic marker expression. In conclusion, our data support the hypothesis that statin treatments could be beneficial for patients in the early asymptomatic phase of CAVD. Therefore, new clinical trials should be designed to test the impact of lowering lipid therapy to halt the progression of this disease in its earliest phase.

7.2 References

1. Beckmann, E., Grau, J. B., Sainger, R., Poggio, P. & Ferrari, G. Insights into the use of biomarkers in calcific aortic valve disease. *J. Heart Valve Dis.* **19,** 441–452 (2010).

2. Cosmi, J. E. *et al.* The risk of the development of aortic stenosis in patients with 'benign' aortic valve thickening. *Arch Intern Med* **162,** 2345–2347 (2002).

3. Faggiano, P. *et al.* Progression of aortic valve sclerosis to aortic stenosis. *Am. J. Cardiol.* **91,** 99–101 (2003).

4. Carabello, B. A. Introduction to aortic stenosis. *Circ. Res.* **113,** 179–185 (2013).

5. Mathers, C. D. & Loncar, D. Projections of global mortality and burden of disease from 2002 to 2030. *PLoS Med.* **3,** e442 (2006).

6. Poggio, P. *et al.* Noggin attenuates the osteogenic activation of human valve interstitial cells in aortic valve sclerosis. *Cardiovasc. Res.* **98,** 402–410 (2013).

7. Otto, C. M. Calcific aortic valve disease: outflow obstruction is the end stage of a systemic disease process. *European Heart Journal* **30,** 1940–1942 (2009).

8. Rajamannan, N. M. *et al.* Calcific Aortic Valve Disease: Not Simply a Degenerative Process: A Review and Agenda for Research From the National Heart and Lung and Blood Institute Aortic Stenosis Working Group * Executive Summary: Calcific Aortic Valve Disease - 2011 Update. *Circulation* **124,** 1783–1791 (2011).

9. Yu, P.-J. *et al.* Correlation between plasma osteopontin levels and aortic valve calcification: potential insights into the pathogenesis of aortic valve calcification and stenosis. *J. Thorac. Cardiovasc. Surg.* **138,** 196–199 (2009).

10. Steitz, S. A. *et al.* Osteopontin inhibits mineral deposition and promotes regression of ectopic calcification. *Am. J. Pathol.* **161,** 2035–2046 (2002).

11. Pastor-Pérez, F. & Marín, F. Hypertension, aortic sclerosis and the prothrombotic

state: understanding the complex interaction. *J Hum Hypertens* **23,** 287–288 (2009).

12. Mulholland, D. L. & Gotlieb, A. I. Cell biology of valvular interstitial cells. *Can J Cardiol* **12,** 231–236 (1996).

13. Merryman, W. D. *et al.* Correlation between heart valve interstitial cell stiffness and transvalvular pressure: implications for collagen biosynthesis. *Am. J. Physiol. Heart Circ. Physiol.* **290,** H224–31 (2006).

14. Blevins, T. L., Carroll, J. L., Raza, A. M. & Grande-Allen, K. J. Phenotypic characterization of isolated valvular interstitial cell subpopulations. *J. Heart Valve Dis.* **15,** 815–822 (2006).

15. Otto, C. M., Kuusisto, J., Reichenbach, D. D., Gown, A. M. & O'Brien, K. D. Characterization of the early lesion of 'degenerative' valvular aortic stenosis. Histological and immunohistochemical studies. *Circulation* **90,** 844–853 (1994).

16. Rosenhek, R. *et al.* Mild and moderate aortic stenosis. Natural history and risk stratification by echocardiography. *Eur. Heart J.* **25,** 199–205 (2004).

17. Sacks, M. S., David Merryman, W. & Schmidt, D. E. On the biomechanics of heart valve function. *J Biomech* **42,** 1804–1824 (2009).

18. Parolari, A. *et al.* Do statins improve outcomes and delay the progression of non-rheumatic calcific aortic stenosis? *Heart* **97,** 523–529 (2011).

19. Moura, L. M. *et al.* Rosuvastatin affecting aortic valve endothelium to slow the progression of aortic stenosis. *J. Am. Coll. Cardiol.* **49,** 554–561 (2007).

20. Cowell, S. J. *et al.* A randomized trial of intensive lipid-lowering therapy in calcific aortic stenosis. *N. Engl. J. Med.* **352,** 2389–2397 (2005).

21. Benton, J. A., Kern, H. B., Leinwand, L. A., Mariner, P. D. & Anseth, K. S. Statins block calcific nodule formation of valvular interstitial cells by inhibiting alpha-smooth muscle actin expression. *Arteriosclerosis, Thrombosis, and Vascular Biology* **29,** 1950–1957 (2009).

22. Rossebø, A. B. *et al.* Intensive lipid lowering with simvastatin and ezetimibe in aortic stenosis. *N. Engl. J. Med.* **359,** 1343–1356 (2008).

23. Aikawa, E. & Otto, C. M. Look more closely at the valve: imaging calcific aortic valve disease. *Circulation* **125,** 9–11 (2012).

24. Rosenhek, R. *et al.* ESC Working Group on Valvular Heart Disease Position Paper: assessing the risk of interventions in patients with valvular heart disease. *European Heart Journal* **33,** 822–8– 828a– 828b (2012).

25. Baumgartner, H. & Otto, C. M. Aortic stenosis severity: do we need a new concept? *J. Am. Coll. Cardiol.* **54,** 1012–1013 (2009).

26. Gould, S. T., Srigunapalan, S., Simmons, C. A. & Anseth, K. S. Hemodynamic and cellular response feedback in calcific aortic valve disease. *Circ. Res.* **113,** 186–197 (2013).

27. Towler, D. A. Molecular and cellular aspects of calcific aortic valve disease. *Circ. Res.* **113,** 198–208 (2013).

28. Heistad, D. D., Shanahan, C. & Demer, L. L. Introduction to the compendium on calcific aortic valve disease. *Circ. Res.* **113,** 176–178 (2013).

29. Côté, N. *et al.* Inflammation is associated with the remodeling of calcific aortic valve disease. *Inflammation* **36,** 573–581 (2013).

30. Dweck, M. R. *et al.* Aortic stenosis, atherosclerosis, and skeletal bone: is there a common link with calcification and inflammation? *European Heart Journal* **34,** 1567–1574 (2013).

31. Poggio, P. *et al.* Osteopontin controls endothelial cell migration in vitro and in excised human valvular tissue from patients with calcific aortic stenosis and controls. *J. Cell. Physiol.* **226,** 2139–2149 (2011).

32. Grau, J. B. *et al.* Analysis of Osteopontin Levels for the Identification of Asymptomatic Patients With Calcific Aortic Valve Disease. (2011).

33. Sainger, R. *et al.* Dephosphorylation of circulating human osteopontin correlates with severe valvular calcification in patients with calcific aortic valve disease. 1–8 (2012).

Appendix A

Table 1. List of Primers used.

Gene		Primer sequence
BMP4	Fw	5'- CAC TGG TCC CTG GGA TGT TC -3'
	Rv	5'- GAT CCA CAG CAC TGG TCT TGA CTA -3'
ON	Fw	5’- GAG AAA GAA GAT CCA GGC CC -3’
	Rv	5’- GCC TGT CTC TAA ACC CCT CC -3’
OPN	Fw	5'- TTG CAG CCT TCT CAG CCA A -3'
	Rv	5'- GGA GGC AAA AGC AAA TCA CTG -3'
RUNX2	Fw	5’- CCA ACC CAC GAA TGC ACT ATC -3’
	Rv	5’- TAG TGA GTG GTG GCG GAC ATA C -3’
ALP	Fw	5’- GCT GGC AGT GGT CAG ATG TT -3’
	Rv	5’- CTA TCC TGG CTC CGT GCT C -3’
FN	Fw	5’- CCG TGG GCA ACT CTG TC -3’
	Rv	5’- TGC GGC AGT TGT CAC AG -3’
THBS1	Fw	5’- CAC AGC TCG TAG AAC AGG AGG -3’
	Rv	5’- CAA TGC CAC AGT TCC TGA TG -3’
THBS2	Fw	5’- GCA GCG TCT CTG TGT TCT CA -3’
	Rv	5’- GAG TCA CTT CAG GGG TTT CG -3’
Col1A1	Fw	5’- GGA CAC AGA GGT TTC AGT GG -3’
	Rv	5’- CCA GTA GCA CCA TCA TTT CC -3’
DCN	Fw	5’- ATC CTC CTT CTG CTT GCA CA -3’
	Rv	5’- TGC TCC AGG ACT AAC TTT GCT -3’
BGN	Fw	5’- CCC TCT CCA GGT CCA TCC GC -3’
	Rv	5’- GAG CTG GTA GGT TGG GCG GG -3’
CD44v6	Fw	5’- TCC CAG TAT GAC ACA TAT TGC -3’
	Rv	5’- CCC ACA TGC CAT CTG TTG CC -3’
CD44v3	Fw	5’- TCC CAG TAT GAC ACA TAT TGC -3’
	Rv	5'- TCA TTT GGC TCC CAG CCT GG -3'
GAPDH	Fw	5’- CCCATCACCATCTTCCAGGAG -3’
	Rv	5’- CTTCTCCATGGTGGTGAAGACG -3’
18S	Fw	5’- GTA ACC CGT TGA ACC CCA TT -3’
	Rv	5’- CCA TCC AAT CGG TAG TAG CG -3’

Table 2. RT^{2}Profiler PCR Array list of genes analyzed.

GeneBank	Symbol	Description
NM_006988	ADAMTS1	ADAM metallopeptidase with thrombospondin type 1 motif, 1
NM_139025	ADAMTS13	ADAM metallopeptidase with thrombospondin type 1 motif, 13
NM_007037	ADAMTS8	ADAM metallopeptidase with thrombospondin type 1 motif, 8
NM_000610	CD44	CD44 molecule (Indian blood group)
NM_004360	CDH1	Cadherin 1, type 1, E-cadherin (epithelial)
NM_001843	CNTN1	Contactin 1
NM_080629	COL11A1	Collagen, type XI, alpha 1
NM_004370	COL12A1	Collagen, type XII, alpha 1
NM_021110	COL14A1	Collagen, type XIV, alpha 1
NM_001855	COL15A1	Collagen, type XV, alpha 1
NM_001856	COL16A1	Collagen, type XVI, alpha 1
NM_000088	COL1A1	Collagen, type I, alpha 1
NM_001846	COL4A2	Collagen, type IV, alpha 2
NM_000093	COL5A1	Collagen, type V, alpha 1
NM_001848	COL6A1	Collagen, type VI, alpha 1
NM_001849	COL6A2	Collagen, type VI, alpha 2
NM_000094	COL7A1	Collagen, type VII, alpha 1
NM_001850	COL8A1	Collagen, type VIII, alpha 1
NM_004385	VCAN	Versican
NM_001901	CTGF	Connective tissue growth factor
NM_001903	CTNNA1	Catenin (cadherin-associated protein), alpha 1, 102kDa
NM_001904	CTNNB1	Catenin (cadherin-associated protein), beta 1, 88kDa
NM_001331	CTNND1	Catenin (cadherin-associated protein), delta 1
NM_001332	CTNND2	Catenin (cadherin-associated protein), delta 2 (neural plakophilin-related arm-repeat protein)
NM_004425	ECM1	Extracellular matrix protein 1
NM_002026	FN1	Fibronectin 1
NM_001523	HAS1	Hyaluronan synthase 1
NM_000201	ICAM1	Intercellular adhesion molecule 1
NM_181501	ITGA1	Integrin, alpha 1
NM_002203	ITGA2	Integrin, alpha 2 (CD49B, alpha 2 subunit of VLA-2 receptor)
NM_002204	ITGA3	Integrin, alpha 3 (antigen CD49C, alpha 3 subunit of VLA-3 receptor)
NM_000885	ITGA4	Integrin, alpha 4 (antigen CD49D, alpha 4 subunit of VLA-4 receptor)
NM_002205	ITGA5	Integrin, alpha 5 (fibronectin receptor, alpha polypeptide)
NM_000210	ITGA6	Integrin, alpha 6
NM_002206	ITGA7	Integrin, alpha 7
NM_003638	ITGA8	Integrin, alpha 8
NM_002209	ITGAL	Integrin, alpha L (antigen CD11A (p180), lymphocyte function-associated antigen 1; alpha polypeptide)
NM_000632	ITGAM	Integrin, alpha M (complement component 3 receptor 3 subunit)
NM_002210	ITGAV	Integrin, alpha V (vitronectin receptor, alpha polypeptide, antigen CD51)
NM_002211	ITGB1	Integrin, beta 1 (fibronectin receptor, beta polypeptide, antigen CD29 includes MDF2, MSK12)
NM_000211	ITGB2	Integrin, beta 2 (complement component 3 receptor 3 and 4 subunit)
NM_000212	ITGB3	Integrin, beta 3 (platelet glycoprotein IIIa, antigen CD61)
NM_000213	ITGB4	Integrin, beta 4
NM_002213	ITGB5	Integrin, beta 5
NM_000216	KAL1	Kallmann syndrome 1 sequence
NM_005559	LAMA1	Laminin, alpha 1
NM_000426	LAMA2	Laminin, alpha 2
NM_000227	LAMA3	Laminin, alpha 3
NM_002291	LAMB1	Laminin, beta 1
NM_000228	LAMB3	Laminin, beta 3
NM_002293	LAMC1	Laminin, gamma 1 (formerly LAMB2)
NM_002421	MMP1	Matrix metallopeptidase 1 (interstitial collagenase)
NM_002425	MMP10	Matrix metallopeptidase 10 (stromelysin 2)
NM_005940	MMP11	Matrix metallopeptidase 11 (stromelysin 3)
NM_002426	MMP12	Matrix metallopeptidase 12 (macrophage elastase)
NM_002427	MMP13	Matrix metallopeptidase 13 (collagenase 3)
NM_004995	MMP14	Matrix metallopeptidase 14 (membrane-inserted)
NM_002428	MMP15	Matrix metallopeptidase 15 (membrane-inserted)
NM_005941	MMP16	Matrix metallopeptidase 16 (membrane-inserted)
NM_004530	MMP2	Matrix metallopeptidase 2 (gelatinase A, 72kDa gelatinase, 72kDa type IV collagenase)
NM_002422	MMP3	Matrix metallopeptidase 3 (stromelysin 1, progelatinase)
NM_002423	MMP7	Matrix metallopeptidase 7 (matrilysin, uterine)
NM_002424	MMP8	Matrix metallopeptidase 8 (neutrophil collagenase)
NM_004994	MMP9	Matrix metallopeptidase 9 (gelatinase B, 92kDa gelatinase, 92kDa type IV collagenase)